

Analysis and Optimization of Loss Functions for Multiclass, Top-k, and Multilabel Classification

Maksim Lapin, Matthias Hein, and Bernt Schiele

Abstract—Top-k error is currently a popular performance measure on large scale image classification benchmarks such as ImageNet and Places. Despite its wide acceptance, our understanding of this metric is limited as most of the previous research is focused on its special case, the top-1 error. In this work, we explore two directions that shed more light on the top-k error. First, we provide an in-depth analysis of established and recently proposed single-label multiclass methods along with a detailed account of efficient optimization algorithms for them. Our results indicate that the softmax loss and the smooth multiclass SVM are surprisingly competitive in top-k error uniformly across all k , which can be explained by our analysis of multiclass top-k calibration. Further improvements for a specific k are possible with a number of proposed top-k loss functions. Second, we use the top-k methods to explore the transition from multiclass to multilabel learning. In particular, we find that it is possible to obtain effective multilabel classifiers on Pascal VOC using a single label per image for training, while the gap between multiclass and multilabel methods on MS COCO is more significant. Finally, our contribution of efficient algorithms for training with the considered top-k and multilabel loss functions is of independent interest.

Index Terms—Multiclass classification, multilabel classification, top-k error, top-k calibration, SDCA optimization



1 INTRODUCTION

MODERN computer vision benchmarks are large scale [1]–[3], and are only likely to grow further both in terms of the sample size as well as the number of classes. While simply collecting more data may be a relatively straightforward exercise, obtaining high quality ground truth annotation is hard. Even when the annotation is just a list of image level tags, collecting a *consistent* and *exhaustive* list of labels for every image requires significant effort. Instead, existing benchmarks often offer only a single label per image, albeit the images may be inherently multilabel. The increased number of classes then leads to ambiguity in the labels as classes start to overlap or exhibit a hierarchical structure. The issue is illustrated in Figure 1, where it is difficult even for humans to guess the ground truth label correctly on the first attempt [2], [4].

Allowing k guesses instead of one leads to what we call the *top-k error*, which is one of the main subjects of this work. While previous research is focused on minimizing the top-1 error, we consider $k \geq 1$. We are mainly interested in two cases: (i) achieving small top- k error for *all* k simultaneously; and (ii) minimization of a specific top- k error. These goals are pursued in the first part of the paper which is concerned with single label multiclass classification. We propose extensions of the established multiclass loss functions to address top- k error minimization and derive appropriate optimization schemes based on stochastic dual coordinate ascent (SDCA) [5]. We analyze which of the multiclass methods are calibrated for the top- k error and perform an extensive



Fig. 1: Class ambiguity with a single label on Places 205 [2]. **Labels:** Valley, Pasture, Mountain; Ski resort, Chalet, Sky. Note that multiple labels apply to each image and k guesses may be required to guess the ground truth label correctly.

empirical evaluation to better understand their benefits and limitations. An earlier version of this work appeared in [6].

Moving forward, we see top- k classification as a natural transition step between multiclass learning with a single label per training example and multilabel learning with a complete set of relevant labels. Multilabel learning forms the second part of this work, where we introduce a smoothed version of the multilabel SVM loss [7], and contribute two novel projection algorithms for efficient optimization of multilabel losses in the SDCA framework. Furthermore, we compare all multiclass, top- k , and multilabel methods in a novel experimental setting, where we want to quantify the utility of multilabel annotation. Specifically, we want to understand if it is possible to obtain effective multilabel classifiers from single label annotation.

The contributions of this work are as follows.

- In § 2, we provide an overview of the related work and establish connections to a number of related research directions. In particular, we point to an intimate link

- M. Lapin and B. Schiele are with the Computer Vision and Multimodal Computing group, Max Planck Institute for Informatics, Saarbrücken, Saarland, Germany. E-mail: {mlapin, schiele}@mpi-inf.mpg.de.
- M. Hein is with the Department of Mathematics and Computer Science, Saarland University, Saarbrücken, Saarland, Germany. E-mail: hein@cs.uni-saarland.de.

TABLE 1: Overview of the methods considered in this work and our contributions.

Method	Name	Loss function	Conjugate	SDCA update	Top- k calibrated
SVM ^{OVA}	One-vs-all (OVA) SVM	$\max\{0, 1 - yf(x)\}$			no [†] (Prop. 8)
LR ^{OVA}	OVA logistic regression	$\log(1 + \exp(-yf(x)))$	[8]	[8]	yes (Prop. 9)
SVM ^{Multi}	Multiclass SVM	$\max\{0, (a + c)\pi_1\}$	[8], [9]	[8], [9]	no (Prop. 11)
LR ^{Multi}	Softmax (cross entropy)	$\log(\sum_{j \in \mathcal{Y}} \exp(a_j))$	Prop. 3	Prop. 15	yes (Prop. 12)
top- k SVM ^{α}	Top- k SVM (α)	$\max\{0, \frac{1}{k} \sum_{j=1}^k (a + c)\pi_j\}$			open question
top- k SVM ^{β}	Top- k SVM (β)	$\frac{1}{k} \sum_{j=1}^k \max\{0, (a + c)\pi_j\}$	[9]	[9]	
top- k SVM ^{α_γ}	Smooth top- k SVM (α)	L_γ in Prop. 2 w/ Δ_k^α	Prop. 2	Prop. 14	
top- k SVM ^{β_γ}	Smooth top- k SVM (β)	L_γ in Prop. 2 w/ Δ_k^β			
top- k Ent	Top- k entropy	L in Prop. 4	Eq. 4 w/ Δ_k^α	Prop. 15	
top- k Ent _{tr}	Truncated top- k entropy	$\log(1 + \sum_{j \in \mathcal{J}_y^k} \exp(a_j))$	-	-	yes (Prop. 13)
SVM ^{ML}	Multilabel SVM	$\max_{y \in \mathcal{Y}, \bar{y} \in \bar{\mathcal{Y}}} \max\{0, 1 + u_{\bar{y}} - u_y\}$	Prop. 5	Prop. 18	see e.g. [10]
SVM ^{ML} _{γ}	Smooth multilabel SVM	L_γ in Prop. 6	Prop. 6	Prop. 18	for multilabel
LR ^{ML}	Multilabel Softmax	$\frac{1}{ \bar{\mathcal{Y}} } \sum_{y \in \mathcal{Y}} \log(\sum_{\bar{y} \in \bar{\mathcal{Y}}} \exp(u_{\bar{y}} - u_y))$	Prop. 7	Prop. 20	consistency

Let $a \triangleq (f_j(x) - f_y(x))_{j \in \mathcal{Y}}$, $c \triangleq 1 - e_y$ (multiclass); $u \triangleq (f_y(x))_{y \in \mathcal{Y}}$ (multilabel); $\pi : a_{\pi_1} \geq \dots \geq a_{\pi_m}$; \mathcal{J}_y^k is defined in § 3.2. SVM^{Multi} \equiv top-1 SVM ^{α} \equiv top-1 SVM ^{β} ; LR^{Multi} \equiv top-1 Ent \equiv top-1 Ent_{tr}. [†]Smooth SVM^{OVA} _{γ} is top- k calibrated (Prop. 10).

that exists between top- k classification, label ranking, and learning to rank in information retrieval.

- In § 3, we introduce the learning problem for multiclass and multilabel classification, and discuss the respective performance metrics. We also propose 4 novel loss functions for minimizing the top- k error and a novel smooth multilabel SVM loss. A brief summary of the methods that we consider is given in Table 1.
- In § 4, we introduce the notion of top- k calibration and analyze which of the multiclass methods are calibrated for the top- k error. In particular, we highlight that the softmax loss is uniformly top- k calibrated for all $k \geq 1$.
- In § 5, we develop efficient optimization schemes based on the SDCA framework. Specifically, we contribute a set of algorithms for computing the proximal maps that can be used to train classifiers with the specified multiclass, top- k , and multilabel loss functions.
- In § 6, the methods are evaluated empirically in three different settings: on synthetic data (§ 6.1), on multiclass datasets (§ 6.2), and on multilabel datasets (§ 6.3).
- In § 6.2, we perform a set of experiments on 11 multiclass benchmarks including the ImageNet 2012 [1] and the Places 205 [2] datasets. Our evaluation reveals, in particular, that the softmax loss and the proposed smooth SVM^{Multi} _{γ} loss are competitive uniformly in all top- k errors, while improvements for a specific k can be obtained with the new top- k losses.
- In § 6.3, we evaluate the multilabel methods on 10 datasets following [11], where our smooth multilabel SVM^{ML} _{γ} shows particularly encouraging results. Next, we perform experiments on Pascal VOC 2007 [12] and Microsoft COCO [3], where we train multiclass and top- k methods using only a single label of the most prominent object per image, and then compare their multilabel performance on test data to that of multilabel

methods trained with full annotation. Surprisingly, we observe a gap of just above 2% mAP on Pascal VOC between the best multiclass and multilabel methods.

We release our implementation of SDCA-based solvers for training models with the loss functions considered in this work¹. We also publish code for the corresponding proximal maps, which may be of independent interest.

2 RELATED WORK

In this section, we place our work in a broad context of related research directions. First, we draw connections to the general problem of *learning to rank*. While it is mainly studied in the context of information search and retrieval, there are clear ties to multiclass and multilabel classification. Second, we briefly review related results on *consistency* and classification calibration. These form the basis for our theoretical analysis of top- k calibration. Next, we focus on the technical side including the *optimization method* and the algorithms for efficient computation of proximal operators. Finally, we consider multiclass and multilabel *image classification*, which are the main running examples in this paper.

Learning to rank. Learning to rank is a supervised learning problem that arises whenever the structure in the output space admits a partial order [13]. The classic example is ranking in information retrieval (IR), see e.g. [14] for a recent review. There, a feature vector $\Phi(q, d)$ is computed for every query q and every document d , and the task is to learn a model that ranks the relevant documents for the given query before the irrelevant ones. Three main approaches are recognized within that framework: the pointwise, the pairwise, and the listwise approach. Pointwise methods cast the problem of predicting document relevance as a regression [15] or a classification [16] problem. Instead, the pairwise

1. <https://github.com/mlapin/libsdca>

approach is focused on predicting the relative order between documents [17]–[19]. Finally, the listwise methods attempt to optimize a given performance measure directly on the full list of documents [20]–[22], or propose a loss function on the predicted and the ground truth lists [23], [24].

Different from ranking in IR, our main interest in this work is *label ranking* which generalizes the basic binary classification problem to multiclass, multilabel, and even hierarchical classification, see [25] for a survey. A link between the two settings is established if we consider queries to be examples (e.g. images) and documents to be class labels. The main contrast, however, is in the employed loss functions and performance evaluation at test time (§ 3).

Most related to our work is a general family of convex loss functions for ranking and classification introduced by Usunier et al. [26]. One of the loss functions that we consider (top- k SVM ^{β} [9]) is a member of that family. Another example is WSABIE [27], [28], which learns a joint embedding model optimizing an approximation of a loss from [26].

Top- k classification in our setting is directly related to label ranking as the task is to place the ground truth label in the set of top k labels as measured by their prediction scores. An alternative approach is suggested by [29] who use structured learning to aggregate the outputs of pre-trained one-vs-all binary classifiers and directly predict a set of k labels, where the labels missing from the annotation are modelled with latent variables. That line of work is pursued further in [30]. The task of predicting a set of items is also considered in [31], who frame it as a problem of maximizing a submodular reward function. A probabilistic model for ranking and top- k classification is proposed by [32], while [33], [34] use metric learning to train a nearest neighbor model. An interesting setting related to top- k classification is learning with positive and unlabeled data [35], [36], where the absence of a label does not imply it is a negative label, and also learning with label noise [37], [38].

Label ranking is closely related to multilabel classification [11], [39], which we consider later in this paper, and to tag ranking [40]. Ranking objectives have been also considered for training convolutional architectures [41], most notably with a loss on triplets [42], [43], that considers both positive and negative examples. Many recent works focus on the top of the ranked list [44]–[48]. However, they are mainly interested in search and retrieval, where the number of relevant documents by far exceeds what users are willing to consider. That setting suggests a different trade-off for recall and precision compared to our setting with only a few relevant labels. This is correspondingly reflected in performance evaluation, as mentioned above.

Consistency and calibration. Classification is a discrete prediction problem where minimizing the expected (0-1) error is known to be computationally hard. Instead, it is common to minimize a *surrogate* loss that leads to efficient learning algorithms. An important question, however, is whether the minimizers of the expected surrogate loss also minimize the expected error. Loss functions which have that property are called *calibrated* or *consistent* with respect to the given discrete loss. Consistency in binary classification is well understood [49]–[51], and significant progress has been made in the analysis of multiclass [52]–[54], multilabel [10], [55], and ranking [56]–[58] methods. In this work,

we investigate calibration of a number of surrogate losses with respect to the top- k error, which generalizes previously established results for multiclass methods.

Optimization. To facilitate experimental evaluation of the proposed loss functions, we also implement the corresponding optimization routines. We choose the stochastic dual coordinate ascent (SDCA) framework of [5] for its ease of implementation, strong convergence guarantees, and the possibility to compute certificates of optimality via the duality gap. While [5] describe the general SDCA algorithm that we implement, their analysis is limited to *scalar* loss functions (both Lipschitz and smooth) with ℓ_2 regularization, which is only suitable for binary problems. A more recent work [8] extends the analysis to *vector valued* smooth (or Lipschitz) functions and general strongly convex regularizers, which is better suited to our multiclass and multilabel loss functions. A detailed comparison of recent coordinate descent algorithms is given in [8], [59].

Following [60] and [8], the main step in the optimization algorithm updates the dual variables by computing a projection or, more generally, the proximal operator [61]. The proximal operators that we consider here can be equivalently expressed as instances of a continuous nonlinear resource allocation problem, which has a long research history, see [62] for a recent survey. Most related to our setting is the Euclidean projection onto the unit simplex or the ℓ_1 -ball in \mathbb{R}^n , which can be computed approximately via bisection in $O(n)$ time [63], or exactly via breakpoint searching [64] and variable fixing [65]. The former can be done in $O(n \log n)$ time with a simple implementation based on sorting, or in $O(n)$ time with an efficient median finding algorithm. In this work, we choose the variable fixing scheme which does not require sorting and is easy to implement. Although its complexity is $O(n^2)$ on pathological inputs with elements growing exponentially [66], the observed complexity in practice is linear and is competitive with breakpoint searching algorithms [65], [66].

While there exist efficient projection algorithms for optimizing the SVM hinge loss and its descendants, the situation is a bit more complicated for logistic regression, both binary and multiclass. There exists no analytical solution for an update with the logistic loss, and [8] suggest a formula in the binary case which computes an approximate update in closed form. Multiclass logistic (softmax) loss is optimized in the SPAMS toolbox [67], which implements FISTA [68]. Alternative optimization methods are considered in [69] who also propose a two-level coordinate descent method in the multiclass case. Different from these works, we propose to follow closely the same variable fixing scheme that is used for SVM training and use the Lambert W function [70] in the resulting entropic proximal map. Our runtime compares favourably with SPAMS, as we show in § 6.2.

Image classification. Multiclass and multilabel image classification are the main applications that we consider in this work to evaluate the proposed loss functions. We employ a relatively simple image recognition pipeline following [71], where feature vectors are extracted from a convolutional neural network (ConvNet), such as the VGGNet [71] or the ResNet [72], and are then used to train a linear classifier with the different loss functions. The ConvNets that we use are pre-trained on the large scale ImageNet [1]

dataset, where there is a large number of object categories (1000), but relatively little variation in scale and location of the central object. For scene recognition, we also use a VGGNet-like architecture [73] that was trained on the Places 205 [2] dataset.

Despite the differences between the benchmarks [74], image representations learned by ConvNets on large datasets have been observed to transfer well [75], [76]. We follow that scheme in single-label experiments, e.g. when recognizing birds [77] and flowers [78] using a network trained on ImageNet, or when transferring knowledge in scene recognition [4], [79]. However, moving on to multi-label classification on Pascal VOC [12] and Microsoft COCO [3], we need to account for increased variation in scale and object placement.

While the earlier works ignore explicit search for object location [80], [81], or require bounding box annotation [82]–[84], recent results indicate that effective classifiers for images with multiple objects in cluttered scenes can be trained from weak image-level annotation by explicitly searching over multiple scales and locations [85]–[89]. Our multilabel setup follows closely the pipeline of [87] with a few exceptions detailed in § 6.3.

3 LOSS FUNCTIONS FOR CLASSIFICATION

When choosing a loss function, one may want to consider several aspects. First, at the basic level, the loss function depends on the available annotation and the performance metric one is interested in, e.g. we distinguish between (single label) multiclass and multilabel losses in this work. Next, there are two fundamental factors that control the *statistical* and the *computational* behavior of learning. For computational reasons, we work with convex surrogate losses rather than with the performance metric directly. In that context, a relevant distinction is between the nonsmooth Lipschitz functions (SVM^{Multi}, top-k SVM) and the smooth functions (LR^{Multi}, SVM_γ^{Multi}, top-k SVM_γ) with strongly convex conjugates that lead to faster convergence rates. From the statistical perspective, it is important to understand if the surrogate loss is classification calibrated as it is an attractive asymptotic property that leads to Bayes consistent classifiers. Finally, one may exploit duality and introduce modifications to the conjugates of existing functions that have desirable effects on the primal loss (top-k Ent).

The rest of this section covers the technical background that is used later in the paper. We discuss our notation, introduce multiclass and multilabel classification, recall the standard approaches to classification, and introduce our recently proposed methods for top- k error minimization.

In § 3.1, we discuss multiclass and multilabel performance evaluation measures that are used later in our experiments. In § 3.2, we review established multiclass approaches and introduce our novel top- k loss functions; we also recall Moreau-Yosida regularization as a smoothing technique and compute convex conjugates for SDCA optimization. In § 3.3, we discuss multilabel classification methods, introduce the smooth multilabel SVM, and compute the corresponding convex conjugates. To enhance readability, we defer all the proofs to the appendix.

Notation. We consider classification problems with a predefined set of m classes. We begin with *multiclass* classification, where every example $x_i \in \mathcal{X}$ has exactly *one* label $y_i \in \mathcal{Y} \triangleq \{1, \dots, m\}$, and later generalize to the *multilabel* setting, where each example is associated with a *set* of labels $Y_i \subset \mathcal{Y}$. In this work, a classifier is a function $f : \mathcal{X} \rightarrow \mathbb{R}^m$ that induces a ranking of class labels via the prediction scores $f(x) = (f_y(x))_{y \in \mathcal{Y}}$. In the linear case, each predictor f_y has the form $f_y(x) = \langle w_y, x \rangle$, where $w_y \in \mathbb{R}^d$ is the parameter to be learned. We stack the individual parameters into a weight matrix $W \in \mathbb{R}^{d \times m}$, so that $f(x) = W^\top x$. While we focus on linear classifiers with $\mathcal{X} \equiv \mathbb{R}^d$ in the exposition below and in most of our experiments, all loss functions are formulated in the general setting where the kernel trick [90] can be employed to construct nonlinear decision surfaces. In fact, we have a number of experiments with the RBF kernel as well.

At test time, prediction depends on the evaluation metric and generally involves sorting / producing the top- k highest scoring class labels in the multiclass setting, and predicting the labels that score above a certain threshold δ in multilabel classification. We come back to performance metrics shortly.

We use π and τ to denote permutations of (indexes) \mathcal{Y} . Unless stated otherwise, a_π reorders components of a vector a in descending order, $a_{\pi_1} \geq a_{\pi_2} \geq \dots \geq a_{\pi_m}$. Therefore, for example, $a_{\pi_1} = \max_j a_j$. If necessary, we make it clear which vector is being sorted by writing $\pi(a)$ to mean $\pi(a) \in \arg \text{sort } a$ and let $\pi_{1:k}(a) \triangleq \{\pi_1(a), \dots, \pi_k(a)\}$. We also use the Iverson bracket defined as $\llbracket P \rrbracket = 1$ if P is true and 0 otherwise; and introduce a shorthand for the conditional probability $p_y(x) \triangleq \Pr(Y = y | X = x)$. Finally, we let $a^{\setminus y}$ be obtained by removing the y -th coordinate from a .

We consider ℓ_2 -regularized objectives in this work, so that if $L : \mathcal{Y} \times \mathbb{R}^m \rightarrow \mathbb{R}_+$ is a multiclass loss and $\lambda > 0$ is a regularization parameter, classifier training amounts to solving $\min_W \frac{1}{n} \sum_{i=1}^n L(y_i, W^\top x_i) + \lambda \|W\|_F^2$. Binary and multilabel classification problems only differ in the loss L .

3.1 Performance Metrics

Here, we briefly review performance evaluation metrics employed in multiclass and multilabel classification.

Multiclass. A standard performance measure for classification problems is the zero-one loss, which simply counts the number of classification mistakes [91], [92]. While that metric is well understood and inspired such popular surrogate losses as the SVM hinge loss, it naturally becomes more stringent as the number of classes increases. An alternative to the standard zero-one error is to allow k guesses instead of one. Formally, the **top- k zero-one loss (top- k error)** is

$$\text{err}_k(y, f(x)) \triangleq \llbracket f_{\pi_k}(x) > f_y(x) \rrbracket. \quad (1)$$

That is, we count a mistake if the ground truth label y scores below k other class labels. Note that for $k = 1$ we recover the standard zero-one error. **Top- k accuracy** is defined as 1 minus the top- k error, and performance on the full test sample is computed as the mean across all test examples.

Multilabel. Several groups of multilabel evaluation metrics are established in the literature and it is generally suggested that multiple contrasting measures should be

reported to avoid skewed results. Here, we give a brief overview of the metrics that we report and refer the interested reader to [11], [39], [55], where multilabel metrics are discussed in more detail.

Ranking based. This group of performance measures compares the ranking of the labels induced by $f_y(x)$ to the ground truth ranking. We report the **rank loss** defined as

$$\text{RLoss}(f) = \frac{1}{n} \sum_{i=1}^n |D_i| / (|Y_i| |\bar{Y}_i|),$$

where $D_i = \{(y, \bar{y}) \mid f_y(x_i) \leq f_{\bar{y}}(x_i), (y, \bar{y}) \in Y_i \times \bar{Y}_i\}$ is the set of reversely ordered pairs, and $\bar{Y}_i \triangleq \mathcal{Y} \setminus Y_i$ is the complement of Y_i . This is the loss that is implicitly optimized by all multiclass / multilabel loss functions that we consider since they induce a penalty when $f_{\bar{y}}(x_i) - f_y(x_i) > 0$.

Ranking class labels for a given image is similar to ranking documents for a user query in information retrieval [14]. While there are many established metrics [93], a popular measure that is relevant to our discussion is **precision-at- k** ($P@k$), which is the fraction of relevant items within the top k retrieved [94], [95]. Although this measure makes perfect sense when $k \ll |Y_i|$, i.e. there are many more relevant documents than we possibly want to examine, it is not very useful when there are only a few correct labels per image – once all the relevant labels are in the top k list, $P@k$ starts to decrease as k increases. A better alternative in our multilabel setting is a complementary measure, **recall-at- k** , defined as

$$\text{R@}k(f) = \frac{1}{n} \sum_{i=1}^n (\pi_{1:k}(f(x_i)) \cap |Y_i|) / |Y_i|,$$

which measures the fraction of relevant labels in the top k list. Note that $\text{R@}k$ is a natural generalization of the top- k error to the multilabel setting and coincides with that multiclass metric whenever Y_i is singleton.

Finally, we report the standard Pascal VOC [12] performance measure, mean average precision (**mAP**), which is computed as the one-vs-all AP averaged over all classes.

Partition based. In contrast to ranking evaluation, partition based measures assess the quality of the actual multilabel prediction which requires a cut-off **threshold** $\delta \in \mathbb{R}$. Several threshold selection strategies have been proposed in the literature: (i) setting a constant threshold prior to experiments [96]; (ii) selecting a threshold *a posteriori* by matching label cardinality [97]; (iii) tuning the threshold on a validation set [55], [98]; (iv) learning a regression function [99]; (v) bypassing threshold selection altogether by introducing a (dummy) calibration label [100]. We have experimented with options (ii) and (iii), as discussed in § 6.3.

Let $h(x) \triangleq \{y \in \mathcal{Y} \mid f_y(x) \geq \delta\}$ be the set of predicted labels for a given threshold δ , and let

$$\begin{aligned} \widehat{\text{TP}}_{i,j} &= \llbracket j \in h(x_i), j \in Y_i \rrbracket, & \widehat{\text{TN}}_{i,j} &= \llbracket j \notin h(x_i), j \notin Y_i \rrbracket, \\ \widehat{\text{FP}}_{i,j} &= \llbracket j \in h(x_i), j \notin Y_i \rrbracket, & \widehat{\text{FN}}_{i,j} &= \llbracket j \notin h(x_i), j \in Y_i \rrbracket, \end{aligned}$$

be a set of $m \cdot n$ primitives defined as in [55]. Now, one can use any performance measure Ψ that is based on the binary confusion matrix, but, depending on where the averaging occurs, the following three groups of metrics are recognized.

Instance-averaging. The binary metrics are computed on the averages over labels and then averaged across examples:

$$\Psi^{\text{inst}}(h) = \frac{1}{n} \sum_{i=1}^n \Psi\left(\frac{1}{m} \sum_{j=1}^m \widehat{\text{TP}}_{i,j}, \dots, \frac{1}{m} \sum_{j=1}^m \widehat{\text{FN}}_{i,j}\right).$$

Macro-averaging. The metrics are averaged across labels:

$$\Psi^{\text{mac}}(h) = \frac{1}{m} \sum_{j=1}^m \Psi\left(\frac{1}{n} \sum_{i=1}^n \widehat{\text{TP}}_{i,j}, \dots, \frac{1}{n} \sum_{i=1}^n \widehat{\text{FN}}_{i,j}\right).$$

Micro-averaging. The metric is applied on the averages over both labels and examples:

$$\Psi^{\text{mic}}(h) = \Psi\left(\frac{1}{mn} \sum_{i,j} \widehat{\text{TP}}_{i,j}, \dots, \frac{1}{mn} \sum_{i,j} \widehat{\text{FN}}_{i,j}\right).$$

Following [11], we consider the **F_1 score** as the binary metric Ψ with all three types of averaging. We also report multilabel **accuracy**, **subset accuracy**, and the **hamming loss** defined respectively as

$$\text{Acc}(h) = \frac{1}{n} \sum_{i=1}^n (|h(x_i) \cap Y_i|) / (|h(x_i) \cup Y_i|),$$

$$\text{SAcc}(h) = \frac{1}{n} \sum_{i=1}^n \llbracket h(x_i) = Y_i \rrbracket,$$

$$\text{HLoss}(h) = \frac{1}{mn} \sum_{i=1}^n |h(x_i) \Delta Y_i|,$$

where Δ is the symmetric set difference.

3.2 Multiclass Methods

In this section, we switch from performance evaluation at test time to how the quality of a classifier is measured during training. In particular, we introduce the loss functions used in established multiclass methods as well as our novel loss functions for optimizing the top- k error (1).

OVA. A multiclass problem is often solved using the one-vs-all (OVA) reduction to m independent binary classification problems. Every class is trained versus the rest which yields m classifiers $\{f_y\}_{y \in \mathcal{Y}}$. Typically, each classifier f_y is trained with a convex margin-based loss function $L(\tilde{y}f_y(x))$, where $L: \mathbb{R} \rightarrow \mathbb{R}_+$, $\tilde{y} = \pm 1$. Simplifying the notation, we consider

$$L(yf(x)) = \max\{0, 1 - yf(x)\}, \quad (\text{SVM}^{\text{OVA}})$$

$$L(yf(x)) = \log(1 + e^{-yf(x)}). \quad (\text{LR}^{\text{OVA}})$$

The hinge (SVM^{OVA}) and logistic (LR^{OVA}) losses correspond to the SVM and logistic regression methods respectively.

Multiclass. An alternative to the OVA scheme above is to use a *multiclass* loss $L: \mathcal{Y} \times \mathbb{R}^m \rightarrow \mathbb{R}_+$ directly. All multiclass losses that we consider only depend on pairwise differences between the ground truth score $f_y(x)$ and all the other scores $f_j(x)$. Loss functions from the SVM family additionally require a *margin* $\Delta(y, j)$, which can be interpreted as a distance in the label space [13] between y and j . To simplify the notation, we use vectors a (for the differences) and c (for the margin) defined for a given (x, y) pair as

$$a_j \triangleq f_j(x) - f_y(x), \quad c_j \triangleq 1 - \llbracket y = j \rrbracket, \quad j = 1, \dots, m.$$

We also write $L(a)$ instead of the full $L(y, f(x))$.

We consider two generalizations of SVM^{OVA} and LR^{OVA} :

$$L(a) = \max_{j \in \mathcal{Y}} \{a_j + c_j\}, \quad (\text{SVM}^{\text{Multi}})$$

$$L(a) = \log\left(\sum_{j \in \mathcal{Y}} \exp(a_j)\right). \quad (\text{LR}^{\text{Multi}})$$

Both the multiclass SVM loss ($\text{SVM}^{\text{Multi}}$) of [101] and the softmax loss (LR^{Multi}) are common in multiclass problems. The latter is particularly popular in deep architectures [71], [102], [103], while $\text{SVM}^{\text{Multi}}$ is also competitive in large-scale image classification [104].

The OVA and multiclass methods were designed with the goal of minimizing the standard zero-one loss. Now,

if we consider the top- k error (1) which does not penalize $(k - 1)$ mistakes, we discover that convexity of the above losses leads to phenomena where $\text{err}_k(y, f(x)) = 0$, but $L(y, f(x)) \gg 0$. That happens, for example, when $f_{\pi_1}(x) \gg f_y(x) \geq f_{\pi_k}(x)$, and creates a bias if we are working with rigid function classes such as linear classifiers. Next, we introduce loss functions that are modifications of the above losses with the goal of alleviating that phenomenon.

Top- k SVM. Recently, we introduced Top- k Multiclass SVM [9], where two modifications of the multiclass hinge loss (SVM^{Multiti}) were proposed. The first version (α) is motivated directly by the top- k error while the second version (β) falls into a general family of ranking losses introduced earlier by Usunier et al. [26]. The two top- k SVM losses are

$$L(a) = \max \left\{ 0, \frac{1}{k} \sum_{j=1}^k (a + c)_{\pi_j} \right\}, \quad (\text{top-}k \text{ SVM}^\alpha)$$

$$L(a) = \frac{1}{k} \sum_{j=1}^k \max \{ 0, (a + c)_{\pi_j} \}, \quad (\text{top-}k \text{ SVM}^\beta)$$

where π reorders the components of $(a + c)$ in descending order. We show in [9] that top- k SVM $^\alpha$ offers a tighter upper bound on the top- k error than top- k SVM $^\beta$. However, both losses perform similarly in our experiments with only a small advantage of top- k SVM $^\beta$ in some settings. Therefore, when the distinction is not important, we simply refer to them as the top- k hinge or the top- k SVM loss. Note that they both reduce to SVM^{Multiti} for $k = 1$.

Top- k SVM losses are not smooth which has implications for their optimization (§ 5) and top- k calibration (§ 4.1). Following [8], who employed Moreau-Yosida regularization [105], [106] to obtain a smoothed version of the binary hinge loss (SVM^{OVA}), we applied the same technique in [6] and introduced smooth top- k SVM.

Moreau-Yosida regularization. We follow [61] and give the main points here for completeness. The Moreau envelope or Moreau-Yosida regularization M_f of the function f is

$$M_f(v) \triangleq \inf_x (f(x) + (1/2) \|x - v\|_2^2).$$

It is a smoothed or regularized form of f with the following nice properties: it is continuously differentiable on \mathbb{R}^d , even if f is not, and the sets of minimizers of f and M_f are the same². To compute a smoothed top- k hinge loss, we use

$$M_f = (f^* + (1/2) \|\cdot\|_2^2)^*,$$

where f^* is the convex conjugate³ of f . A classical result in convex analysis [107] states that a conjugate of a strongly convex function has Lipschitz smooth gradient, therefore, M_f is indeed a smooth function.

Top- k hinge conjugate. Here, we compute the conjugates of the top- k hinge losses α and β . As we show in [9], their effective domains⁴ are given by the **top- k simplex** (α and β respectively) of radius r defined as

$$\Delta_k^\alpha(r) \triangleq \{x \mid \langle \mathbf{1}, x \rangle \leq r, 0 \leq x_i \leq \frac{1}{k} \langle \mathbf{1}, x \rangle, \forall i\}, \quad (2)$$

$$\Delta_k^\beta(r) \triangleq \{x \mid \langle \mathbf{1}, x \rangle \leq r, 0 \leq x_i \leq \frac{1}{k} r, \forall i\}. \quad (3)$$

We let $\Delta_k^\alpha = \Delta_k^\alpha(1)$, $\Delta_k^\beta = \Delta_k^\beta(1)$, and note the relation $\Delta_k^\alpha \subset \Delta_k^\beta \subset \Delta$, where $\Delta = \{x \mid \langle \mathbf{1}, x \rangle \leq 1, x_i \geq 0\}$ is the

2. That does not imply that we get the same classifiers since we are minimizing a regularized sum of individually smoothed loss terms.

3. The **convex conjugate** of f is $f^*(x^*) = \sup_x \{\langle x^*, x \rangle - f(x)\}$.

4. The **effective domain** of f is $\text{dom } f = \{x \in X \mid f(x) < +\infty\}$.

unit simplex and the inclusions are proper for $k > 1$, while for $k = 1$ all three sets coincide.

Proposition 1 ([9]). *The convex conjugate of top- k SVM $^\alpha$ is*

$$L^*(v) = \begin{cases} -\sum_{j \neq y} v_j & \text{if } \langle \mathbf{1}, v \rangle = 0 \text{ and } v^{\setminus y} \in \Delta_k^\alpha, \\ +\infty & \text{otherwise.} \end{cases}$$

The conjugate of top- k SVM $^\beta$ is defined in the same way, but with the set Δ_k^β instead of Δ_k^α .

Note that the conjugates of both top- k SVM losses coincide and are equal to the conjugate of the SVM^{Multiti} loss with the exception of their effective domains, which are Δ_k^α , Δ_k^β , and Δ respectively. As becomes evident in § 5, the effective domain of the conjugate is the feasible set for the dual variables. Therefore, as we move from SVM^{Multiti} to top- k SVM $^\beta$, to top- k SVM $^\alpha$, we introduce more and more constraints on the dual variables thus limiting the extent to which a single training example can influence the classifier.

Smooth top- k SVM. We apply the smoothing technique introduced above to top- k SVM $^\alpha$. Smoothing of top- k SVM $^\beta$ is done similarly, but the set $\Delta_k^\alpha(r)$ is replaced with $\Delta_k^\beta(r)$.

Proposition 2. *Let $\gamma > 0$ be the smoothing parameter. The smooth top- k hinge loss (α) and its conjugate are*

$$L_\gamma(a) = \frac{1}{\gamma} (\langle (a + c)^{\setminus y}, p \rangle - \frac{1}{2} \|p\|^2), \quad (\text{top-}k \text{ SVM}_\gamma^\alpha)$$

$$L_\gamma^*(v) = \begin{cases} \frac{\gamma}{2} \|v^{\setminus y}\|^2 - \langle v^{\setminus y}, c^{\setminus y} \rangle & \text{if } \langle \mathbf{1}, v \rangle = 0, v^{\setminus y} \in \Delta_k^\alpha, \\ +\infty & \text{otherwise,} \end{cases}$$

where $p = \text{proj}_{\Delta_k^\alpha(\gamma)}(a + c)^{\setminus y}$ is the Euclidean projection of $(a + c)^{\setminus y}$ onto $\Delta_k^\alpha(\gamma)$. Moreover, $L_\gamma(a)$ is $1/\gamma$ -smooth.

While there is no analytic formula for the top- k SVM $_\gamma^\alpha$ loss, it can be computed efficiently via the projection onto the top- k simplex [9]. We can also compute its gradient as

$$\nabla L_\gamma(a) = (1/\gamma) (\mathbf{I}_y - e_y \mathbf{1}_y^\top) \text{proj}_{\Delta_k^\alpha(\gamma)}(a + c)^{\setminus y},$$

where \mathbf{I}_y is the identity matrix w/o the y -th column, e_y is the y -th standard basis vector, and $\mathbf{1}_y$ is the $(m - 1)$ -dimensional vector of all ones. This follows from the definition of a , the fact that $L_\gamma(a)$ can be written as $\frac{1}{2\gamma} (\|x\|^2 - \|x - p\|^2)$ for $x = (a + c)^{\setminus y}$ and $p = \text{proj}_{\Delta_k^\alpha(\gamma)}(x)$, and a known result [108] which says that $\nabla_x \frac{1}{2} \|x - \text{proj}_C(x)\|^2 = x - \text{proj}_C(x)$ for any closed convex set C .

Smooth multiclass SVM (SVM $_\gamma^{\text{Multiti}}$). We also highlight an important special case of top- k SVM $_\gamma^\alpha$ that performed remarkably well in our experiments. It is a smoothed version of SVM^{Multiti} and is obtained with $k = 1$ and $\gamma > 0$.

Softmax conjugate. Before we introduce a top- k version of the softmax loss (LR^{Multiti}), we need to recall its conjugate.

Proposition 3. *The convex conjugate of the LR^{Multiti} loss is*

$$L^*(v) = \begin{cases} \sum_{j \neq y} v_j \log v_j + (1 + v_y) \log(1 + v_y), & \text{if } \langle \mathbf{1}, v \rangle = 0 \text{ and } v^{\setminus y} \in \Delta, \\ +\infty & \text{otherwise,} \end{cases} \quad (4)$$

where $\Delta = \{x \mid \langle \mathbf{1}, x \rangle \leq 1, x_j \geq 0\}$ is the unit simplex.

Note that the conjugates of both the SVM^{Multiti} and the LR^{Multiti} losses share the same effective domain, the unit

simplex Δ , and differ only in their functional form: a linear function for SVM^{Multi} and a negative entropy for LR^{Multi}. While we motivated top- k SVM directly from the top- k error, we see that the only change compared to SVM^{Multi} was in the effective domain of the conjugate loss. This suggests a general way to *construct novel losses* with specific properties by taking the conjugate of an existing loss function, and modifying its effective domain in a way that enforces the desired properties. The motivation for doing so comes from the interpretation of the dual variables as forces with which every training example pushes the decision surface in the direction given by the ground truth label. Therefore, by reducing the feasible set we can limit the maximal contribution of any given training example.

Top- k entropy. As hinted above, we first construct the conjugate of the top- k entropy loss (α) by taking the conjugate of LR^{Multi} and replacing Δ in (4) with Δ_k^α , and then take the conjugate again to obtain the primal loss top- k Ent. A β version can be constructed using the set Δ_k^β instead.

Proposition 4. *The top- k entropy loss is defined as*

$$L(a) = \max\{\langle a^{\setminus y}, x \rangle - (1-s) \log(1-s) - \langle x, \log x \rangle \mid x \in \Delta_k^\alpha, \langle \mathbf{1}, x \rangle = s\}. \quad (\text{top-}k \text{ Ent})$$

Moreover, we recover the LR^{Multi} loss when $k = 1$.

While there is no closed-form solution for the top- k Ent loss when $k > 1$, we can compute and optimize it efficiently as we discuss later in § 5.

Truncated top- k entropy. A major limitation of the softmax loss for top- k error optimization is that it cannot ignore the $(k-1)$ highest scoring predictions. This can lead to a situation where the loss is high even though the top- k error is zero. To see that, let us rewrite the LR^{Multi} loss as

$$L(y, f(x)) = \log(1 + \sum_{j \neq y} \exp(f_j(x) - f_y(x))). \quad (5)$$

If there is only a *single* j such that $f_j(x) - f_y(x) \gg 0$, then $L(y, f(x)) \gg 0$ even though $\text{err}_2(y, f(x))$ is zero.

This problem is also present in all top- k hinge losses considered above and is an inherent limitation due to their convexity. The origin of the problem is the fact that ranking based losses [26] are based on functions such as

$$\phi(f(x)) = (1/m) \sum_{j \in \mathcal{Y}} \alpha_j f_{\pi_j}(x) - f_y(x).$$

The function ϕ is convex if the sequence (α_j) is monotonically non-increasing [109]. This implies that convex ranking based losses have to put *more* weight on the highest scoring classifiers, while we would like to put *less* weight on them. To that end, we drop the first $(k-1)$ highest scoring predictions from the sum in (5), sacrificing convexity of the loss, and define the truncated top- k entropy loss as follows

$$L(a) = \log(1 + \sum_{j \in \mathcal{J}_y^k} \exp(a_j)), \quad (\text{top-}k \text{ Ent}_{\text{tr}})$$

where \mathcal{J}_y^k are the indexes corresponding to the $(m-k)$ *smallest* components of $(f_j(x))_{j \neq y}$. This loss can be seen as a smooth version of the top- k error (1), as it is small whenever the top- k error is zero. We show a synthetic experiment in § 6.1, where the advantage of discarding the highest scoring classifier in top- k Ent_{tr} becomes apparent.

3.3 Multilabel Methods

In this section, we introduce natural extensions of the classic multiclass methods discussed above to the setting where there is a *set* of ground truth labels $Y \subset \mathcal{Y}$ for each example x . We focus on the loss functions that produce a ranking of labels and optimize a multilabel loss $L : 2^{\mathcal{Y}} \times \mathbb{R}^m \rightarrow \mathbb{R}_+$. We let $u \triangleq f(x)$ and use a simplified notation $L(u) = L(Y, f(x))$. A more complete overview of multilabel classification methods is given in [11], [39], [110].

Binary relevance (BR). Binary relevance is the standard one-vs-all scheme applied to multilabel classification. It is the default baseline for direct multilabel methods as it does not consider possible correlations between the labels.

Multilabel SVM. We follow the line of work by [7] and consider the Multilabel SVM loss below:

$$\begin{aligned} L(u) &= \max_{y \in Y} \max_{j \in \bar{Y}} \max\{0, 1 + u_j - u_y\} \\ &= \max\{0, 1 + \max_{j \in \bar{Y}} u_j - \min_{y \in Y} u_y\}. \end{aligned} \quad (\text{SVM}^{\text{ML}})$$

This method is also known as the *multiclass multilabel perceptron* (MMP) [100] and the *separation ranking loss* [111]. It can be contrasted with another SVM^{Multi} extension, the RankSVM of Elisseeff and Weston [99], which optimizes the *pairwise ranking loss*:

$$\frac{1}{|Y_i| |\bar{Y}_i|} \sum_{(y,j) \in Y \times \bar{Y}} \max\{0, 1 + u_j - u_y\}.$$

Note that both the SVM^{ML} that we consider and RankSVM avoid expensive enumeration of all the $2^{\mathcal{Y}}$ possible labellings by considering only pairwise label ranking. A principled large margin approach that accounts for all possible label interactions is structured output prediction [13].

Multilabel SVM conjugate. Here, we compute the convex conjugate of the SVM^{ML} loss which is used later to define a Smooth Multilabel SVM. Note that the SVM^{ML} loss depends on the partitioning of \mathcal{Y} into Y and \bar{Y} for every given (x, Y) pair. This is reflected in the definition of a set S_Y below, which is the effective domain of the conjugate:

$$S_Y \triangleq \{x \mid -\sum_{y \in Y} x_y = \sum_{j \in \bar{Y}} x_j \leq 1, x_y \leq 0, x_j \geq 0\}.$$

In the multiclass setting, the set Y is singleton, therefore $x_y = -\sum_{j \in \bar{Y}} x_j$ has no degrees of freedom and we recover the unit simplex Δ over (x_j) , as in (4). In the true multilabel setting, on the other hand, there is freedom to distribute the weight across all the classes in Y .

Proposition 5. *The convex conjugate of the SVM^{ML} loss is*

$$L^*(v) = -\sum_{j \in \bar{Y}} v_j, \text{ if } v \in S_Y, +\infty, \text{ otherwise.} \quad (6)$$

Note that when $|Y| = 1$, (6) naturally reduces to the conjugate of SVM^{Multi} given in Proposition 1 with $k = 1$.

Smooth multilabel SVM. Here, we apply the smoothing technique, which worked very well for multiclass problems [6], [8], to the multilabel SVM^{ML} loss.

As with the smooth top- k SVM, there is no analytic formula for the smoothed loss. However, we can both compute and optimize it within our framework by solving the Euclidean projection problem onto what we call a **bipartite simplex**. It is a convenient modification of the set S_Y above:

$$B(r) \triangleq \{(x, y) \mid \langle \mathbf{1}, x \rangle = \langle \mathbf{1}, y \rangle \leq r, x \in \mathbb{R}_+^m, y \in \mathbb{R}_+^n\}. \quad (7)$$

Proposition 6. Let $\gamma > 0$ be the smoothing parameter. The smooth multilabel SVM loss and its conjugate are

$$L_\gamma(u) = \frac{1}{\gamma} \left(\langle b, p \rangle - \frac{1}{2} \|p\|^2 + \langle \bar{b}, \bar{p} \rangle - \frac{1}{2} \|\bar{p}\|^2 \right), \quad (\text{SVM}_\gamma^{\text{ML}})$$

$$L_\gamma^*(v) = \begin{cases} \frac{1}{2} \left(\sum_{y \in Y} v_y - \sum_{j \in \bar{Y}} v_j \right) + \frac{\gamma}{2} \|v\|^2, & v \in S_Y, \\ +\infty, & \text{o/w,} \end{cases}$$

where $(p, \bar{p}) = \text{proj}_{B(\gamma)}(b, \bar{b})$ is the projection onto $B(\gamma)$ of $b = (\frac{1}{2} - u_y)_{y \in Y}$, $\bar{b} = (\frac{1}{2} + u_j)_{j \in \bar{Y}}$. $L_\gamma(u)$ is $1/\gamma$ -smooth.

Note that the smooth $\text{SVM}_\gamma^{\text{ML}}$ loss is a nice generalization of the smooth multiclass loss $\text{SVM}_\gamma^{\text{Multi}}$ and we naturally recover the latter when Y is singleton. In § 5, we extend the variable fixing algorithm of [65] and obtain an efficient method to compute Euclidean projections onto $B(r)$.

Multilabel cross-entropy. Here, we discuss an extension of the LR^{Multi} loss to multilabel learning. We use the softmax function to model the distribution over the class labels $p_y(x)$, which recovers the well-known multinomial logistic regression [112] and the maximum entropy [69] models.

Assume that all the classes given in the ground truth set Y are equally likely. We define an empirical distribution for a given (x, Y) pair as $\hat{p}_y = (1/|Y|)\mathbb{1}[y \in Y]$, and model the conditional probability $p_y(x)$ via the softmax:

$$p_y(x) = (\exp u_y) / \left(\sum_{j \in Y} \exp u_j \right), \quad \forall y \in Y.$$

The cross-entropy of the distributions \hat{p} and $p(x)$ is given by

$$H(\hat{p}, p(x)) = -\frac{1}{|Y|} \sum_{y \in Y} \log \left(\frac{\exp u_y}{\sum_j \exp u_j} \right),$$

and the corresponding multilabel cross entropy loss is:

$$L(u) = \frac{1}{|Y|} \sum_{y \in Y} \log \left(\sum_{j \in Y} \exp(u_j - u_y) \right). \quad (\text{LR}^{\text{ML}})$$

Multilabel cross-entropy conjugate. Next, we compute the convex conjugate of the LR^{ML} loss, which is used later in our optimization framework.

Proposition 7. The convex conjugate of the LR^{ML} loss is

$$L^*(v) = \begin{cases} \sum_{y \in Y} (v_y + \frac{1}{k}) \log(v_y + \frac{1}{k}) + \sum_{j \in \bar{Y}} v_j \log v_j, & \text{if } v \in D_Y, \\ +\infty & \text{otherwise.} \end{cases} \quad (8)$$

where $k = |Y|$ and D_Y is the effective domain defined as:

$$D_Y \triangleq \left\{ v \mid \sum_{y \in Y} (v_y + \frac{1}{k}) + \sum_{j \in \bar{Y}} v_j = 1, \right. \\ \left. v_y + \frac{1}{k} \geq 0, v_j \geq 0, y \in Y, j \in \bar{Y} \right\}.$$

The conjugates of the multilabel losses SVM^{ML} and LR^{ML} no longer share the same effective domain, which was the case for multiclass losses. However, we still recover the conjugate of the LR^{Multi} loss when Y is singleton.

4 BAYES OPTIMALITY AND TOP-K CALIBRATION

This section is devoted to the theoretical analysis of multiclass losses in terms of their top- k performance. We establish the best top- k error in the Bayes sense, determine when a classifier achieves it, define the notion of top- k calibration, and investigate which loss functions possess this property.

Bayes optimality. Recall that the Bayes optimal zero-one loss in binary classification is simply the probability of the

least likely class [91]. Here, we extend this notion to the top- k error (1) introduced in § 3.1 for multiclass classification and provide a description of top- k Bayes optimal classifier.

Lemma 1. The Bayes optimal top- k error at x is

$$\min_{g \in \mathbb{R}^m} \mathbb{E}_{Y|X} [\text{err}_k(Y, g) \mid X = x] = 1 - \sum_{j=1}^k p_{\tau_j}(x),$$

where $p_{\tau_1}(x) \geq p_{\tau_2}(x) \geq \dots \geq p_{\tau_m}(x)$. A classifier f is **top- k Bayes optimal** at x if and only if

$$\{y \mid f_y(x) \geq f_{\pi_k}(x)\} \subset \{y \mid p_y(x) \geq p_{\tau_k}(x)\},$$

where $f_{\pi_1}(x) \geq f_{\pi_2}(x) \geq \dots \geq f_{\pi_m}(x)$.

Another way to write the optimal top- k error is $\sum_{j=k+1}^m p_{\pi_j}(x)$, which naturally leads to an optimal prediction strategy according to the ranking of $p_y(x)$ in descending order. However, the description of a top- k Bayes optimal classifier reveals that optimality for any given k is better understood as a *partitioning*, rather than ranking, where the labels are split into $\pi_{1:k}$ and the rest, without any preference on the ranking in either subset. If, on the other hand, we want a classifier that is top- k Bayes optimal for all $k \geq 1$ simultaneously, a proper ranking according to $p_y(x)$ is both necessary and sufficient.

Top- k calibration. Optimization of the zero-one loss and the top- k error leads to hard combinatorial problems. Instead of tackling a combinatorial problem directly, an alternative is to use a convex surrogate loss which upper bounds the discrete error. Under mild conditions on the loss function [49], [52], an optimal classifier for the surrogate yields a Bayes optimal solution for the zero-one loss. Such loss functions are called *classification calibrated*, which is known in statistical learning theory as a necessary condition for a classifier to be universally Bayes consistent [49]. We introduce now the notion of calibration for the top- k error.

Definition 1. A multiclass loss function $L : \mathcal{Y} \times \mathbb{R}^m \rightarrow \mathbb{R}_+$ is called **top- k calibrated** if for all possible data generating measures on $\mathcal{X} \times \mathcal{Y}$ and all $x \in \mathcal{X}$

$$\arg \min_{g \in \mathbb{R}^m} \mathbb{E}_{Y|X} [L(Y, g) \mid X = x] \\ \subseteq \arg \min_{g \in \mathbb{R}^m} \mathbb{E}_{Y|X} [\text{err}_k(Y, g) \mid X = x].$$

If a loss is *not* top- k calibrated, it implies that even in the limit of infinite data, one does not obtain a classifier with the Bayes optimal top- k error from Lemma 1. It is thus an important property, even though of an asymptotic nature. Next, we analyse which of the multiclass classification methods covered in § 3.2 are top- k calibrated.

4.1 Multiclass Top- k Calibration

In this section, we consider top- k calibration of the standard OVA scheme, established multiclass classification methods, and the proposed top- k Ent_{tr} loss. First, we state a condition under which an OVA scheme is uniformly top- k calibrated, not only for $k = 1$, which corresponds to the standard zero-one loss, but for all $k \geq 1$ simultaneously. The condition is given in terms of the Bayes optimal classifier for each of the corresponding binary problems and with respect to a given loss function L , e.g. the hinge or logistic losses.

Lemma 2. *The OVA reduction is top- k calibrated for any $1 \leq k \leq m$ if the Bayes optimal function of a convex margin-based loss L is a strictly monotonically increasing function of $p_y(x) = \Pr(Y = y | X = x)$ for every class $y \in \mathcal{Y}$.*

Proof. Let the Bayes optimal classifier for the binary problem corresponding to a $y \in \mathcal{Y}$ have the form

$$f_y(x) = g(\Pr(Y = y | X = x)),$$

where g is a strictly monotonically increasing function. The ranking of f_y corresponds to the ranking of $p_y(x)$ and hence the OVA reduction is top- k calibrated for any $k \geq 1$. \square

Next, we use Lemma 2 and the corresponding Bayes optimal classifiers to check if the one-vs-all schemes employing hinge and logistic regression losses are top- k calibrated.

Proposition 8. *OVA SVM is not top- k calibrated.*

Proposition 9. *OVA logistic regression is top- k calibrated.*

The hinge loss is not calibrated since the corresponding binary classifiers, being piecewise constant, are subject to degenerate cases that result in arbitrary rankings of classes. Surprisingly, the smoothing technique based on Moreau-Yosida regularization (§ 3.2) makes a smoothed loss more attractive not only from the optimization side, but also in terms of top- k calibration. Here, we show that a smooth binary hinge loss from [8] fulfills the conditions of Lemma 2 and leads to a top- k calibrated OVA scheme.

Proposition 10. *OVA smooth SVM is top- k calibrated.*

An alternative to the OVA scheme with binary losses is to use a *multiclass* loss $L : \mathcal{Y} \times \mathbb{R}^m \rightarrow \mathbb{R}_+$ directly. First, we consider the multiclass hinge loss SVM^{Multi}, which is known to be *not* calibrated for the top-1 error [52], and show that it is not top- k calibrated for any k .

Proposition 11. *Multiclass SVM is not top- k calibrated.*

Tewari and Bartlett [52] provide a general framework to study classification calibration that is applicable to a large family of multiclass methods. However, their characterization of calibration is derived in terms of the properties of the convex hull of $\{(L(1, f), \dots, L(m, f)) | f \in \mathcal{F}\}$, which might be difficult to verify in practice. In contrast, our proofs of Propositions 11 and 12 are straightforward and based on direct derivation of the corresponding Bayes optimal classifiers for the SVM^{Multi} and the LR^{Multi} losses respectively.

Proposition 12. *Multiclass softmax loss is top- k calibrated.*

The implicit reason for top- k calibration of the OVA schemes and the softmax loss is that one can estimate the probabilities $p_y(x)$ from the Bayes optimal classifier. Loss functions which allow this are called *proper*. We refer to [113] and references therein for a detailed discussion.

We have established that the OVA logistic regression and the softmax loss are top- k calibrated for any k , so why should we be interested in defining new loss functions for the top- k error? The reason is that calibration is an asymptotic property since the Bayes optimal functions are obtained by *pointwise* minimization of $\mathbb{E}_{Y|X}[L(Y, f(x)) | X = x]$ at every $x \in \mathcal{X}$. The picture changes if we use linear classifiers, since they obviously cannot be minimized independently at

each point. Indeed, the Bayes optimal classifiers, in general, cannot be realized by linear functions.

Furthermore, convexity of the softmax and multiclass hinge losses leads to phenomena where $\text{err}_k(y, f(x)) = 0$, but $L(y, f(x)) \gg 0$. We discussed this issue § 3.2 and motivated modifications of the above losses for the top- k error. Next, we show that one of the proposed top- k losses is also top- k calibrated.

Proposition 13. *The truncated top- k entropy loss is top- s calibrated for any $k \leq s \leq m$.*

Top- k calibration of the remaining top- k losses is an open problem, which is complicated by the absence of a closed-form expression for most of them.

5 OPTIMIZATION FRAMEWORK

This section is mainly devoted to efficient optimization of the multiclass and multilabel methods from § 3 within the stochastic dual coordinate ascent (SDCA) framework of Shalev-Shwartz and Zhang [5]. The core reason for efficiency of the optimization scheme is the ability to formulate variable updates in terms of projections onto the effective domain of the conjugate loss, which, in turn, can be solved in time $O(m \log m)$ or faster. These projections fall into a broad area of nonlinear resource allocation [62], where we already have a large selection of specialized algorithms. For example, we use an algorithm of Kiwiel [65] for SVM^{Multi} and top- k SVM ^{β} , and contribute analogous algorithms for the remaining losses. In particular, we propose an entropic projection algorithm based on the Lambert W function for the LR^{Multi} loss, and a variable fixing algorithm for projecting onto the bipartite simplex (7) for the SVM^{ML}. We also discuss how the proposed loss functions that do not have a closed-form expression can be evaluated efficiently, and perform a runtime comparison against FISTA [68] using the SPAMS optimization toolbox [67].

In § 5.1, we state the primal and Fenchel dual optimization problems, and introduce the Lambert W function. In § 5.2, we consider SDCA update steps and loss computation for multiclass methods, as well as present our runtime evaluation experiments. In § 5.3, we cover multilabel optimization and present our algorithm for the Euclidean projection onto the bipartite simplex.

5.1 Technical Background

We briefly recall the main facts about the SDCA framework [5], Fenchel duality [108], and the Lambert W function [70].

The primal and dual problems. Let $X \in \mathbb{R}^{d \times n}$ be the matrix of training examples $x_i \in \mathbb{R}^d$, $K = X^T X$ the corresponding Gram matrix, $W \in \mathbb{R}^{d \times m}$ the matrix of primal variables, $A \in \mathbb{R}^{m \times n}$ the matrix of dual variables, and $\lambda > 0$ the regularization parameter. The primal and Fenchel dual [108] objective functions are given as

$$\begin{aligned} P(W) &= +\frac{1}{n} \sum_{i=1}^n L(y_i, W^T x_i) + \frac{\lambda}{2} \text{tr}(W^T W), \\ D(A) &= -\frac{1}{n} \sum_{i=1}^n L^*(y_i, -\lambda n a_i) - \frac{\lambda}{2} \text{tr}(AKA^T), \end{aligned} \quad (9)$$

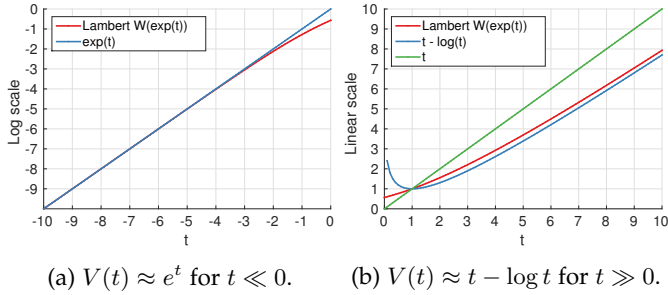


Fig. 2: Behavior of the Lambert W function of the exponent ($V(t) = W(e^t)$). **(a)** Log scale plot with $t \in (-10, 0)$. **(b)** Linear scale plot with $t \in (0, 10)$.

where L^* is the convex conjugate of L and y_i is interpreted as a set Y_i if L is a multilabel loss.

SDCA proceeds by sampling a dual variable $a_i \in \mathbb{R}^m$, which corresponds to a training example $x_i \in \mathbb{R}^d$, and modifying it to achieve maximal increase in the dual objective $D(A)$ while keeping other dual variables fixed. Several sampling strategies can be used, e.g. [114], but we use a simple scheme where the set of indexes is randomly shuffled before every epoch and then all a_i 's are updated sequentially. The algorithm terminates when the relative duality gap $(P(W) - D(A))/P(W)$ falls below a pre-defined $\varepsilon > 0$, or the computational budget is exhausted, in which case we still have an estimate of suboptimality via the duality gap.

Since the algorithm operates entirely on the dual variables and the prediction scores $f(x_i)$, it is directly applicable to training both linear $f(x_i) = W^\top x_i$ as well as nonlinear $f(x_i) = AK_i$ classifiers (K_i being the i -th column of the Gram matrix K). When $d \ll n$, which is often the case in our experiments, and we are training a linear classifier, then it is less expensive to maintain the primal variables $W = XA^\top$ [9] and compute the dot products $W^\top x_i$ in \mathbb{R}^d . In that case, whenever a_i is updated, we perform a rank-1 update of W .

It turns out that every update step $\max_{a_i} D(A)$ is equivalent to the proximal operator⁵ of a certain function, which can be seen as a projection onto the effective domain of L^* .

Lambert W function. The Lambert W function is defined as the inverse of the mapping $w \mapsto we^w$. It is widely used in many fields of computer science [70], [115], [116], and can often be recognized in nonlinear equations involving the exp and the log functions. Taking logarithms on both sides of the defining equation $z = We^W$, we get $\log z = W(z) + \log W(z)$. Therefore, if we are given an equation of the form $x + \log x = t$ for some $t \in \mathbb{R}$, we can directly “solve” it in closed-form as $x = W(e^t)$. The crux of the problem is that the function $V(t) \triangleq W(e^t)$ is transcendental [115] just like the logarithm and the exponent. There exist highly optimized implementations for the latter and we argue that the same can be done for the Lambert W function. In fact, there is already some work on this topic [115], [116], which we also employ in our implementation.

To develop intuition about the function $V(t) = W(e^t)$, which is the Lambert W function of the exponent, we look at how it behaves for different values of t . An illustration is

5. The **proximal operator**, or the **proximal map**, of a function f is defined as $\text{prox}_f(v) = \arg \min_x (f(x) + \frac{1}{2} \|x - v\|^2)$.

provided in Figure 2. One can see directly from the equation $x + \log x = t$ that the behavior of $x = V(t)$ changes dramatically depending on whether t is a large positive or a large negative number. In the first case, the linear part dominates the logarithm and the function is approximately linear; a better approximation is $x(t) \approx t - \log t$, when $t \gg 1$. In the second case, the function behaves like an exponent e^t . To see this, we write $x = e^t e^{-x}$ and note that $e^{-x} \approx 1$ when $t \ll 0$, therefore, $x(t) \approx e^t$, if $t \ll 0$.

To compute $V(t)$, we use these approximations as initial points in a 5-th order Householder method [117]. A *single* iteration of that method is already sufficient to get full float precision and at most two iterations are needed for double, which makes the function $V(t)$ an attractive tool for computing entropic projections.

5.2 Multiclass Methods

In this section, we cover optimization of the multiclass methods from § 3.2 within the SDCA framework. We discuss how to efficiently compute the smoothed losses that were introduced via conjugation and do not have a closed-form expression. Finally, we evaluate SDCA convergence in terms of runtime and show that smoothing with Moreau-Yosida regularization leads to significant improvements in speed.

As mentioned in § 5.1 above, the core of the SDCA algorithm is the update step $a_i \leftarrow \arg \max_{a_i} D(A)$. Even the primal objective $P(W)$ is only computed for the duality gap and could conceivably be omitted if the certificate of optimality is not required. Next, we focus on how the updates are computed for the different multiclass methods.

SDCA update: SVM^{OVA}, LR^{OVA}. SDCA updates for the binary hinge and logistic losses are covered in [118] and [8]. We highlight that the SVM^{OVA} update has a closed-form expression that leads to scalable training of linear SVMs [118], and is implemented in LibLinear [119].

SDCA update: SVM^{Multi}, LR^{Multi}, SVM^{Multi} _{γ} . Although SVM^{Multi} is also covered in [8], they use a different algorithm based on sorting, while we do a case distinction [9]. First, we solve an easier continuous quadratic knapsack problem using a variable fixing algorithm of Kiwiel [65] which does not require sorting. This corresponds to enforcing the equality constraint in the simplex and generally already gives the optimal solution. The computation is also fast: we observe linear time complexity in practice, as shown in Figure 3a. For the remaining hard cases, however, we fall back to sorting and use a scheme similar to [8]. In our experience, performing the case distinction seemed to offer significant time savings.

For the SVM^{Multi} and SVM^{Multi} _{γ} , we note that they are special cases of top- k SVM ^{α} _{γ} and top- k SVM ^{β} _{γ} with $k = 1$, as well as LR^{Multi} is a special case of top- k Ent.

SDCA update: top- k SVM ^{α/β} , top- k SVM ^{α/β} _{γ} . Here, we consider the update step for the smooth top- k SVM ^{α} _{γ} loss. The nonsmooth version is directly recovered by setting $\gamma = 0$, while the update for top- k SVM ^{β} _{γ} is derived similarly using the set Δ_k^β in (10) instead of Δ_k^α .

We show that performing the update step is equivalent to projecting a certain vector b , computed from the prediction scores $f(x_i) = W^\top x_i$, onto the effective domain of L^* , the top- k simplex, with an added regularization $\rho \langle \mathbf{1}, x \rangle^2$, which biases the solution to be orthogonal to $\mathbf{1}$.

Proposition 14. Let L and L^* in (9) be respectively the top- k SVM $_{\gamma}^{\alpha}$ loss and its conjugate as in Proposition 2. The dual variables a_i corresponding to (x_i, y_i) are updated as:

$$\begin{cases} a_i^{y_i} = -\arg \min_{x \in \Delta_k^{\alpha}(1/(\lambda n))} \{ \|x - b\|^2 + \rho \langle \mathbf{1}, x \rangle^2 \}, \\ a_{y_i, i} = -\sum_{j \neq y_i} a_{j, i}, \end{cases} \quad (10)$$

where $b = \frac{1}{\langle x_i, x_i \rangle + \gamma \lambda n} (q^{y_i} + (1 - q_{y_i}) \mathbf{1})$,
 $q = W^{\top} x_i - \langle x_i, x_i \rangle a_i$, and $\rho = \frac{\langle x_i, x_i \rangle}{\langle x_i, x_i \rangle + \gamma \lambda n}$.

We solve (10) using the algorithm for computing a (biased) projection onto the top- k simplex, which we introduced in [9], with a minor modification of b and ρ . Similarly, the update step for the top- k SVM $_{\gamma}^{\beta}$ loss is solved using a (biased) continuous quadratic knapsack problem, which we discuss in the supplement of [9].

Smooth top- k hinge losses converge significantly faster than their nonsmooth variants as we show in the scaling experiments below. This can be explained by the theoretical results of [8] on the convergence rate of SDCA. They also had similar observations for the smoothed binary hinge loss.

SDCA update: top- k Ent. Finally, we derive an optimization problem for the proposed top- k entropy loss.

Proposition 15. Let L in (9) be the top- k Ent loss and L^* be its convex conjugate as in (4) with Δ replaced by Δ_k^{α} . The dual variables a_i corresponding to (x_i, y_i) are updated as:

$$\begin{cases} a_i^{y_i} = -\frac{1}{\lambda n} \arg \min_{x \in \Delta_k^{\alpha}} \left\{ \frac{\alpha}{2} (\langle x, x \rangle + s^2) - \langle b, x \rangle + \langle x, \log x \rangle \right. \\ \left. + (1 - s) \log(1 - s) \mid s = \langle \mathbf{1}, x \rangle \right\}, \\ a_{y_i, i} = -\sum_{j \neq y_i} a_{j, i}, \end{cases} \quad (11)$$

where $\alpha = \frac{\langle x_i, x_i \rangle}{\lambda n}$, $b = q^{y_i} - q_{y_i} \mathbf{1}$, $q = W^{\top} x_i - \langle x_i, x_i \rangle a_i$.

Problems (10) and (11) have similar structure, but the latter is considerably more difficult to solve due to the presence of logarithms. We propose to tackle this problem using the function $V(t)$ introduced in § 5.1 above.

Our algorithm is an instance of the variable fixing scheme with the following steps: (i) partition the variables into disjoint sets and compute an auxiliary variable t from the optimality conditions; (ii) compute the values of the variables using t and verify them against a set of constraints (e.g. an upper bound in the top- k simplex); (iii) if there are no violated constraints, we have computed the solution, and otherwise examine the next partitioning.

As we discuss in [9], there can be at most k partitionings that we need to consider for Δ_k^{α} and Δ_k^{β} . To see this, let $x \in \Delta_k^{\alpha}$ be a feasible point for (11), and define the subsets

$$U \triangleq \{j \mid x_j = \frac{s}{k}\}, \quad M \triangleq \{j \mid x_j < \frac{s}{k}\}. \quad (12)$$

Clearly, $|U| \leq k$ must hold, and $|U| = k$ we consider as a degenerate fall back case. Therefore, we are primarily interested in the k partitions when $0 \leq |U| < k$. Due to monotonicity in the optimality conditions, one can show that U always corresponds to the largest elements b_j of the vector being projected. Hence, we start with an empty U and add indexes of the largest b_j 's until the solution is found.

Next, we show how to actually compute t and x , given a candidate partition into U and M .

Proposition 16. Let x^* be the solution of (11) and let the sets U and M be defined for the given x^* as in (12), then

$$x_j^* = \min \left\{ \frac{1}{\alpha} V(b_j - t), \frac{s}{k} \right\}, \quad \forall j,$$

and the variables s, t satisfy the nonlinear system

$$\begin{cases} \alpha(1 - \rho)s - \sum_{j \in M} V(b_j - t) = 0, \\ (1 - \rho)t + V^{-1}(\alpha(1 - s)) - \rho V^{-1}(\frac{\alpha s}{k}) + A - \alpha = 0, \end{cases} \quad (13)$$

where $\rho \triangleq \frac{|U|}{k}$, $A \triangleq \frac{1}{k} \sum_{j \in U} b_j$, V^{-1} is the inverse of V .

Moreover, if U is empty, then $x_j^* = \frac{1}{\alpha} V(b_j - t)$ for all j , and t can be found from

$$V(\alpha - t) + \sum_j V(b_j - t) = \alpha. \quad (14)$$

We solve (13) using the Newton's method [120], while for the Eq. (14) we use a 4-th order Householder's method [117] with a faster convergence rate. The latter is particularly attractive, since the set U can always be assumed empty for $k = 1$, i.e. for the LR^{Multi} loss, and is often also empty for the general top- k Ent loss. As both methods require the derivatives of $V(t)$, we note that $\partial_t V(t) = V(t)/(1 + V(t))$ [70], which means that the derivatives come at no additional cost. Finally, we note that $V^{-1}(v) = v + \log v$ by definition.

Loss computation: SVM $_{\gamma}^{\text{Multi}}$, top- k SVM $_{\gamma}^{\alpha/\beta}$. Here, we discuss how to evaluate smoothed losses that do not have a closed-form expression for the primal loss. Recall that the smooth top- k SVM $_{\gamma}^{\alpha}$ loss is given by

$$L_{\gamma}(a) = \frac{1}{\gamma} (\langle (a + c)^y, p \rangle - \frac{1}{2} \|p\|^2),$$

where $a_j = f_j(x) - f_y(x)$, $c_j = 1 - \mathbb{I}[y = j]$ for all $j \in \mathcal{Y}$, and $p = \text{proj}_{\Delta_k^{\alpha}(\gamma)}(a + c)^y$ is the Euclidean projection of $(a + c)^y$ onto $\Delta_k^{\alpha}(\gamma)$. We describe an $O(m \log m)$ algorithm to compute the projection p in [9]. For the special case $k = 1$, i.e. the SVM $_{\gamma}^{\text{Multi}}$ loss, the algorithm is particularly efficient and exhibits essentially linear scaling in practice. Moreover, since we only need the dot products with p in $L_{\gamma}(a)$, we exploit its special structure, $p = \min\{\max\{l, b - t\}, u\}$ with $b = (a + c)^y$, and avoid explicit computation of p . The same procedure is done for the top- k SVM $_{\gamma}^{\beta}$ loss.

Loss computation: top- k Ent. Next, we discuss how to evaluate the top- k Ent loss that was defined via the conjugate of the softmax loss as

$$\max_{x \in \Delta_k^{\alpha}, s = \langle \mathbf{1}, x \rangle} \left\{ \langle a^y, x \rangle - (1 - s) \log(1 - s) - \langle x, \log x \rangle \right\}. \quad (15)$$

Note that (15) is similar to (11) and we use a similar variable fixing scheme, as described above. However, this problem is much easier: the auxiliary variables s and t are computed directly without having to solve a nonlinear system, and their computation does not involve the $V(t)$ function.

Proposition 17. Let x^* be the solution of (15) and let the sets U and M be defined for the given x^* as in (12), then

$$x_j^* = \min \left\{ \exp(a_j - t), \frac{s}{k} \right\}, \quad \forall j,$$

and the variables s, t are computed from

$$\begin{cases} s = 1/(1 + Q), \\ t = \log Z + \log(1 + Q) - \log(1 - \rho), \end{cases} \quad (16)$$

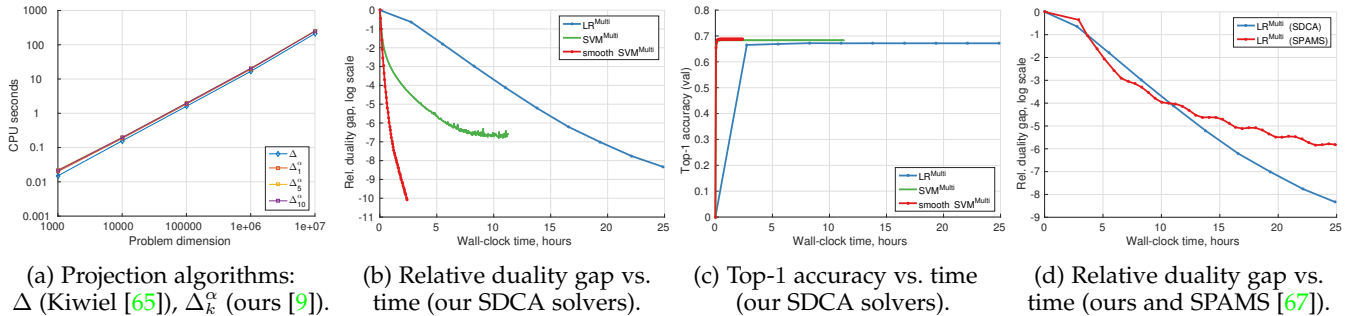


Fig. 3: (a) Scaling of the projection algorithms used in SDCA optimization. (b-c) SDCA convergence of the LR^{Multi} , $\text{SVM}^{\text{Multi}}$, and smooth $\text{SVM}_\gamma^{\text{Multi}}$ methods on the ImageNet 2012 dataset. (d) SDCA vs. FISTA as implemented in the SPAMS toolbox.

where $\rho \triangleq \frac{|U|}{k}$, $A \triangleq \frac{1}{k} \sum_{j \in U} a_j$, $Z \triangleq \sum_{j \in M} \exp a_j$, and

$$Q \triangleq (1 - \rho)^{(1-\rho)} / (k^\rho Z^{(1-\rho)} \exp A).$$

The top- k Ent loss is then computed as

$$L(a) = (A + (1 - \rho)t - \rho \log(\frac{s}{k}))s - (1 - s) \log(1 - s).$$

Moreover, if U is empty, then $x_j^* = \exp(a_j - t)$ for all j , and we recover the softmax loss LR^{Multi} as

$$L(a) = t = \log(1 + Z) = \log(1 + \sum_j \exp a_j).$$

As before, we only need to examine at most k partitions U , adding the next maximal a_j to U until there are no violated constraints. Therefore, the overall complexity of the procedure to compute the top- k Ent loss is $O(km)$.

The efficiency of the outlined approach for optimizing the top- k Ent loss crucially depends on fast computation of $V(t)$ in the SDCA update. Our implementation was able to scale to large datasets as we show next.

Runtime evaluation. First, we highlight the efficiency of our algorithm from [9] for computing the Euclidean projection onto the top- k simplex, which is used, in particular, for optimization of the $\text{SVM}_\gamma^{\text{Multi}}$ loss. The scaling plot is given in Figure 3a and shows results of an experiment following [63]. We sample 1000 points from the normal distribution $\mathcal{N}(0, 1)$ and solve the projection problems using the algorithm of Kiwiel [65] (denoted as Δ) and using our method of projecting onto the set Δ_k^α for different values of $k = 1, 5, 10$. We report the total CPU time taken on a single Intel(R) Xeon(R) E5-2680 2.70GHz processor. As was also observed by [65], we see that the scaling is essentially linear in the problem dimension and makes the method applicable to problems with a large number of classes.

Next in Figure 3, we compare the wall-clock training time of $\text{SVM}^{\text{Multi}}$ with a smoothed $\text{SVM}_\gamma^{\text{Multi}}$ and the LR^{Multi} objectives. We plot the relative duality gap (3b) and the validation accuracy (3c) versus time for the best performing models on the ImageNet 2012 benchmark. We obtain substantial improvement of the convergence rate for the smooth $\text{SVM}_\gamma^{\text{Multi}}$ compared to the nonsmooth baseline. Moreover, we see that the top-1 accuracy saturates after a few passes over the training data, which justifies the use of a fairly loose stopping criterion (we use $\varepsilon = 10^{-3}$). For the LR^{Multi} loss, the cost of each epoch is significantly higher compared to $\text{SVM}^{\text{Multi}}$, which is due to the difficulty of solving (11). This suggests that the smooth top-1 $\text{SVM}_\gamma^{\text{Multi}}$ loss can offer competitive performance (see § 6) at a lower training cost.

Finally, we also compare our implementation of LR^{Multi} (marked SDCA in 3d) with the SPAMS optimization toolbox [67], which provides an efficient implementation of FISTA [68]. We note that the rate of convergence of SDCA is competitive with FISTA for $\epsilon \geq 10^{-4}$ and is noticeably better for $\epsilon < 10^{-4}$. We conclude that our approach for training the LR^{Multi} model is competitive with the state-of-the-art, and faster computation of $V(t)$ can lead to a further speedup.

5.3 Multilabel Methods

This section covers optimization of the multilabel objectives introduced in § 3.3. First, we reduce computation of the SDCA update step and evaluation of the smoothed loss $\text{SVM}_\gamma^{\text{ML}}$ to the problem of computing the Euclidean projection onto what we called the bipartite simplex $B(r)$, see Eq. (7). Next, we contribute a novel variable fixing algorithm for computing that projection. Finally, we discuss SDCA optimization of the multilabel cross-entropy loss LR^{ML} .

SDCA update: SVM^{ML} , $\text{SVM}_\gamma^{\text{ML}}$. Here, we discuss optimization of the smoothed $\text{SVM}_\gamma^{\text{ML}}$ loss. The update step for the nonsmooth counterpart is recovered by setting $\gamma = 0$.

Proposition 18. Let L and L^* in (9) be respectively the $\text{SVM}_\gamma^{\text{ML}}$ loss and its conjugate as in Proposition 6. The dual variables $a \triangleq a_i$ corresponding to the training pair (x_i, Y_i) are updated as $(a_y)_{y \in Y_i} = p$ and $(a_j)_{j \in \bar{Y}_i} = -\bar{p}$, where

$$(p, \bar{p}) = \text{proj}_{B(1/\lambda n)}(b, \bar{b}),$$

$b = \rho(\frac{1}{2} - q_y)_{y \in Y_i}$, $\bar{b} = \rho(\frac{1}{2} + q_j)_{j \in \bar{Y}_i}$, $q = W^\top x_i - \langle x_i, x_i \rangle a_i$, and $\rho = \frac{1}{\langle x_i, x_i \rangle + \gamma \lambda n}$.

Let us make two remarks regarding optimization of the multilabel SVM. First, we see that the update step involves exactly the same projection that was used in Proposition 6 to define the smoothed $\text{SVM}_\gamma^{\text{ML}}$ loss, with the difference in the vectors being projected and the radius of the bipartite simplex. Therefore, we can use the same projection algorithm both during optimization as well as when computing the loss. And second, even though SVM^{ML} reduces to $\text{SVM}^{\text{Multi}}$ when Y_i is singleton, the derivation of the smoothed loss and the projection algorithm proposed below for the bipartite simplex are substantially different from what we proposed in the multiclass setting. Most notably, the treatment of the dimensions in Y_i and \bar{Y}_i is now symmetric.

Loss computation: SVM $_{\gamma}^{\text{ML}}$. The smooth multilabel SVM loss SVM $_{\gamma}^{\text{ML}}$ is given by

$$L_{\gamma}(u) = \frac{1}{\gamma} (\langle b, p \rangle - \frac{1}{2} \|p\|^2 + \langle \bar{b}, \bar{p} \rangle - \frac{1}{2} \|\bar{p}\|^2),$$

where $b = (\frac{1}{2} - u_y)_{y \in Y}$, $\bar{b} = (\frac{1}{2} + u_j)_{j \in \bar{Y}}$, $u = f(x)$, and $(p, \bar{p}) = \text{proj}_{B(\gamma)}(b, \bar{b})$. Below, we propose an efficient variable fixing algorithm to compute the Euclidean projection onto $B(\gamma)$. We also note that we can use the same trick that we used for top-k SVM $_{\gamma}^{\alpha}$ and exploit the special form of the projection to avoid explicit computation of p and \bar{p} .

Euclidean projection onto the bipartite simplex $B(\rho)$. The optimization problem that we seek to solve is:

$$(p, \bar{p}) = \arg \min_{x \in \mathbb{R}_+^m, y \in \mathbb{R}_+^n} \frac{1}{2} \|x - b\|^2 + \frac{1}{2} \|y - \bar{b}\|^2 \quad (17)$$

$$\langle \mathbf{1}, x \rangle = \langle \mathbf{1}, y \rangle \leq \rho.$$

This problem has been considered by Shalev-Shwartz and Singer [60], who proposed a breakpoint searching algorithm based on sorting, as well as by Liu and Ye [63], who formulated it as a root finding problem that is solved via bisection. Next, we contribute a novel variable fixing algorithm that is inspired by the algorithm of Kiwiel [65] for the continuous quadratic knapsack problem (a.k.a. projection onto simplex).

1) *Initialization.* Define the sets $I_x = \{1, \dots, m\}$, $L_x = \{\}$, $I_y = \{1, \dots, n\}$, $L_y = \{\}$, and solve the independent subproblems below using the algorithm of [65].

$$p = \arg \min_{x \in \mathbb{R}_+^m} \left\{ \frac{1}{2} \|x - b\|^2 \mid \langle \mathbf{1}, x \rangle = \rho \right\},$$

$$\bar{p} = \arg \min_{y \in \mathbb{R}_+^n} \left\{ \frac{1}{2} \|y - \bar{b}\|^2 \mid \langle \mathbf{1}, y \rangle = \rho \right\}.$$

Let t' and s' be the resulting optimal thresholds, such that $p = \max\{0, b - t'\}$ and $\bar{p} = \max\{0, \bar{b} - s'\}$. If $t' + s' \geq 0$, then (p, \bar{p}) is the solution to (17); stop.

2) *Restricted subproblem.* Compute t as

$$t = (\sum_{I_x} b_j - \sum_{I_y} \bar{b}_j) / (|I_x| + |I_y|),$$

and let $x_j(t) = b_j - t$, $y_j(t) = \bar{b}_j + t$.

3) *Feasibility check.* Compute

$$\Delta_x = \sum_{I_x^L} (b_j - t), \text{ where } I_x^L = \{j \in I_x \mid x_j(t) \leq 0\},$$

$$\Delta_y = \sum_{I_y^L} (\bar{b}_j + t), \text{ where } I_y^L = \{j \in I_y \mid y_j(t) \leq 0\}.$$

4) *Stopping criterion.* If $\Delta_x = \Delta_y$, then the solution to (17) is given by $p = \max\{0, b - t\}$ and $\bar{p} = \max\{0, \bar{b} + t\}$; stop.

5) *Variable fixing.* If $\Delta_x > \Delta_y$, update $I_x \leftarrow I_x \setminus I_x^L$, $L_x \leftarrow L_x \cup I_x^L$. If $\Delta_x < \Delta_y$, update $I_y \leftarrow I_y \setminus I_y^L$, $L_y \leftarrow L_y \cup I_y^L$. Go to step 2.

Proposition 19. *The algorithm above solves (17).*

The proposed algorithm is easy to implement, does not require sorting, and scales well in practice, as demonstrated by our experiments on VOC 2007 and MS COCO.

Runtime evaluation. We also compare the runtime of the proposed variable fixing algorithm and the sorting based algorithm of [60]. We perform no comparison to [63] as their code is not available. Furthermore, the algorithms that we consider are exact, while the method of [63] is approximate and its runtime is dependent on the required precision. The experimental setup is the same as in § 5.2 above, and our results are reported in Table 2.

Dimension d	10^3	10^4	10^5	10^6	10^7
Sorting based [60]	0.07	0.56	6.92	85.56	1364.94
Variable fixing (ours)	0.02	0.15	1.48	16.46	169.81
Improvement factor	3.07	3.79	4.69	5.20	8.04

TABLE 2: Runtime (in seconds) for solving 1000 projection problems onto $B(\rho)$ with $\rho = 10$ and $m = n = d/2$, see Eq. (17). The data is generated i.i.d. from $\mathcal{N}(0, 1)$.

We observe consistent improvement in runtime over the sorting based implementation, and we use our algorithm to train SVM $_{\gamma}^{\text{ML}}$ in further experiments.

SDCA update: LR $^{\text{ML}}$. Finally, we discuss optimization of the multilabel cross-entropy loss LR $^{\text{ML}}$. We show that the corresponding SDCA update step is equivalent to a certain entropic projection problem, which we propose to tackle using the $V(t)$ function introduced above.

Proposition 20. *Let L and L^* in (9) be respectively the LR $^{\text{ML}}$ loss and its conjugate from Proposition 7. The dual variables $a \triangleq a_i$ corresponding to the training pair (x_i, Y_i) are updated as $(a_y)_{y \in Y_i} = -\frac{1}{\lambda n} (p - \frac{1}{k})$ and $(a_j)_{j \in \bar{Y}_i} = -\frac{1}{\lambda n} \bar{p}$, where*

$$(p, \bar{p}) = \arg \min_{x \geq 0, y \geq 0} \frac{\alpha}{2} \|x - b\|^2 + \langle x, \log x \rangle + \frac{\alpha}{2} \|y - \bar{b}\|^2 + \langle y, \log y \rangle, \quad (18)$$

$$\text{s.t. } \langle \mathbf{1}, x \rangle + \langle \mathbf{1}, y \rangle = 1,$$

$k = |Y_i|$, $\alpha = \frac{\langle x_i, x_i \rangle}{\lambda n}$, $b = (\frac{1}{\alpha} q_j + \frac{1}{k})_{j \in Y_i}$, $\bar{b} = (\frac{1}{\alpha} q_j)_{j \in \bar{Y}_i}$, and $q = W^T x_i - \langle x_i, x_i \rangle a_i$.

Moreover, the solution of (18) is given by

$$p_j = \frac{1}{\alpha} V(\alpha b_j - t), \quad \forall j, \quad \bar{p}_j = \frac{1}{\alpha} V(\alpha \bar{b}_j - t), \quad \forall j,$$

where t is computed from

$$\sum_{j \in Y_i} V(q_j + \frac{\alpha}{k} - t) + \sum_{j \in \bar{Y}_i} V(q_j - t) = \alpha. \quad (19)$$

We use a 4-th order Householder's method [117] to solve (19), similar to the top-k Ent loss above. Solving the nonlinear equation in t is the main computational challenge when updating the dual variables. However, as this procedure does not require iteration over the index partitions, it is generally faster than optimization of the top-k Ent loss.

6 EXPERIMENTS

This section provides a broad array of experiments on 24 different datasets comparing multiclass and multilabel performance of the 13 loss functions from § 3. We look at different aspects of empirical evaluation: performance on synthetic and real data, use of handcrafted features and the features extracted from a ConvNet, targeting a specific performance measure and being generally competitive over a range of metrics.

In § 6.1, we show on synthetic data that the top-k Ent $_{\text{tr}}$ loss targeting specifically the top-2 error outperforms all competing methods by a large margin. In § 6.2, we focus on evaluating top- k performance of multiclass methods on 11 real-world benchmark datasets including ImageNet and Places. In § 6.3, we cover multilabel classification in two groups of experiments: (i) a comparative study following [11] on 10 popular multilabel datasets; (ii) image classification on Pascal VOC and MS COCO in a novel setting contrasting multiclass, top- k , and multilabel methods.

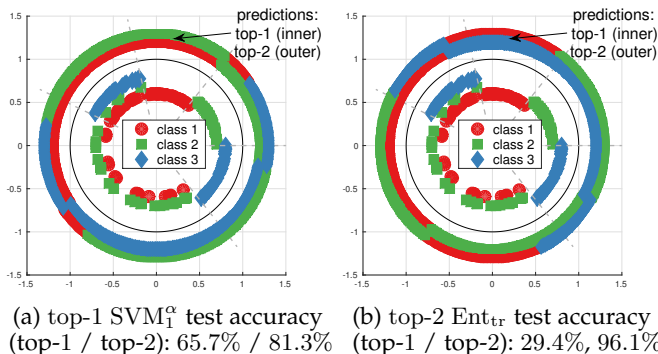


Fig. 4: Synthetic data in \mathbb{R}^2 (color markers inside of the black circle) and visualization of top-1 and top-2 predictions (resp. outside of the circle). (a) top-1 SVM₁^α optimizes the top-1 error which increases its top-2 error. (b) top-2 Ent_{tr} ignores top-1 mistakes and optimizes directly the top-2 error.

6.1 Synthetic Example

In this section, we demonstrate in a synthetic experiment that our proposed top-2 losses outperform the top-1 losses when the aim is optimal top-2 performance. The dataset with three classes is shown in the inner circle of Figure 4.

Sampling scheme. First, we generate samples in $[0, 7] \subset \mathbb{R}$ which is subdivided into 5 segments. All segments have unit length, except for the 4-th segment which has length 3. We sample in each of the 5 segments according to the following distribution: $(0, 1, .4, .3, 0)$ for class 1; $(1, 0, .1, .7, 0)$ for class 2; $(0, 0, .5, 0, 1)$ for class 3. Finally, the data is rescaled to $[0, 1]$ and mapped onto the unit circle.

Samples of different classes are plotted next to each other for better visibility as there is significant class overlap. We visualize top-1/2 predictions with two colored circles outside of the black circle. We sample 200/200/200K points for training/validation/test and tune $C = 1/(\lambda n)$ in the range 2^{-18} to 2^{18} . Results are shown in Table 3.

Circle (synthetic)					
Method	Top-1	Top-2	Method	Top-1	Top-2
SVM ^{OVA}	54.3	85.8	top-1 SVM ₁	65.7	83.9
LR ^{OVA}	54.7	81.7	top-2 SVM _{0/1}	54.4 / 54.5	87.1 / 87.0
SVM ^{Multi}	58.9	89.3	top-2 Ent	54.6	87.6
LR ^{Multi}	54.7	81.7	top-2 Ent _{tr}	58.4	96.1

TABLE 3: Top- k accuracy (%) on synthetic data. **Left:** Baseline methods. **Right:** Top- k SVM (nonsmooth / smooth) and top- k softmax losses (convex and nonconvex).

In each column, we provide the results for the model (as determined by the hyperparameter C) that optimizes the corresponding top- k accuracy. First, we note that all top-1 baselines perform similar in top-1 performance, except for SVM^{Multi} and top-1 SVM₁ which show better results. Next, we see that our top-2 losses improve the top-2 accuracy and the improvement is most significant for the nonconvex top-2 Ent_{tr} loss, which is close to the optimal solution for this dataset. This is because top-2 Ent_{tr} provides a tight bound on the top-2 error and ignores the top-1 errors in the loss. Unfortunately, similar significant improvements are not observed on the real-world datasets that we tried. This

might be due to the high dimension of the feature spaces, which yields well separable problems.

6.2 Multiclass Experiments

The goal of this section is to provide an extensive empirical evaluation of the loss functions from § 3.2 in terms of top- k performance. To that end, we compare multiclass and top- k methods on 11 datasets ranging in size (500 to 2.4M training examples, 10 to 1000 classes), problem domain (vision, non-vision), and granularity (scene, object, and fine-grained classification). The detailed statistics is given in Table 4.

Dataset	m	n	d	Dataset	m	n	d
ALOI [121]	1K	54K	128	Indoor 67 [79]	67	5354	4K
Caltech 101 Sil [32]	101	4100	784	Letter [122]	26	10.5K	16
CUB [77]	202	5994	4K	News 20 [123]	20	15.9K	16K
Flowers [78]	102	2040	4K	Places 205 [2]	205	2.4M	4K
FMD [124]	10	500	4K	SUN 397 [4]	397	19.9K	4K
ImageNet 2012 [1]	1K	1.3M	4K				

TABLE 4: Statistics of multiclass classification benchmarks (m : # classes, n : # training examples, d : # features).

Please refer to Table 1 for an overview of the methods and our naming convention. Further comparison with other established ranking based losses can be found in [9].

Solvers. We use LibLinear [119] for the one-vs-all baselines SVM^{OVA} and LR^{OVA}; and our code from [9] for top- k SVM_γ and the top- k Ent losses. The multiclass baselines SVM^{Multi} and LR^{Multi} correspond respectively to top-1 SVM and top-1 Ent. For the nonconvex top- k Ent_{tr}, we use the LR^{Multi} solution as an initial point and perform gradient descent with line search [120]. We cross-validate hyper-parameters in the range 10^{-5} to 10^3 , extending it when the optimal value is at the boundary.

Features. For ALOI, Letter, and News20 datasets, we use the features provided by the LibSVM [125] datasets. For ALOI, we randomly split the data into equally sized training and test sets preserving class distributions. The Letter dataset comes with a separate validation set, which we use for model selection only. For News20, we use PCA to reduce dimensionality of sparse features from 62060 to 15478 preserving all non-singular PCA components⁶.

For Caltech101 Silhouettes, we use the features and the train/val/test splits provided by [32].

For CUB, Flowers, FMD, and ImageNet 2012, we use MatConvNet [126] to extract the outputs of the last fully connected layer of the VGGNet-16 model [71].

For Indoor 67, SUN 397, and Places 205, we perform the same feature extraction, but use the VGGNet-16 model of [73] which was pre-trained on Places 205.

Discussion. The results are given in Table 5, and we can make several interesting observations. First, while the OVA schemes perform quite similar to the multiclass approaches (OVA logistic regression vs. softmax, OVA SVM vs. multiclass SVM), which confirms earlier observations in [104], [130], the OVA schemes performed worse on ALOI and Letter. Thus, we generally recommend the multiclass losses instead of the OVA schemes.

6. Our SDCA-based solvers are designed for dense inputs.

	ALOI				Letter				News 20				Caltech 101 Silhouettes			
Reference:	Top-1: 93 ± 1.2 [121]				Top-1: 97.98 [122] (RBF)				Top-1: 86.9 [127]				62.1	79.6	83.4	[32]
Method	Top-1	Top-3	Top-5	Top-10	Top-1	Top-3	Top-5	Top-10	Top-1	Top-3	Top-5	Top-10	Top-1	Top-3	Top-5	Top-10
SVM ^{OVA}	82.4	89.5	91.5	93.7	63.0	82.0	88.1	94.6	84.3	95.4	97.9	99.5	61.8	76.5	80.8	86.6
LR ^{OVA}	86.1	93.0	94.8	96.6	68.1	86.1	90.6	96.2	84.9	96.3	97.8	99.3	63.2	80.4	84.4	89.4
SVM ^{Multi}	90.0	95.1	96.7	98.1	76.5	89.2	93.1	97.7	85.4	94.9	97.2	99.1	62.8	77.8	82.0	86.9
LR ^{Multi}	89.8	95.7	97.1	98.4	75.3	90.3	94.3	98.0	84.5	96.4	98.1	99.5	63.2	81.2	85.1	89.7
top-3 SVM	89.2	95.5	97.2	98.4	74.0	91.0	94.4	97.8	85.1	96.6	98.2	99.3	63.4	79.7	83.6	88.3
top-5 SVM	87.3	95.6	97.4	98.6	70.8	91.5	95.1	98.4	84.3	96.7	98.4	99.3	63.3	80.0	84.3	88.7
top-10 SVM	85.0	95.5	97.3	98.7	61.6	88.9	96.0	99.6	82.7	96.5	98.4	99.3	63.0	80.5	84.6	89.1
top-1 SVM ₁	90.6	95.5	96.7	98.2	76.8	89.9	93.6	97.6	85.6	96.3	98.0	99.3	63.9	80.3	84.0	89.0
top-3 SVM ₁	89.6	95.7	97.3	98.4	74.1	90.9	94.5	97.9	85.1	96.6	98.4	99.4	63.3	80.1	84.0	89.2
top-5 SVM ₁	87.6	95.7	97.5	98.6	70.8	91.5	95.2	98.6	84.5	96.7	98.4	99.4	63.3	80.5	84.5	89.1
top-10 SVM ₁	85.2	95.6	97.4	98.7	61.7	89.1	95.9	99.7	82.9	96.5	98.4	99.5	63.1	80.5	84.8	89.1
top-3 Ent	89.0	95.8	97.2	98.4	73.0	90.8	94.9	98.5	84.7	96.6	98.3	99.4	63.3	81.1	85.0	89.9
top-5 Ent	87.9	95.8	97.2	98.4	69.7	90.9	95.1	98.8	84.3	96.8	98.6	99.4	63.2	80.9	85.2	89.9
top-10 Ent	86.0	95.6	97.3	98.5	65.0	89.7	96.2	99.6	82.7	96.4	98.5	99.4	62.5	80.8	85.4	90.1
top-3 Ent _{tr}	89.3	95.9	97.3	98.5	63.6	91.1	95.6	98.8	83.4	96.4	98.3	99.4	60.7	81.1	85.2	90.2
top-5 Ent _{tr}	87.9	95.7	97.3	98.6	50.3	87.7	96.1	99.4	83.2	96.0	98.2	99.4	58.3	79.8	85.2	90.2
top-10 Ent _{tr}	85.2	94.8	97.1	98.5	46.5	80.9	93.7	99.6	82.9	95.7	97.9	99.4	51.9	78.4	84.6	90.2
	Indoor 67				CUB				Flowers				FMD			
Reference (Top-1):	82.0 [73]				62.8 [128] / 76.37 [129]				86.8 [76]				77.4 [128] / 82.4 [128]			
Method	Top-1	Top-3	Top-5	Top-10	Top-1	Top-3	Top-5	Top-10	Top-1	Top-3	Top-5	Top-10	Top-1	Top-3	Top-5	Top-10
SVM ^{OVA}	81.9	94.3	96.5	98.0	60.6	77.1	83.4	89.9	82.0	91.7	94.3	96.8	77.4	92.4	96.4	
LR ^{OVA}	82.0	94.9	97.2	98.7	62.3	80.5	87.4	93.5	82.6	92.2	94.8	97.6	79.6	94.2	98.2	
SVM ^{Multi}	82.5	95.4	97.3	99.1	61.0	79.2	85.7	92.3	82.5	92.2	94.8	96.4	77.6	93.8	97.2	
LR ^{Multi}	82.4	95.2	98.0	99.1	62.3	81.7	87.9	93.9	82.9	92.4	95.1	97.8	79.0	94.6	97.8	
top-3 SVM	81.6	95.1	97.7	99.0	61.3	80.4	86.3	92.5	81.9	92.2	95.0	96.1	78.8	94.6	97.8	
top-5 SVM	79.9	95.0	97.7	99.0	60.9	81.2	87.2	92.9	81.7	92.4	95.1	97.8	78.4	94.4	97.6	
top-10 SVM	78.4	95.1	97.4	99.0	59.6	81.3	87.7	93.4	80.5	91.9	95.1	97.7				
top-1 SVM ₁	82.6	95.2	97.6	99.0	61.9	80.2	86.9	93.1	83.0	92.4	95.1	97.6	78.6	93.8	98.0	
top-3 SVM ₁	81.6	95.1	97.8	99.0	61.9	81.1	86.6	93.2	82.5	92.3	95.2	97.7	79.0	94.4	98.0	
top-5 SVM ₁	80.4	95.1	97.8	99.1	61.3	81.3	87.4	92.9	82.0	92.5	95.1	97.8	79.4	94.4	97.6	
top-10 SVM ₁	78.3	95.1	97.5	99.0	59.8	81.4	87.8	93.4	80.6	91.9	95.1	97.7				
top-3 Ent	81.4	95.4	97.6	99.2	62.5	81.8	87.9	93.9	82.5	92.0	95.3	97.8	79.8	94.8	98.0	
top-5 Ent	80.3	95.0	97.7	99.0	62.0	81.9	88.1	93.8	82.1	92.2	95.1	97.9	79.4	94.4	98.0	
top-10 Ent	79.2	95.1	97.6	99.0	61.2	81.6	88.2	93.8	80.9	92.1	95.0	97.7				
top-3 Ent _{tr}	79.8	95.0	97.5	99.1	62.0	81.4	87.6	93.4	82.1	92.2	95.2	97.6	78.4	95.4	98.2	
top-5 Ent _{tr}	76.4	94.3	97.3	99.0	61.4	81.2	87.7	93.7	81.4	92.0	95.0	97.7	77.2	94.0	97.8	
top-10 Ent _{tr}	72.6	92.8	97.1	98.9	59.7	80.7	87.2	93.4	77.9	91.1	94.3	97.3				
	SUN 397 (10 splits)				Places 205 (val)				ImageNet 2012 (val)							
Reference:	Top-1: 66.9 [73]				60.6				88.5 [73]				76.3	93.2	[71]	
Method	Top-1	Top-3	Top-5	Top-10	Top-1	Top-3	Top-5	Top-10	Top-1	Top-3	Top-5	Top-10	Top-1	Top-3	Top-5	Top-10
SVM ^{Multi}	65.8 ± 0.1	85.1 ± 0.2	90.8 ± 0.1	95.3 ± 0.1	58.4	78.7	84.7	89.9	68.3	82.9	87.0	91.1				
LR ^{Multi}	67.5 ± 0.1	87.7 ± 0.2	92.9 ± 0.1	96.8 ± 0.1	59.0	80.6	87.6	94.3	67.2	83.2	87.7	92.2				
top-3 SVM	66.5 ± 0.2	86.5 ± 0.1	91.8 ± 0.1	95.9 ± 0.1	58.6	80.3	87.3	93.3	68.2	84.0	88.1	92.1				
top-5 SVM	66.3 ± 0.2	87.0 ± 0.2	92.2 ± 0.2	96.3 ± 0.1	58.4	80.5	87.4	94.0	67.8	84.1	88.2	92.4				
top-10 SVM	64.8 ± 0.3	87.2 ± 0.2	92.6 ± 0.1	96.6 ± 0.1	58.0	80.4	87.4	94.3	67.0	83.8	88.3	92.6				
top-1 SVM ₁	67.4 ± 0.2	86.8 ± 0.1	92.0 ± 0.1	96.1 ± 0.1	59.2	80.5	87.3	93.8	68.7	83.9	88.0	92.1				
top-3 SVM ₁	67.0 ± 0.2	87.0 ± 0.1	92.2 ± 0.1	96.2 ± 0.0	58.9	80.5	87.6	93.9	68.2	84.1	88.2	92.3				
top-5 SVM ₁	66.5 ± 0.2	87.2 ± 0.1	92.4 ± 0.2	96.3 ± 0.0	58.5	80.5	87.5	94.1	67.9	84.1	88.4	92.5				
top-10 SVM ₁	64.9 ± 0.3	87.3 ± 0.2	92.6 ± 0.2	96.6 ± 0.1	58.0	80.4	87.5	94.3	67.1	83.8	88.3	92.6				
top-3 Ent	67.2 ± 0.2	87.7 ± 0.2	92.9 ± 0.1	96.8 ± 0.1	58.7	80.6	87.6	94.2	66.8	83.1	87.8	92.2				
top-5 Ent	66.6 ± 0.3	87.7 ± 0.2	92.9 ± 0.1	96.8 ± 0.1	58.1	80.4	87.4	94.2	66.5	83.0	87.7	92.2				
top-10 Ent	65.2 ± 0.3	87.4 ± 0.1	92.8 ± 0.1	96.8 ± 0.1	57.0	80.0	87.2	94.1	65.8	82.8	87.6	92.1				

TABLE 5: Top- k accuracy (%) on various datasets. The first line is a reference performance on each dataset and reports top-1 accuracy except when the numbers are aligned with Top- k . We compare the one-vs-all and multiclass baselines with the top- k SVM ^{α} [9] as well as the proposed smooth top- k SVM ^{α} , top- k Ent, and the nonconvex top- k Ent_{tr}.

Comparing the softmax loss and multiclass SVM, we see that there is no clear winner in top-1 performance, but softmax consistently outperforms multiclass SVM in top- k performance for $k > 1$. This might be due to the strong property of softmax being top- k calibrated for all k . Note that this trend is uniform across all datasets, in particular, also for the ones where the features are not coming from a ConvNet. Both the smooth top- k SVM and the top- k entropy losses perform slightly better than softmax if one compares specific top- k errors. However, the good performance of the truncated top- k entropy loss on synthetic data did not transfer to the real world datasets.

Places 205 (val)				
Method	Top-1	Top-3	Top-5	Top-10
LR ^{Multi}	59.97	81.39	88.17	94.59
top-3 SVM ₁ (FT)	60.73	82.09	88.58	94.56
top-5 SVM ₁ (FT)	60.88	82.18	88.78	94.75
top-3 Ent _{tr} (FT)	60.51	81.86	88.69	94.78
top-5 Ent _{tr} (FT)	60.48	81.66	88.66	94.80
LR ^{Multi} (FT)	60.73	82.07	88.71	94.82

ImageNet 2012 (val)				
Method	Top-1	Top-3	Top-5	Top-10
LR ^{Multi}	68.60	84.29	88.66	92.83
top-3 SVM ₁ (FT)	71.66	86.63	90.55	94.17
top-5 SVM ₁ (FT)	71.60	86.67	90.56	94.23
top-3 Ent _{tr} (FT)	71.41	86.80	90.77	94.35
top-5 Ent _{tr} (FT)	71.20	86.57	90.75	94.38
LR ^{Multi} (FT)	72.11	87.08	90.88	94.38

TABLE 6: Top- k accuracy (%), as reported by Caffe [131], on large scale datasets after fine-tuning (FT) for approximately one epoch on Places and 3 epochs on ImageNet. The first line (LR^{Multi}) is the reference performance w/o fine-tuning.

Fine-tuning experiments. We also performed a number of fine-tuning experiments where the original network was trained further for 1-3 epochs with the smooth top- k hinge and the truncated top- k entropy losses⁷. The motivation was to see if the full end-to-end training would be more beneficial compared to training just the classifier. Results are reported in Table 6. We should note that the setting is now slightly different: there is no feature extraction step with the MatConvNet and there is a non-regularized bias term in Caffe [131]. We see that the top- k specific losses are able to improve the performance compared to the reference model, and that, on Places 205, the smooth top-5 SVM₁ loss achieves the best top-1..5 performance. However, in this set of experiments, we also observed similar improvements when fine-tuning with the standard softmax loss, which achieves the best performance on ImageNet 2012. Further training beyond 3 epochs did not change the results significantly.

Conclusion. We see that a safe choice for multiclass problems seems to be the LR^{Multi} loss as it yields reasonably good results in all top- k errors. A competitive alternative is the smooth SVM _{γ} ^{Multi} loss which can be faster to train (see runtime experiments in § 5.2). If one wants to optimize directly for a top- k error (at the cost of a higher top-1 error),

7. Code: <https://github.com/mlapin/caffe/tree/topk>

emotions							
Method	RLoss	HLoss	Acc	SAcc	F ₁ ^{mic}	F ₁ ^{mac}	F ₁ ^{inst}
RF-PCT [11]	0.151	0.189	51.9	30.7	67.2	65.0	61.1
HOMER [11]	0.297	0.361	47.1	16.3	58.8	57.0	61.4
BR [11] (RBF)	0.246	0.257	36.1	12.9	50.9	44.0	46.9
LR ^{ML}	0.186	0.239	53.6	22.8	66.9	66.6	64.0
SVM ^{ML}	0.217	0.238	50.4	23.3	63.4	65.2	63.9
SVM _{γ} ^{ML}	0.178	0.230	54.0	23.3	67.3	66.7	65.5
LR ^{ML} (RBF)	0.225	0.266	47.2	19.3	61.1	62.0	58.4
SVM ^{ML} (RBF)	0.186	0.224	53.0	21.3	65.5	64.3	64.1
SVM _{γ} ^{ML} (RBF)	0.187	0.224	49.3	21.3	65.5	64.2	61.1

TABLE 9: Continuation of Table 7.

then further improvements are possible using either the smooth top- k SVM or the top- k entropy losses.

6.3 Multilabel Experiments

The aim of this section is threefold. First, we establish competitive performance of our multilabel classification methods from § 3.3 comparing them to the top 3 methods from an extensive experimental study by Madjarov et al. [11] on 10 multilabel benchmark datasets of varying scale and complexity. Next, we discuss an interesting learning setting when top- k classification methods emerge as a transition step between multiclass and multilabel approaches. Finally, we evaluate multiclass, top- k , and multilabel classification methods on Pascal VOC 2007 [12] and the more challenging Microsoft COCO [3] image classification benchmarks.

Dataset	m	n	d	l_c	Dataset	m	n	d	l_c
bibtex [134]	159	5K	2K	2.40	enron [135]	53	1K	1K	3.38
bookmarks [134]	208	60K	2K	2.03	mediamill [136]	101	31K	120	4.38
corel5k [137]	374	4.5K	499	3.52	medical [97]	45	645	1.5K	1.25
delicious [133]	983	13K	500	19.02	scene [138]	6	1.2K	294	1.07
emotions [139]	6	391	72	1.87	yeast [99]	14	1.5K	103	4.24
VOC 2007 [12]	20	5K	2K	1.46	MS COCO [3]	80	83K	2K	2.91

TABLE 8: Statistics of multilabel benchmarks (m : # classes, n : # training examples, d : # features, l_c : label cardinality).

Multilabel classification. Here, we seek to establish a solid baseline to evaluate our implementation of the multilabel SVM^{ML}, smooth SVM _{γ} ^{ML}, and the LR^{ML} methods. To that end, we follow the work of Madjarov et al. [11] who provide a clear description of the evaluation protocol and an extensive experimental comparison of 12 multilabel classification methods on 11 datasets reporting 16 performance metrics. We limit our comparison to the 3 best performing methods from their study, namely the random forest of predicting clustering trees [132], the hierarchy of multilabel classifiers [133], and the binary relevance method using SVM^{OVA}. We report results on 10 datasets as there was an issue with the published train/test splits on the remaining benchmark⁸. The datasets vary greatly in size and **label cardinality** (the average number of labels per example), as can be seen from the basic statistics in Table 8. Further details about each of the datasets can be found in [11].

We follow closely the evaluation protocol of [11] except for the selection of the cut-off threshold δ (see § 3.1 for

8. See <https://github.com/tsoumakas/mulan/issues/4> for details.

bibtex									bookmarks						corel5k								
Method	RLoss	HLoss	Acc	SAcc	F ₁ ^{mic}	F ₁ ^{mac}	F ₁ ^{inst}		RLoss	HLoss	Acc	SAcc	F ₁ ^{mic}	F ₁ ^{mac}	F ₁ ^{inst}		RLoss	HLoss	Acc	SAcc	F ₁ ^{mic}	F ₁ ^{mac}	F ₁ ^{inst}
RF-PCT [11]	0.093	0.013	16.6	9.8	23.0	5.5	21.2		0.104	0.009	20.4	18.9	23.6	10.1	21.3		0.117	0.009	0.9	0.0	1.8	0.4	1.4
HOMER [11]	0.255	0.014	33.0	16.5	42.9	26.6	42.6		-	-	-	-	-	-	-		0.352	0.012	17.9	0.2	27.5	3.6	28.0
BR [11] (RBF)	0.068	0.012	34.8	19.4	45.7	30.7	43.3		-	-	-	-	-	-	-		0.117	0.017	3.0	0.0	5.9	2.1	4.7
LR ^{ML}	0.053	0.013	30.9	14.2	42.5	35.0	38.8		0.079	0.009	22.5	16.5	29.5	21.7	27.0		0.101	0.009	17.5	0.0	27.1	6.4	27.3
SVM ^{ML}	0.094	0.013	28.6	13.2	40.6	31.5	36.1		0.140	0.009	24.0	19.8	27.5	18.4	26.7		0.205	0.009	9.9	0.8	18.5	5.0	17.5
SVM _γ ^{ML}	0.073	0.013	31.4	16.2	43.5	33.5	39.3		0.091	0.009	28.0	20.7	34.0	22.6	32.4		0.174	0.009	18.8	1.0	29.4	5.9	26.3
LR ^{ML} (RBF)	0.054	0.013	33.8	14.6	45.4	31.8	42.0		0.072	0.009	25.1	19.7	33.1	24.6	29.0		0.101	0.009	18.0	1.0	28.5	6.0	27.8
SVM ^{ML} (RBF)	0.067	0.013	36.2	19.0	46.5	37.1	44.6		0.103	0.009	30.3	22.9	35.8	26.0	34.9		0.107	0.009	18.1	1.8	28.8	6.7	27.2
SVM _γ ^{ML} (RBF)	0.067	0.012	36.6	18.4	46.5	37.2	44.6		0.079	0.008	31.8	23.0	38.0	28.0	36.7		0.105	0.009	19.3	1.8	30.2	6.8	28.8
delicious									enron						mediamill								
Method	RLoss	HLoss	Acc	SAcc	F ₁ ^{mic}	F ₁ ^{mac}	F ₁ ^{inst}		RLoss	HLoss	Acc	SAcc	F ₁ ^{mic}	F ₁ ^{mac}	F ₁ ^{inst}		RLoss	HLoss	Acc	SAcc	F ₁ ^{mic}	F ₁ ^{mac}	F ₁ ^{inst}
RF-PCT [11]	0.106	0.018	14.6	0.7	24.8	8.3	24.4		0.079	0.046	41.6	13.1	53.7	12.2	55.2		0.047	0.029	44.1	12.2	56.3	11.2	58.9
HOMER [11]	0.379	0.022	20.7	0.1	33.9	10.3	34.3		0.183	0.051	47.8	14.5	59.1	16.7	61.3		0.177	0.038	41.3	5.3	55.3	7.3	57.9
BR [11] (RBF)	0.114	0.018	13.6	0.4	23.4	9.6	23.0		0.084	0.045	44.6	14.9	56.4	14.3	58.2		0.061	0.032	40.3	8.0	53.3	5.6	55.7
LR ^{ML}	0.123	0.019	11.6	0.3	21.4	10.9	19.5		0.074	0.055	38.5	7.8	53.0	21.9	50.4		0.042	0.033	41.2	7.8	54.8	17.1	54.4
SVM ^{ML}	0.184	0.019	6.9	0.2	11.1	6.6	12.2		0.136	0.055	38.9	10.5	50.3	21.6	50.9		0.102	0.034	35.6	7.9	47.2	16.5	49.2
SVM _γ ^{ML}	0.163	0.019	14.9	0.3	27.1	12.1	23.6		0.095	0.050	42.8	10.5	56.2	23.2	54.9		0.058	0.032	41.8	8.4	56.1	17.7	54.7
LR ^{ML} (RBF)	0.096	0.019	22.1	1.5	37.2	12.4	34.5		0.070	0.047	46.3	13.0	58.4	20.3	57.9		0.042	0.033	42.0	10.0	56.2	21.8	53.3
SVM ^{ML} (RBF)	0.137	0.018	17.8	1.7	32.4	16.7	26.4		0.090	0.047	46.6	15.0	58.1	26.8	58.4		0.072	0.031	43.3	11.8	57.6	25.9	55.3
SVM _γ ^{ML} (RBF)	0.099	0.018	23.1	1.6	39.0	18.2	35.7		0.076	0.047	48.6	16.1	59.5	26.9	59.9		0.046	0.029	46.6	13.3	61.0	27.1	58.7
medical									scene						yeast								
Method	RLoss	HLoss	Acc	SAcc	F ₁ ^{mic}	F ₁ ^{mac}	F ₁ ^{inst}		RLoss	HLoss	Acc	SAcc	F ₁ ^{mic}	F ₁ ^{mac}	F ₁ ^{inst}		RLoss	HLoss	Acc	SAcc	F ₁ ^{mic}	F ₁ ^{mac}	F ₁ ^{inst}
RF-PCT [11]	0.024	0.014	59.1	53.8	69.3	20.7	61.6		0.072	0.094	54.1	51.8	66.9	65.8	55.3		0.167	0.197	47.8	15.2	61.7	32.2	61.4
HOMER [11]	0.090	0.012	71.3	61.0	77.3	28.2	76.1		0.119	0.082	71.7	66.1	76.4	76.8	74.5		0.205	0.207	55.9	21.3	67.3	44.7	68.7
BR [11] (RBF)	0.021	0.077	20.6	0.0	34.3	36.1	32.8		0.060	0.079	68.9	63.9	76.1	76.5	71.4		0.164	0.190	52.0	19.0	65.2	39.2	65.0
LR ^{ML}	0.024	0.013	68.7	56.9	76.2	35.1	75.2		0.081	0.120	58.3	39.4	67.2	68.4	66.3		0.352	0.264	36.0	8.4	48.3	44.4	48.0
SVM ^{ML}	0.026	0.013	72.9	62.8	78.4	34.8	77.5		0.082	0.114	60.7	46.0	68.7	69.5	67.7		0.424	0.280	31.3	5.8	46.7	42.9	45.6
SVM _γ ^{ML}	0.023	0.012	73.1	60.2	78.7	36.7	77.4		0.081	0.114	60.4	44.1	68.7	69.5	67.6		0.366	0.261	35.6	9.5	46.6	44.7	47.3
LR ^{ML} (RBF)	0.031	0.016	64.9	46.5	72.6	28.0	71.4		0.068	0.096	63.6	54.3	72.0	73.0	70.5		0.160	0.193	55.1	19.0	67.5	47.1	66.9
SVM ^{ML} (RBF)	0.027	0.012	72.5	61.7	78.9	36.6	76.6		0.069	0.088	69.1	58.0	75.1	75.9	75.4		0.159	0.188	56.2	21.6	68.2	48.1	66.7
SVM _γ ^{ML} (RBF)	0.027	0.012	72.5	61.6	78.9	36.6	77.2		0.064	0.088	68.0	58.0	74.7	75.2	75.0		0.157	0.187	56.2	19.8	68.4	48.2	67.0

TABLE 7: Multilabel classification. The 3 best performing methods from the study by Madjarov et al. [11] are compared to our multilabel methods from § 3.3. **Baselines:** RF-PCT – random forest of predicting clustering trees [132]; HOMER – hierarchy of multilabel classifiers [133]; BR – binary relevance method using SVM^{OVA}. HOMER and all the methods marked with (RBF) use an RBF kernel. Following [55], the cut-off threshold δ for our methods is chosen by cross validation.

definition). Following [97], Madjarov et al. choose δ by matching label cardinality between the training and test data. While it is fast and easy to compute, that approach has two drawbacks: (i) being an instance of transductive learning, the method requires re-computation of δ every time test data changes; (ii) the choice of δ is not tuned to any performance measure and is likely to be suboptimal. In our experiments (not reported here), we observed generally comparable, but slightly lower results compared to when δ is selected on a validation set as discussed next.

Instead, Koyejo et al. [55] recently showed that a consistent classifier is obtained when one computes δ by optimizing a given performance measure on a hold-out validation set. While there are at most mn distinct values of δ that would need to be considered, we limit the search to the grid $\{-10^{(-5.9:2:1)}, 0, 10^{(-5.9:2:1)}\}$ of 71 values.

Following [11], we use 10-fold cross-validation to select $C = 1/(\lambda n)$, the RBF kernel parameter $\theta = 1/(2\sigma^2)$, and the threshold δ , as described above. We use rather large and fine-grained grids both for C (from 2^{-20} to 2^5) and θ (from 2^{-15} to 2^3). The smoothing parameter is always set $\gamma = 1$.

Tables 7 and 9 present our experimental results. We

report 7 performance metrics previously introduced in § 3.1 and tune the hyper-parameters for each metric individually. All metrics, except the rank loss and the hamming loss, are given in percents. Since the RF-PCT method did not use the RBF kernel in [55], we also report results with the linear kernel for our methods in the middle section of each table.

Overall, experimental results indicate competitive performance of our methods across all datasets and evaluation measures. Specifically, we highlight that the smooth SVM_γ^{ML} with the RBF kernel yields the best performance in 38 out of 70 cases. On the two largest datasets, bookmarks and delicious, where the previous methods even struggled to complete training, we are able to achieve significant performance improvements both in rank loss as well as in partition-based measures. Finally, we note that while the previous methods show rather large variability in performance, all three of our multilabel methods tend to be more stable and show results that are concentrated around the best performing method in each of the cases.

Multiclass to multilabel. Collecting ground truth annotation is hard. Even when the annotation is simply an image level tag, providing a *consistent* and *exhaustive* list of labels

Labels	Method	aero	bike	bird	boat	bottle	bus	car	cat	chair	cow	table	dog	horse	mbike	prsn	plant	sheep	sofa	train	tv	mAP	
multi-class	LR ^{Multi}	99.2	95.0	92.5	92.3	61.9	86.6	93.4	95.8	55.3	85.8	82.0	92.1	97.2	91.5	93.2	70.8	82.1	82.6	97.8	81.1	86.4	
	top-k Ent	99.1	96.0	92.3	95.4	62.1	89.2	93.9	95.3	58.5	88.1	72.8	94.2	97.3	93.8	93.0	67.9	87.7	83.4	97.6	85.3	87.1	
	SVM ^{Multi}	99.5	94.0	97.0	96.8	62.1	93.4	94.6	97.5	65.0	89.9	85.1	97.4	97.8	95.5	93.7	71.0	90.2	84.4	98.7	82.3	89.3	
	top-k SVM ^α	99.3	95.5	94.7	95.5	61.5	91.9	94.6	97.4	66.7	89.0	80.8	97.1	97.7	95.4	95.3	70.7	90.2	84.3	98.5	84.8	89.0	
	top-k SVM ^β	99.4	95.5	96.0	95.9	63.5	92.6	94.6	97.4	66.1	90.2	84.1	97.1	97.8	95.5	95.0	70.9	91.7	84.6	98.5	83.9	89.5	
	SVM _γ ^{Multi}	99.4	95.4	95.0	95.5	64.3	91.9	94.4	97.0	64.0	90.0	84.7	96.1	97.7	94.8	94.2	70.6	89.7	84.6	98.3	83.3	89.0	
	top-k SVM _γ ^α	99.3	96.0	93.2	95.0	63.6	90.7	94.3	97.0	62.4	89.3	79.7	96.0	97.6	95.0	95.0	70.2	89.5	84.4	98.3	83.9	88.5	
	top-k SVM _γ ^β	99.3	95.6	94.7	95.2	64.4	91.8	94.5	97.1	65.1	89.8	84.2	96.3	97.7	94.9	94.8	70.6	89.7	84.6	98.4	84.0	89.1	
	multi-label	LR ^{ML}	98.8	94.2	92.3	90.6	56.6	83.3	92.1	95.8	65.0	85.3	84.0	93.9	96.5	93.6	92.5	69.4	83.8	81.2	97.7	78.2	86.2
		SVM ^{ML}	99.5	96.5	97.5	96.7	71.8	93.6	95.3	97.8	79.3	92.0	87.6	98.4	98.2	96.6	97.9	73.1	93.3	83.8	98.7	88.5	91.8
		SVM _γ ^{ML}	99.6	96.3	97.1	96.4	69.5	93.3	94.9	97.5	76.7	91.3	88.0	98.0	98.3	96.6	98.1	72.6	93.2	83.7	98.6	88.0	91.4

TABLE 10: Pascal VOC 2007 **classification** results. Evaluation of multiclass, top- k , and multilabel classification methods. Methods in the “multiclass” section above use only a *single* label per image, while methods in the “multilabel” section use all annotated labels. Please see the section **Multiclass to multilabel** for further details on the learning setting.

Method	R@0	R@3	R@5	RLoss	HLoss	Acc	SAcc	F ₁ ^{mic}	F ₁ ^{mac}	F ₁ ^{inst}
LR ^{Multi}	76.2	94.3	98.0	0.016	0.029	73.2	54.4	78.1	75.0	80.0
top-k Ent	76.1	94.3	97.8	0.016	0.038	48.1	44.0	59.8	72.1	61.7
SVM ^{Multi}	76.5	94.1	97.6	0.017	0.025	76.0	60.6	80.3	77.5	81.9
top-k SVM ^α	76.4	94.6	98.0	0.015	0.025	76.6	61.3	81.4	77.9	81.7
top-k SVM ^β	76.8	95.2	98.1	0.014	0.024	77.3	62.0	82.0	78.6	83.1
SVM _γ ^{Multi}	76.6	94.7	98.0	0.015	0.025	75.9	60.0	81.2	78.3	82.3
top-k SVM _γ ^α	76.4	95.0	98.2	0.015	0.025	76.2	59.3	81.2	76.7	81.5
top-k SVM _γ ^β	76.7	95.2	98.1	0.014	0.024	76.7	60.5	82.2	78.1	82.8
LR ^{ML}	76.5	96.3	98.9	0.010	0.027	75.2	59.8	81.3	77.4	80.7
SVM ^{ML}	78.0	96.8	98.9	0.008	0.019	81.6	69.8	85.8	81.9	86.1
SVM _γ ^{ML}	77.9	97.3	99.1	0.008	0.018	82.4	70.8	86.8	83.0	86.4

TABLE 11: Pascal VOC 2007 multilabel classification results.

for every image in the training set would require significant effort. It is much easier to provide a weaker form of annotation where only a single prominent object is tagged. An interesting question is then whether it is still possible to train multilabel classifiers from multiclass annotation. And if so, how large is the performance gap compared to methods trained with full multilabel annotation? In the following, we set to explore that setting and answer the questions above.

We also note that top- k classification emerges naturally as an intermediate step between multiclass and multilabel learning. Recall that top- k loss functions operate in the multiclass setting where there is a single label per example, but that label is hard to guess correctly on the first attempt. One could imagine that the example is actually associated with k labels, but only a single label is revealed in the annotation. Therefore, it is also interesting to see if our top- k loss functions can offer an advantage over the classic multiclass losses in this setting.

To evaluate the multiclass, top- k , and multilabel loss functions on a common task, we choose two multilabel image classification benchmarks: Pascal VOC 2007 and Microsoft COCO. Multilabel methods are trained using full image level annotation (i.e. all class labels, but no bounding boxes or segmentation), while multiclass and top- k methods are trained using a *single* label per image. Both datasets offer object level bounding box annotations which can be used to estimate relative sizes of objects in the scene. For multiclass training, we only keep the label of the largest object, which

is our proxy to estimating the prominent object in the image. All methods are evaluated using full annotation at test time. Note that except for pruning the training labels, we do *not* use bounding boxes anywhere during training or testing.

Experimental setup. We use 5K images for training and 5K for testing on Pascal VOC 2007, and 83K for training and 40K for testing on the MS COCO validation set. We split the training data in half for parameter tuning, and re-train on the full set for testing. We tune the regularization parameter $C = 1/(\lambda n)$ in the range from 2^{-20} to 2^{15} , and the top- k parameter k in the range $\{2, 3, 4, 5\}$. For the partition-based measures, we also tune the threshold δ in the range $[0.1, 10]$ with 100 equally spaced points. That range was chosen by observing the distribution of δ when it is computed by matching the label cardinality between training and test data. All hyper-parameters are tuned for each method and performance metric individually.

To isolate the effect of loss functions on classifier training from feature learning, we follow the classic approach of extracting features as a pre-processing step and then train our classifiers on the fixed image representation. We use our own implementation of SDCA based solvers for all of the methods considered in this section. That offers strong convergence guarantees due to (i) convexity of the objective and (ii) having the duality gap as the stopping criterion.

Our feature extraction pipeline is fairly common and follows the steps outlined in [71], [87]. We compute multiple feature vectors per image. Every original image is resized isotropically so that the smallest side is equal to $Q \in \{256, 384, 512\}$ pixels, and then horizontal flips are added for a total of 6 images at 3 scales. We use MatConvNet [126] and apply the ResNet-152 model [72] which has been pre-trained on ImageNet. We extract features from the pool5 layer and obtain about 500 feature vectors of dimension 2048 per image on Pascal VOC (the exact number depends on the size of the original image). To reduce computational costs on COCO, we increase the stride of that layer to 2 for $Q \in \{384, 512\}$, which yields about 140 feature vectors per image and a total of $n = 12M$ training examples. Unlike [87], we do not compute an additional global descriptor and also perform no normalization. Our preliminary experiments showed no advantage in doing so, and we decided to keep the pipeline close to the original ResNet network.

Labels	Method	mAP	P@1	P@2	P@3	P@5	R@1	R@3	R@5	R@10	RLoss	HLoss	Acc	SAcc	F_1^{mic}	F_1^{mac}	F_1^{inst}
multi-class	LR ^{Multi}	54.6	92.6	66.9	52.2	37.0	44.8	65.8	73.9	82.9	0.066	0.028	43.4	15.9	52.4	41.1	55.8
	SVM ^{Multi}	54.2	92.8	66.9	51.9	36.6	44.9	65.6	73.4	83.5	0.057	0.025	48.3	20.7	55.6	43.3	60.1
	top-k SVM ^α	58.3	92.8	68.1	53.2	37.5	44.9	66.8	74.8	83.7	0.054	0.025	48.8	20.8	56.8	44.4	59.9
	top-k SVM ^β	59.0	93.2	68.4	53.2	37.5	45.0	66.9	74.7	84.0	0.053	0.025	49.7	21.2	57.5	44.5	61.3
	SVM ^{γMulti}	58.1	93.0	67.7	52.8	37.2	45.0	66.5	74.3	83.6	0.056	0.025	48.9	20.2	56.5	44.6	60.6
	top-k SVM ^α _γ	58.4	92.8	68.1	53.2	37.5	44.9	66.8	74.8	83.7	0.055	0.025	48.4	20.4	57.0	44.5	60.3
	top-k SVM ^β _γ	59.1	93.2	68.4	53.3	37.4	45.0	66.9	74.7	83.7	0.054	0.025	49.3	20.9	57.2	44.4	60.9
multi-label	LR ^{ML}	58.2	92.8	76.3	61.8	44.2	44.9	75.5	84.6	93.2	0.021	0.030	43.7	16.9	52.9	49.6	55.6
	SVM ^{ML}	63.0	92.1	72.9	57.4	40.6	44.1	70.8	78.9	89.1	0.040	0.024	49.5	25.6	58.3	50.6	60.5
	SVM ^{ML} _γ	71.0	95.7	79.5	63.4	44.6	46.2	77.1	85.3	93.2	0.020	0.021	57.4	29.8	65.5	58.9	67.9

TABLE 12: MS COCO multilabel **classification** results. Methods in the “multiclass” section use only a *single* label per image, while methods in the “multilabel” section use all annotated labels. Please see the section **Multiclass to multilabel** for further details on the learning setting, and § 3.1 for details on the evaluation measures.

Every feature vector can be mapped to a region in the original image. For training, we simply replicate the same image labels effectively increasing the size of the training set. At test time, we obtain a single ranking of class labels per image by max pooling the scores for each class. We follow this basic setup, but note that a 1 – 2% improvement is possible with a more sophisticated aggregation of information from the different image regions [84], [87].

Pascal VOC 2007. Here, we discuss the results presented in Tables 10 and 11. We start with the first table which reports the standard VOC evaluation measure, the mean AP. First, we compare top-1 (multiclass) and top- k classification methods. As before, although the differences are small, we see consistent improvements in each of the three groups: LR^{Multi} to top- k Ent, SVM^{Multi} to top- k SVM^β, and SVM^{γMulti} to top- k SVM^β_γ. The best top-1 method is SVM^{Multi} with 89.3% mAP, which is outperformed by top- k SVM^β reporting the best multiclass result of 89.5% mAP.

Next, we look at the performance gap between multiclass and multilabel settings. The best mAP of 91.8% is achieved by the multilabel SVM, SVM^{ML}, which exploits full annotation to boost its performance. However, the gap of just above 2% suggests a non-trivial trade-off between the additional annotation effort and the resulting classification performance. One limitation of the results on VOC 2007 is the relatively low label cardinality of only 1.5 labels per image. We will see how the picture changes on COCO where the label cardinality is about 3 labels per image.

Comparing the smooth and nonsmooth losses, we see that nonsmooth loss functions tend to perform better on this dataset. Moreover, SVM seems to perform significantly better than softmax. While this is a somewhat surprising result, it has been observed previously, e.g. with the R-CNN detector [140], [141], and with deeply-supervised CNNs [142], even though their comparison was to OVA SVM.

Finally, we note that the current state of the art classification results on VOC 2007 are reported in [84], [87], [89]. Our 91.8% mAP of SVM^{ML} matches exactly the result of LSSVM-Max in [87], which operates in the setting closest to ours in terms of image representation and the learning architecture. Their proposed PRSVM method performs additional inference (as opposed to simple max pooling) and achieves 92.9% mAP. Multiscale orderless pooling from [84] is directly comparable to our setting and yields 90.8% mAP.

Performing inference on the extracted image regions, they too report around 93% mAP, while additionally exploiting bounding box annotations boosts the performance to 93.7%.

While mAP is the established performance measure on Pascal VOC datasets, it does not evaluate how well a method captures inter-class correlations since the AP is computed for each class independently. To address this limitation, we also report a number of multilabel performance metrics from § 3.1 in Table 11. The best performing method in the multiclass category is again top- k SVM^β, but the improvement over the baseline SVM^{Multi} is more pronounced. Furthermore, the smooth SVM^{ML}_γ now clearly outperforms its nonsmooth counterpart also significantly increasing the gap between multiclass and multilabel methods.

MS COCO. Table 12 presents our results on the MS COCO benchmark. The general trend is similar to that observed on VOC 2007: top- k methods tend to outperform top-1 multiclass baselines, but are outperformed by multilabel methods that exploit full annotation. However, the differences between the methods are more meaningful on this dataset. In particular, smooth top- k SVM^β_γ achieves 59.1% mAP, which is a 1% improvement over SVM^{γMulti}, while multilabel SVM^{ML}_γ boosts the performance to 71%. The improvement of over 10% highlights the value of multilabel annotation, even though this result is subject to the bias of our label selection procedure for multiclass methods: small objects may have not been represented well. That class imbalance could be also the reason for relatively poor mAP performance of SVM^{Multi} and LR^{Multi} methods in these experiments.

The current state of the art classification results on COCO are reported in [84]. A comparable architecture achieved 69.7% mAP, while performing inference on the multiple regions per image and exploiting the bounding box annotations boosted the performance to 73% mAP.

Looking at multilabel evaluation measures, we can also make a few interesting observations. First, the rank loss seems to correlate well with the other performance measures, which is good since that is the metric that our loss functions are designed to optimize. Second, strong performance at P@1 suggests that a single guess is generally sufficient to guess a correct label. However, due to high class imbalance this result is not too impressive and is humbled by the performance of R@ k : even 10 attempts may not

suffice to guess all relevant labels. The difficulty of properly ranking the less represented classes is also highlighted by the relatively low accuracy and subset accuracy results, although the latter metric may be too stringent for a large scale benchmark.

7 CONCLUSION

We have done an extensive experimental study of multi-class, top- k , and multilabel performance optimization. We observed that the softmax loss and the smooth hinge loss are competitive across all top- k errors and should be considered the primary candidates in practice. Our new top- k loss functions can further improve these results, especially if one is targeting a particular top- k error as the performance measure, or if the training examples are multilabel in nature. The latter transition from multiclass to multilabel classification indicates that effective multilabel classifiers can be trained from single label annotations. Our results also show that the classical multilabel SVM is competitive in mAP on Pascal VOC 2007, however, the proposed *smooth* multilabel SVM outperforms the competing methods in other metrics on Pascal VOC, and in all metrics on MS COCO. Finally, we would like to highlight our optimization schemes for top- k Ent, top- k SVM $_{\gamma}$, and SVM $_{\gamma}^{ML}$, which include the softmax loss and multiclass, multilabel SVM as special cases.

REFERENCES

- [1] O. Russakovsky, J. Deng, H. Su, J. Krause, S. Satheesh, S. Ma, Z. Huang, A. Karpathy, A. Khosla, M. Bernstein, A. C. Berg, and L. Fei-Fei, "ImageNet Large Scale Visual Recognition Challenge," 2014.
- [2] B. Zhou, A. Lapedriza, J. Xiao, A. Torralba, and A. Oliva, "Learning deep features for scene recognition using places database," in *NIPS*, 2014, pp. 487–495.
- [3] T.-Y. Lin, M. Maire, S. Belongie, J. Hays, P. Perona, D. Ramanan, P. Dollár, and C. L. Zitnick, "Microsoft COCO: Common objects in context," in *ECCV*, 2014, pp. 740–755.
- [4] J. Xiao, J. Hays, K. A. Ehinger, A. Oliva, and A. Torralba, "SUN database: Large-scale scene recognition from abbey to zoo," in *CVPR*, 2010.
- [5] S. Shalev-Shwartz and T. Zhang, "Stochastic dual coordinate ascent methods for regularized loss minimization," *JMLR*, vol. 14, pp. 567–599, 2013.
- [6] M. Lapin, M. Hein, and B. Schiele, "Loss functions for top- k error: Analysis and insights," in *CVPR*, 2016.
- [7] K. Crammer and Y. Singer, "A family of additive online algorithms for category ranking," *JMLR*, vol. 3, pp. 1025–1058, 2003.
- [8] S. Shalev-Shwartz and T. Zhang, "Accelerated proximal stochastic dual coordinate ascent for regularized loss minimization," *Math. Prog.*, pp. 1–41, 2014.
- [9] M. Lapin, M. Hein, and B. Schiele, "Top- k multiclass SVM," in *NIPS*, 2015, pp. 325–333.
- [10] W. Gao and Z.-H. Zhou, "On the consistency of multi-label learning," in *COLT*, vol. 19, 2011, pp. 341–358.
- [11] G. Madjarov, D. Kocev, D. Gjorgjevikj, and S. Džeroski, "An extensive experimental comparison of methods for multi-label learning," *Pattern Recognition*, vol. 45, no. 9, pp. 3084–3104, 2012.
- [12] M. Everingham, L. Van Gool, C. K. Williams, J. Winn, and A. Zisserman, "The PASCAL visual object classes (VOC) challenge," *IJCV*, vol. 88, no. 2, pp. 303–338, 2010.
- [13] I. Tsochantaridis, T. Joachims, T. Hofmann, and Y. Altun, "Large margin methods for structured and interdependent output variables," *JMLR*, pp. 1453–1484, 2005.
- [14] T.-Y. Liu, "Learning to rank for information retrieval," *Foundations and Trends in Information Retrieval*, vol. 3, no. 3, 2009.
- [15] D. Cossock and T. Zhang, "Subset ranking using regression," in *COLT*, 2006, pp. 605–619.
- [16] P. Li, Q. Wu, and C. J. Burges, "McRank: Learning to rank using multiple classification and gradient boosting," in *NIPS*, 2007.
- [17] C. Burges, T. Shaked, E. Renshaw, A. Lazier, M. Deeds, N. Hamilton, and G. Hullender, "Learning to rank using gradient descent," in *ICML*, 2005, pp. 89–96.
- [18] Y. Freund, R. Iyer, R. E. Schapire, and Y. Singer, "An efficient boosting algorithm for combining preferences," *JMLR*, vol. 4, no. Nov, pp. 933–969, 2003.
- [19] T. Joachims, "Optimizing search engines using clickthrough data," in *KDD*, 2002, pp. 133–142.
- [20] M. Taylor, J. Guiver, S. Robertson, and T. Minka, "SoftRank: optimizing non-smooth rank metrics," in *WSDM*, 2008.
- [21] Y. Yue, T. Finley, F. Radlinski, and T. Joachims, "A support vector method for optimizing average precision," in *SIGIR*, 2007.
- [22] J. Xu and H. Li, "AdaRank: a boosting algorithm for information retrieval," in *SIGIR*, 2007, pp. 391–398.
- [23] Z. Cao, T. Qin, T.-Y. Liu, M.-F. Tsai, and H. Li, "Learning to rank: from pairwise approach to listwise approach," in *ICML*, 2007.
- [24] F. Xia, T.-Y. Liu, J. Wang, W. Zhang, and H. Li, "Listwise approach to learning to rank: theory and algorithm," in *ICML*, 2008.
- [25] S. Vembu and T. Gärtner, "Label ranking algorithms: A survey," in *Preference learning*. Springer, 2010, pp. 45–64.
- [26] N. Usunier, D. Buffoni, and P. Gallinari, "Ranking with ordered weighted pairwise classification," in *ICML*, 2009, pp. 1057–1064.
- [27] J. Weston, S. Bengio, and N. Usunier, "Wsabie: scaling up to large vocabulary image annotation," *IJCAI*, pp. 2764–2770, 2011.
- [28] M. R. Gupta, S. Bengio, and J. Weston, "Training highly multiclass classifiers," *JMLR*, vol. 15, pp. 1461–1492, 2014.
- [29] J. J. McAuley, A. Ramisa, and T. S. Caetano, "Optimization of robust loss functions for weakly-labeled image taxonomies," *IJCV*, vol. 104, no. 3, pp. 343–361, 2013.
- [30] X. Xu, A. Shimada, H. Nagahara, R.-i. Taniguchi, and L. He, "Image annotation with incomplete labelling by modelling image specific structured loss," *IEEE T ELECTR ELECTR*, vol. 11, no. 1, pp. 73–82, 2016.
- [31] S. Ross, J. Zhou, Y. Yue, D. Dey, and D. Bagnell, "Learning policies for contextual submodular prediction," in *ICML*, 2013.
- [32] K. Swersky, B. J. Frey, D. Tarlow, R. S. Zemel, and R. P. Adams, "Probabilistic n -choose- k models for classification and ranking," in *NIPS*, 2012, pp. 3050–3058.
- [33] M. Guillaumin, T. Mensink, J. Verbeek, and C. Schmid, "TagProp: Discriminative metric learning in nearest neighbor models for image auto-annotation," in *ICCV*, 2009, pp. 309–316.
- [34] T. Mensink, J. Verbeek, F. Perronnin, and G. Csurka, "Distance-based image classification: Generalizing to new classes at near-zero cost," *PAMI*, vol. 35, no. 11, pp. 2624–2637, 2013.
- [35] A. Kanehira and T. Harada, "Multi-label ranking from positive and unlabeled data," in *CVPR*, 2016.
- [36] M. C. du Plessis, G. Niu, and M. Sugiyama, "Analysis of learning from positive and unlabeled data," in *NIPS*, 2014, pp. 703–711.
- [37] B. Frény and M. Verleysen, "Classification in the presence of label noise: a survey," *NNLS*, vol. 25, no. 5, pp. 845–869, 2014.
- [38] T. Liu and D. Tao, "Classification with noisy labels by importance reweighting," *PAMI*, vol. 38, no. 3, pp. 447–461, 2016.
- [39] M.-L. Zhang and Z.-H. Zhou, "A review on multi-label learning algorithms," *KDE*, vol. 26, no. 8, pp. 1819–1837, 2014.
- [40] M. Wang, B. Ni, X.-S. Hua, and T.-S. Chua, "Assistive tagging: A survey of multimedia tagging with human-computer joint exploration," *ACM Computing Surveys (CSUR)*, vol. 44, no. 4, p. 25, 2012.
- [41] Y. Gong, Y. Jia, T. Leung, A. Toshev, and S. Ioffe, "Deep convolutional ranking for multilabel image annotation," *arXiv:1312.4894*, 2013.
- [42] J. Wang, Y. Song, T. Leung, C. Rosenberg, J. Wang, J. Philbin, B. Chen, and Y. Wu, "Learning fine-grained image similarity with deep ranking," in *CVPR*, 2014, pp. 1386–1393.
- [43] F. Zhao, Y. Huang, L. Wang, and T. Tan, "Deep semantic ranking based hashing for multi-label image retrieval," in *CVPR*, 2015.
- [44] S. Agarwal, "The infinite push: A new support vector ranking algorithm that directly optimizes accuracy at the absolute top of the list," in *SDM*, 2011, pp. 839–850.
- [45] S. Boyd, C. Cortes, M. Mohri, and A. Radovanovic, "Accuracy at the top," in *NIPS*, 2012, pp. 953–961.
- [46] A. Rakotomamonjy, "Sparse support vector infinite push," in *ICML*, 2012, pp. 1335–1342.
- [47] C. Rudin, "The p -norm push: A simple convex ranking algorithm that concentrates at the top of the list," *JMLR*, vol. 10, 2009.

- [48] N. Li, R. Jin, and Z.-H. Zhou, "Top rank optimization in linear time," in *NIPS*, 2014, pp. 1502–1510.
- [49] P. L. Bartlett, M. I. Jordan, and J. D. McAuliffe, "Convexity, classification and risk bounds," *JASA*, vol. 101, pp. 138–156, 2006.
- [50] T. Zhang, "Statistical behavior and consistency of classification methods based on convex risk minimization," *Ann. Stat.*, 2004.
- [51] M. D. Reid and R. C. Williamson, "Composite binary losses," *JMLR*, vol. 11, no. Sep, pp. 2387–2422, 2010.
- [52] A. Tewari and P. L. Bartlett, "On the consistency of multiclass classification methods," *JMLR*, vol. 8, pp. 1007–1025, 2007.
- [53] B. Á. Pires and C. Szepesvári, "Multiclass classification calibration functions," *arXiv:1609.06385*, 2016.
- [54] E. Vernet, M. D. Reid, and R. C. Williamson, "Composite multiclass losses," in *NIPS*, 2011, pp. 1224–1232.
- [55] O. O. Koyejo, N. Natarajan, P. K. Ravikumar, and I. S. Dhillon, "Consistent multilabel classification," in *NIPS*, 2015.
- [56] D. Cossack and T. Zhang, "Statistical analysis of bayes optimal subset ranking," *IEEE Trans. Inf. Theory*, vol. 54, no. 11, 2008.
- [57] J. C. Duchi, L. W. Mackey, and M. I. Jordan, "On the consistency of ranking algorithms," in *ICML*, 2010, pp. 327–334.
- [58] C. Calauzenes, N. Usunier, and P. Gallinari, "On the (non-) existence of convex, calibrated surrogate losses for ranking," in *NIPS*, 2012, pp. 197–205.
- [59] O. Fercoq and P. Richtárik, "Accelerated, parallel, and proximal coordinate descent," *SIOPT*, vol. 25, no. 4, pp. 1997–2023, 2015.
- [60] S. Shalev-Shwartz and Y. Singer, "Efficient learning of label ranking by soft projections onto polyhedra," *JMLR*, vol. 7, pp. 1567–1599, 2006.
- [61] N. Parikh and S. P. Boyd, "Proximal algorithms," *Foundations and Trends in Optimization*, vol. 1, no. 3, pp. 127–239, 2014.
- [62] M. Patriksson and C. Strömberg, "Algorithms for the continuous nonlinear resource allocation problem – new implementations and numerical studies," *EJOR*, vol. 243, no. 3, pp. 703–722, 2015.
- [63] J. Liu and J. Ye, "Efficient Euclidean projections in linear time," in *ICML*, 2009, pp. 657–664.
- [64] K. C. Kiwiel, "Breakpoint searching algorithms for the continuous quadratic knapsack problem," *Math. Prog.*, vol. 112, no. 2, pp. 473–491, 2008.
- [65] K. Kiwiel, "Variable fixing algorithms for the continuous quadratic knapsack problem," *JOTA*, vol. 136, no. 3, 2008.
- [66] L. Condat, "Fast projection onto the simplex and the ℓ_1 ball," *Math. Prog.*, pp. 1–11, 2014.
- [67] J. Mairal, R. Jenatton, F. R. Bach, and G. R. Obozinski, "Network flow algorithms for structured sparsity," in *NIPS*, 2010.
- [68] A. Beck and M. Teboulle, "A fast iterative shrinkage-thresholding algorithm for linear inverse problems," *SIIMS*, vol. 2, no. 1, pp. 183–202, 2009.
- [69] H.-F. Yu, F.-L. Huang, and C.-J. Lin, "Dual coordinate descent methods for logistic regression and maximum entropy models," *Machine Learning*, vol. 85, no. 1-2, pp. 41–75, 2011.
- [70] R. M. Corless, G. H. Gonnet, D. E. Hare, D. J. Jeffrey, and D. E. Knuth, "On the Lambert W function," *Advances in Computational Mathematics*, vol. 5, no. 1, pp. 329–359, 1996.
- [71] K. Simonyan and A. Zisserman, "Very deep convolutional networks for large-scale image recognition," *CoRR*, vol. abs/1409.1556, 2014.
- [72] K. He, X. Zhang, S. Ren, and J. Sun, "Deep residual learning for image recognition," in *CVPR*, 2016.
- [73] L. Wang, S. Guo, W. Huang, and Y. Qiao, "Places205-vggnet models for scene recognition," *CoRR*, vol. abs/1508.01667, 2015.
- [74] A. Torralba and A. A. Efros, "Unbiased look at dataset bias," in *CVPR*, 2011, pp. 1521–1528.
- [75] M. Oquab, L. Bottou, I. Laptev, and J. Sivic, "Learning and transferring mid-level image representations using convolutional neural networks," in *CVPR*, 2014, pp. 1717–1724.
- [76] A. S. Razavian, H. Azizpour, J. Sullivan, and S. Carlsson, "CNN features off-the-shelf: an astounding baseline for recognition," in *CVPRW, DeepVision workshop*, 2014.
- [77] C. Wah, S. Branson, P. Welinder, P. Perona, and S. Belongie, "The Caltech-UCSD Birds-200-2011 dataset," California Institute of Technology, Tech. Rep., 2011.
- [78] M.-E. Nilsback and A. Zisserman, "Automated flower classification over a large number of classes," in *ICVGIP*, 2008.
- [79] A. Quattoni and A. Torralba, "Recognizing indoor scenes," in *CVPR*, 2009.
- [80] K. Chatfield, K. Simonyan, A. Vedaldi, and A. Zisserman, "Return of the devil in the details: Delving deep into convolutional nets," *arXiv:1405.3531*, 2014.
- [81] M. D. Zeiler and R. Fergus, "Visualizing and understanding convolutional networks," in *ECCV*, 2014, pp. 818–833.
- [82] S. Ren, K. He, R. Girshick, and J. Sun, "Faster R-CNN: Towards real-time object detection with region proposal networks," in *NIPS*, 2015, pp. 91–99.
- [83] P. Sermanet, D. Eigen, X. Zhang, M. Mathieu, R. Fergus, and Y. LeCun, "OverFeat: Integrated recognition, localization and detection using convolutional networks," *arXiv:1312.6229*, 2013.
- [84] R.-W. Zhao, J. Li, Y. Chen, J.-M. Liu, Y.-G. Jiang, and X. Xue, "Regional gating neural networks for multi-label image classification," in *BMVC*, 2016.
- [85] M. Oquab, L. Bottou, I. Laptev, and J. Sivic, "Is object localization for free? – Weakly-supervised learning with convolutional neural networks," in *CVPR*, 2015, pp. 685–694.
- [86] Y. Wei, W. Xia, M. Lin, J. Huang, B. Ni, J. Dong, Y. Zhao, and S. Yan, "HCP: A flexible cnn framework for multi-label image classification," *PAMI*, vol. 38, no. 9, pp. 1901–1907, 2016.
- [87] Z. Wei and M. Hoai, "Region ranking svm for image classification," in *CVPR*, 2016.
- [88] J. Wang, Y. Yang, J. Mao, Z. Huang, C. Huang, and W. Xu, "CNN-RNN: A unified framework for multi-label image classification," *arXiv:1604.04573*, 2016.
- [89] M. Wang, C. Luo, R. Hong, J. Tang, and J. Feng, "Beyond object proposals: Random crop pooling for multi-label image recognition," *IEEE Trans. Image Process.*, vol. 25, no. 12, 2016.
- [90] B. Schölkopf and A. J. Smola, *Learning with Kernels: Support Vector Machines, Regularization, Optimization, and Beyond*. The MIT Press, 2002.
- [91] J. Friedman, T. Hastie, and R. Tibshirani, *The elements of statistical learning*. Springer, 2001.
- [92] R. O. Duda, P. E. Hart, and D. G. Stork, *Pattern classification*. John Wiley & Sons, 2012.
- [93] C. D. Manning, P. Raghavan, and H. Schütze, *Introduction to Information Retrieval*. Cambridge University Press, 2008.
- [94] T. Joachims, "A support vector method for multivariate performance measures," in *ICML*, 2005, pp. 377–384.
- [95] B. McFee and G. R. Lanckriet, "Metric learning to rank," in *ICML*, 2010, pp. 775–782.
- [96] K. Dembczynski, W. Cheng, and E. Hüllermeier, "Bayes optimal multilabel classification via probabilistic classifier chains," in *ICML*, 2010, pp. 279–286.
- [97] J. Read, B. Pfahringer, G. Holmes, and E. Frank, "Classifier chains for multi-label classification," in *ECML*, 2009, pp. 254–269.
- [98] Y. Yang, "An evaluation of statistical approaches to text categorization," *Information retrieval*, vol. 1, no. 1-2, pp. 69–90, 1999.
- [99] A. Elisseeff and J. Weston, "A kernel method for multi-labelled classification," in *NIPS*, 2001, pp. 681–687.
- [100] J. Fürnkranz, E. Hüllermeier, E. L. Mencía, and K. Brinker, "Multilabel classification via calibrated label ranking," *Machine Learning*, vol. 73, no. 2, pp. 133–153, 2008.
- [101] K. Crammer and Y. Singer, "On the algorithmic implementation of multiclass kernel-based vector machines," *JMLR*, vol. 2, pp. 265–292, 2001.
- [102] Y. Bengio, "Learning deep architectures for AI," *Foundations and Trends in Machine Learning*, vol. 2, no. 1, pp. 1–127, 2009.
- [103] A. Krizhevsky, I. Sutskever, and G. Hinton, "ImageNet classification with deep convolutional neural networks," in *NIPS*, 2012.
- [104] Z. Akata, F. Perronnin, Z. Harchaoui, and C. Schmid, "Good practice in large-scale learning for image classification," *PAMI*, vol. 36, no. 3, pp. 507–520, 2014.
- [105] A. Beck and M. Teboulle, "Smoothing and first order methods, a unified framework," *SIOPT*, vol. 22, pp. 557–580, 2012.
- [106] Y. Nesterov, "Smooth minimization of non-smooth functions," *Math. Prog.*, vol. 103, no. 1, pp. 127–152, 2005.
- [107] J.-B. Hiriart-Urruty and C. Lemaréchal, *Fundamentals of Convex Analysis*. Berlin: Springer, 2001.
- [108] J. M. Borwein and A. S. Lewis, *Convex Analysis and Nonlinear Optimization: Theory and Examples*, ser. Cms Books in Mathematics Series. Springer Verlag, 2000.
- [109] S. Boyd and L. Vandenberghe, *Convex Optimization*. Cambridge University Press, 2004.
- [110] G. Tsoumakas and I. Katakis, "Multi label classification: An overview," *IJDWM*, vol. 3, no. 3, pp. 1–13, 2007.

- [111] Y. Guo and D. Schuurmans, "Adaptive large margin training for multilabel classification," in *AAAI*, 2011, pp. 374–379.
- [112] B. Krishnapuram, L. Carin, M. A. Figueiredo, and A. J. Hartemink, "Sparse multinomial logistic regression: Fast algorithms and generalization bounds," *PAMI*, vol. 27, no. 6, 2005.
- [113] M. Reid and B. Williamson, "Composite binary losses," *JMLR*, vol. 11, pp. 2387–2422, 2010.
- [114] Z. Qu, P. Richtárik, and T. Zhang, "Quartz: Randomized dual coordinate ascent with arbitrary sampling," in *NIPS*, 2015.
- [115] T. Fukushima, "Precise and fast computation of Lambert W-functions without transcendental function evaluations," *Journal of Computational and Applied Mathematics*, vol. 244, 2013.
- [116] D. Veberič, "Lambert W function for applications in physics," *Computer Physics Communications*, vol. 183, no. 12, 2012.
- [117] A. S. Householder, *The Numerical Treatment of a Single Nonlinear Equation*. McGraw-Hill, 1970.
- [118] C.-J. Hsieh, K.-W. Chang, C.-J. Lin, S. S. Keerthi, and S. Sundararajan, "A dual coordinate descent method for large-scale linear SVM," in *ICML*, 2008, pp. 408–415.
- [119] R.-E. Fan, K.-W. Chang, C.-J. Hsieh, X.-R. Wang, and C.-J. Lin, "LIBLINEAR: A library for large linear classification," *JMLR*, vol. 9, pp. 1871–1874, 2008.
- [120] J. Nocedal and S. J. Wright, *Numerical Optimization*. Springer Science+ Business Media, 2006.
- [121] A. Rocha and S. K. Goldenstein, "Multiclass from binary: Expanding one-versus-all, one-versus-one and ecoc-based approaches," *NNLS*, vol. 25, no. 2, pp. 289–302, 2014.
- [122] C.-W. Hsu and C.-J. Lin, "A comparison of methods for multiclass support vector machines," *Neural Networks*, vol. 13, no. 2, pp. 415–425, 2002.
- [123] K. Lang, "Newsweeder: Learning to filter netnews," in *ICML*, 1995, pp. 331–339.
- [124] L. Sharan, R. Rosenholtz, and E. Adelson, "Material perception: What can you see in a brief glance?" *Journal of Vision*, vol. 9, no. 8, pp. 784–784, 2009.
- [125] C.-C. Chang and C.-J. Lin, "LIBSVM: A library for support vector machines," *ACM TIST*, vol. 2, pp. 1–27, 2011.
- [126] A. Vedaldi and K. Lenc, "MatConvNet – Convolutional neural networks for MATLAB," in *ACM-MM*, 2015.
- [127] J. D. Rennie, "Improving multi-class text classification with naive bayes," Massachusetts Institute of Technology, Tech. Rep., 2001.
- [128] M. Cimpoi, S. Maji, and A. Vedaldi, "Deep filter banks for texture recognition and segmentation," in *CVPR*, 2015.
- [129] N. Zhang, J. Donahue, R. Girshick, and T. Darrell, "Part-based RCNN for fine-grained detection," in *ECCV*, 2014.
- [130] R. Rifkin and A. Klautau, "In defense of one-vs-all classification," *JMLR*, vol. 5, pp. 101–141, 2004.
- [131] Y. Jia, E. Shelhamer, J. Donahue, S. Karayev, J. Long, R. Girshick, S. Guadarrama, and T. Darrell, "Caffe: Convolutional architecture for fast feature embedding," *arXiv:1408.5093*, 2014.
- [132] D. Kocev, C. Vens, J. Struyf, and S. Džeroski, "Ensembles of multi-objective decision trees," in *ECML*, 2007, pp. 624–631.
- [133] G. Tsoumakas, I. Katakis, and I. Vlahavas, "Effective and efficient multilabel classification in domains with large number of labels," in *ECML/PKDD Workshop on Mining Multidimensional Data*, 2008.
- [134] I. Katakis, G. Tsoumakas, and I. Vlahavas, "Multilabel text classification for automated tag suggestion," *ECML PKDD Discovery Challenge*, vol. 75, 2008.
- [135] B. Klimt and Y. Yang, "The Enron corpus: A new dataset for email classification research," in *ECML*, 2004, pp. 217–226.
- [136] C. Snoek, M. Worring, J. Van Gemert, J.-M. Geusebroek, and A. Smeulders, "The challenge problem for automated detection of 101 semantic concepts in multimedia," in *ACM-MM*, 2006.
- [137] P. Duygulu, K. Barnard, J. F. de Freitas, and D. A. Forsyth, "Object recognition as machine translation: Learning a lexicon for a fixed image vocabulary," in *ECCV*, 2002, pp. 97–112.
- [138] M. R. Boutell, J. Luo, X. Shen, and C. M. Brown, "Learning multilabel scene classification," *Pattern Recognition*, vol. 37, no. 9, pp. 1757–1771, 2004.
- [139] K. Trohidis, G. Tsoumakas, G. Kalliris, and I. P. Vlahavas, "Multilabel classification of music into emotions," in *ISMIR*, vol. 8, 2008.
- [140] K. Lenc and A. Vedaldi, "R-CNN minus R," in *BMVC*, 2015.
- [141] R. Girshick, "Fast R-CNN," in *ICCV*, 2015, pp. 1440–1448.
- [142] C.-Y. Lee, S. Xie, P. Gallagher, Z. Zhang, and Z. Tu, "Deeply-supervised nets," in *AISTATS*, 2015.
- [143] K. B. Petersen, M. S. Pedersen *et al.*, "The matrix cookbook," *Technical University of Denmark*, vol. 450, pp. 7–15, 2008.

APPENDIX A

PROOFS FROM § 3

A.1 Proof of Proposition 2

Proof. We take the convex conjugate of the top- k hinge loss, which was derived in [9, Proposition 2], and add a regularizer $\frac{\gamma}{2}\langle v, v \rangle$ to obtain the γ -strongly convex conjugate loss $L_\gamma^*(v)$. Note that since $v_y = -\sum_{j \neq y} v_j$ and $a_y = f_y(x) - \bar{f}_y(x) = 0$, we only need to work with $(m-1)$ -dimensional vectors where the y -th coordinate is removed. The primal loss $L_\gamma(a)$, obtained as the convex conjugate of $L_\gamma^*(v)$, is $1/\gamma$ -smooth due to a known result in convex analysis [107] (see also [8, Lemma 2]). We now derive a formula to compute it based on the Euclidean projection onto the top- k simplex. By definition,

$$\begin{aligned} L_\gamma(a) &= \sup_{v' \in \mathbb{R}^m} \{ \langle a, v' \rangle - L_\gamma^*(v') \} \\ &= \max_{v \in \Delta_k^\alpha(1)} \{ \langle a \setminus y, v \rangle - \frac{\gamma}{2} \langle v, v \rangle + \langle v, c \setminus y \rangle \} \\ &= -\frac{1}{\gamma} \min_{v \in \Delta_k^\alpha(1)} \left\{ \frac{1}{2} \langle v, v \rangle - \langle (a+c) \setminus y, v \rangle \right\}. \end{aligned}$$

For the constraint $\frac{v}{\gamma} \in \Delta_k^\alpha(1)$, we have

$$\begin{aligned} \langle \mathbf{1}, v/\gamma \rangle \leq 1, \quad 0 \leq v_i/\gamma \leq \frac{1}{k} \langle \mathbf{1}, v/\gamma \rangle &\iff \\ \langle \mathbf{1}, v \rangle \leq \gamma, \quad 0 \leq v_i \leq \frac{1}{k} \langle \mathbf{1}, v \rangle &\iff v \in \Delta_k^\alpha(\gamma). \end{aligned}$$

The final expression follows from the fact that

$$\begin{aligned} \arg \min_{v \in \Delta_k^\alpha(\gamma)} \left\{ \frac{1}{2} \langle v, v \rangle - \langle (a+c) \setminus y, v \rangle \right\} \\ \equiv \arg \min_{v \in \Delta_k^\alpha(\gamma)} \| (a+c) \setminus y - v \|^2 \equiv \text{proj}_{\Delta_k^\alpha(\gamma)} (a+c) \setminus y. \end{aligned}$$

□

A.2 Proof of Proposition 3

Proof. Here, we use the notation $u \triangleq f(x)$ as we need to take special care of the differences $f_j(x) - \bar{f}_y(x)$ when computing the conjugate. Therefore, the softmax loss is

$$L(u) = \log \left(\sum_{j \in \mathcal{Y}} \exp(u_j - u_y) \right) = \log \left(\sum_{j \in \mathcal{Y}} \exp(a_j) \right),$$

where $a = H_y u$ as before and $H_y \triangleq \mathbf{I} - \mathbf{1}e_y^\top$. Define

$$\phi(u) \triangleq \log \left(\sum_{j \in \mathcal{Y}} \exp(u_j) \right),$$

then $L(u) = \phi(H_y u)$ and the convex conjugate is computed similar to [9, Lemma 2] as follows.

$$\begin{aligned} L^*(v) &= \sup \{ \langle u, v \rangle - L(u) \mid u \in \mathbb{R}^m \} \\ &= \sup \{ \langle u, v \rangle - \phi(H_y u) \mid u \in \mathbb{R}^m \} \\ &= \sup \{ \langle u^\parallel, v \rangle + \langle u^\perp, v \rangle - \phi(H_y u^\perp) \mid \\ &\quad u^\parallel \in \text{Ker } H_y, u^\perp \in \text{Ker}^\perp H_y \}, \end{aligned}$$

where $\text{Ker } H_y = \{u \mid H_y u = 0\} = \{t\mathbf{1} \mid t \in \mathbb{R}\}$ and $\text{Ker}^\perp H_y = \{u \mid \langle \mathbf{1}, u \rangle = 0\}$. It follows that $L^*(v)$ can only be finite if $\langle u^\parallel, v \rangle = 0$, which implies $v \in \text{Ker}^\perp H_y \iff \langle \mathbf{1}, v \rangle = 0$. Let H_y^\dagger be the Moore-Penrose pseudoinverse of H_y . For a $v \in \text{Ker}^\perp H_y$, we write

$$\begin{aligned} L^*(v) &= \sup \{ \langle H_y^\dagger H_y u^\perp, v \rangle - \phi(H_y u^\perp) \mid u^\perp \} \\ &= \sup \{ \langle z, (H_y^\dagger)^\top v \rangle - \phi(z) \mid z \in \text{Im } H_y \}, \end{aligned}$$

where $\text{Im } H_y = \{H_y u \mid u \in \mathbb{R}^m\} = \{u \mid u_y = 0\}$. Using rank-1 update of the pseudoinverse [143, § 3.2.7], we have

$$(H_y^\dagger)^\top = \mathbf{I} - e_y e_y^\top - \frac{1}{m}(\mathbf{1} - e_y)\mathbf{1}^\top,$$

which together with $\langle \mathbf{1}, v \rangle = 0$ implies $(H_y^\dagger)^\top v = v - v_y e_y$.

$$\begin{aligned} L^*(v) &= \sup\{\langle u, v - v_y e_y \rangle - \phi(u) \mid u_y = 0\} \\ &= \sup\{\langle u^{\setminus y}, v^{\setminus y} \rangle - \log(1 + \sum_{j \neq y} \exp(u_j))\}. \end{aligned}$$

The function inside sup is concave and differentiable, hence the global optimum is at the critical point [109]. Setting the partial derivatives to zero yields

$$v_j = \exp(u_j) / (1 + \sum_{j \neq y} \exp(u_j))$$

for $j \neq y$, from which we conclude, similar to [8, § 5.1], that $\langle \mathbf{1}, v \rangle \leq 1$ and $0 \leq v_j \leq 1$ for all $j \neq y$, i.e. $v^{\setminus y} \in \Delta$. Let $Z \triangleq \sum_{j \neq y} \exp(u_j)$, we have at the optimum

$$u_j = \log(v_j) + \log(1 + Z), \quad \forall j \neq y.$$

Since $\langle \mathbf{1}, v \rangle = 0$, we also have that $v_y = -\sum_{j \neq y} v_j$, hence

$$\begin{aligned} L^*(v) &= \sum_{j \neq y} u_j v_j - \log(1 + Z) \\ &= \sum_{j \neq y} v_j \log(v_j) + \log(1 + Z)(\sum_{j \neq y} v_j - 1) \\ &= \sum_{j \neq y} v_j \log(v_j) - \log(1 + Z)(1 + v_y). \end{aligned}$$

Summing v_j and using the definition of Z ,

$$\sum_{j \neq y} v_j = \sum_{j \neq y} e^{u_j} / (1 + \sum_{j \neq y} e^{u_j}) = Z / (1 + Z).$$

Therefore,

$$1 + Z = 1 / (1 - \sum_{j \neq y} v_j) = 1 / (1 + v_y),$$

which finally yields

$$L^*(v) = \sum_{j \neq y} v_j \log(v_j) + \log(1 + v_y)(1 + v_y),$$

if $\langle \mathbf{1}, v \rangle = 0$ and $v^{\setminus y} \in \Delta$ as stated in the proposition. \square

A.3 Proof of Proposition 4

Proof. The convex conjugate of the top- k entropy loss is

$$L^*(v) \triangleq \begin{cases} \sum_{j \neq y} v_j \log v_j + (1 + v_y) \log(1 + v_y), \\ \quad \text{if } \langle \mathbf{1}, v \rangle = 0 \text{ and } v^{\setminus y} \in \Delta_k^\alpha, \\ +\infty \quad \text{otherwise.} \end{cases}$$

The (primal) top- k entropy loss is defined as the convex conjugate of the $L^*(v)$ above. We have

$$\begin{aligned} L(a) &= \sup\{\langle a, v \rangle - L^*(v) \mid v \in \mathbb{R}^m\} \\ &= \sup\{\langle a, v \rangle - \sum_{j \neq y} v_j \log v_j - (1 + v_y) \log(1 + v_y) \\ &\quad \mid \langle \mathbf{1}, v \rangle = 0, v^{\setminus y} \in \Delta_k^\alpha\} \\ &= \sup\{\langle a^{\setminus y}, v^{\setminus y} \rangle - a_y \sum_{j \neq y} v_j - \sum_{j \neq y} v_j \log v_j \\ &\quad - (1 - \sum_{j \neq y} v_j) \log(1 - \sum_{j \neq y} v_j) \mid v^{\setminus y} \in \Delta_k^\alpha\}. \end{aligned}$$

Note that $a_y = 0$, and hence the corresponding term vanishes. Finally, we let $x \triangleq v^{\setminus y}$ and $s \triangleq \sum_{j \neq y} v_j = \langle \mathbf{1}, x \rangle$.

Next, we discuss how this problem can be solved and show that it reduces to the softmax loss for $k = 1$. Let $a \triangleq a^{\setminus y}$ and consider an equivalent problem below.

$$L(a) = -\min\{\langle x, \log x \rangle + (1 - s) \log(1 - s) - \langle a, x \rangle \mid x \in \Delta_k^\alpha, \langle \mathbf{1}, x \rangle = s\}. \quad (20)$$

The Lagrangian for (20) is

$$\begin{aligned} \mathcal{L}(x, s, t, \lambda, \mu, \nu) &= \langle x, \log x \rangle + (1 - s) \log(1 - s) - \langle a, x \rangle \\ &\quad + t(\langle \mathbf{1}, x \rangle - s) + \lambda(s - 1) - \langle \mu, x \rangle + \langle \nu, x - \frac{s}{k} \mathbf{1} \rangle, \end{aligned}$$

where $t \in \mathbb{R}$ and $\lambda, \mu, \nu \geq 0$ are the dual variables. Computing the partial derivatives of \mathcal{L} w.r.t. x_j and s , and setting them to zero, we obtain

$$\begin{aligned} \log x_j &= a_j - 1 - t + \mu_j - \nu_j, \quad \forall j \\ \log(1 - s) &= -1 - t - \frac{1}{k} \langle \mathbf{1}, \nu \rangle + \lambda. \end{aligned}$$

Note that $x_j = 0$ and $s = 1$ cannot satisfy the above conditions for any choice of the dual variables in \mathbb{R} . Therefore, $x_j > 0$ and $s < 1$, which implies $\mu_j = 0$ and $\lambda = 0$. The only constraint that might be active is $x_j \leq \frac{s}{k}$. Note, however, that in view of $x_j > 0$ it can only be active if either $k > 1$ or we have a one dimensional problem. We consider the case when this constraint is active below.

Consider x_j 's for which $0 < x_j < \frac{s}{k}$ holds at the optimum. The complementary slackness conditions imply that the corresponding $\mu_j = \nu_j = 0$. Let $p \triangleq \langle \mathbf{1}, \nu \rangle$ and re-define t as $t \leftarrow 1 + t$. We obtain the simplified equations

$$\begin{aligned} \log x_j &= a_j - t, \\ \log(1 - s) &= -t - \frac{p}{k}. \end{aligned}$$

If $k = 1$, then $0 < x_j < s$ for all j in a multiclass problem as discussed above, hence also $p = 0$. We have

$$x_j = e^{a_j - t}, \quad 1 - s = e^{-t},$$

where $t \in \mathbb{R}$ is to be found. Plugging that into the objective,

$$\begin{aligned} -L(a) &= \sum_j (a_j - t) e^{a_j - t} - t e^{-t} - \sum_j a_j e^{a_j - t} \\ &= e^{-t} \left[\sum_j (a_j - t) e^{a_j} - t - \sum_j a_j e^{a_j} \right] \\ &= -t e^{-t} [1 + \sum_j e^{a_j}] = -t [e^{-t} + \sum_j e^{a_j - t}] \\ &= -t [1 - s + s] = -t. \end{aligned}$$

To compute t , we note that

$$\sum_j e^{a_j - t} = \langle \mathbf{1}, x \rangle = s = 1 - e^{-t},$$

from which we conclude

$$1 = (1 + \sum_j e^{a_j}) e^{-t} \implies -t = -\log(1 + \sum_j e^{a_j}).$$

Taking into account the minus in front of the min in (20) and the definition of a , we finally recover the softmax loss

$$L(y, f(x)) = \log(1 + \sum_{j \neq y} \exp(f_j(x) - f_y(x))). \quad \square$$

A.4 Proof of Proposition 5

Proof. We compute the convex conjugate of (SVM^{ML}) as

$$L^*(v) = -\inf_{u \in \mathbb{R}^m} \{\max\{0, 1 + \max_{j \in Y} u_j - \min_{y \in Y} u_y\} - \langle u, v \rangle\}.$$

When the infimum is attained, the conjugate can be computed by solving the following optimization problem, otherwise the conjugate is $+\infty$. The corresponding dual variables are given on the right.

$$\min_{u, \alpha, \beta, \xi} \xi - \langle u, v \rangle$$

$$\begin{aligned}
\xi &\geq 1 + \beta - \alpha, & (\lambda &\geq 0) \\
\xi &\geq 0, & (\mu &\geq 0) \\
\alpha &\leq u_y, \quad \forall y \in Y, & (\nu_y &\geq 0) \\
\beta &\geq u_j, \quad \forall j \in \bar{Y}. & (\eta_j &\geq 0)
\end{aligned}
\quad \langle \mathbf{1}, x \rangle = \langle \mathbf{1}, y \rangle \leq \gamma,$$

$$x \geq 0, y \geq 0,$$

which is the Euclidean projection onto the set $B(\gamma)$. \square

The Lagrangian is given as

$$\begin{aligned}
\mathcal{L}(u, \alpha, \beta, \xi, \lambda, \mu, \nu, \eta) &= \xi - \langle u, v \rangle + \lambda(1 + \beta - \alpha - \xi) \\
&\quad - \mu\xi + \sum_{y \in Y} \nu_y(\alpha - u_y) + \sum_{j \in \bar{Y}} \eta_j(u_j - \beta).
\end{aligned}$$

Computing the partial derivatives and setting them to zero,

$$\begin{aligned}
\partial_{u_y} \mathcal{L} &= -v_y - \nu_y, & \nu_y &= -v_y, & \forall y \in Y, \\
\partial_{u_j} \mathcal{L} &= -v_j + \eta_j, & \eta_j &= v_j, & \forall j \in \bar{Y}, \\
\partial_\alpha \mathcal{L} &= -\lambda + \langle \mathbf{1}, \nu \rangle, & \lambda &= \langle \mathbf{1}, \nu \rangle, \\
\partial_\beta \mathcal{L} &= \lambda - \langle \mathbf{1}, \eta \rangle, & \lambda &= \langle \mathbf{1}, \eta \rangle, \\
\partial_\xi \mathcal{L} &= 1 - \lambda - \mu, & \lambda &= 1 - \mu.
\end{aligned}$$

After a basic derivation, we arrive at the solution of the dual problem given by

$$\lambda = -\sum_{y \in Y} v_y = \sum_{j \in \bar{Y}} v_j,$$

where v must be in the following feasible set S_Y :

$$\begin{aligned}
S_Y &\triangleq \{v \in \mathbb{R}^m \mid -\sum_{y \in Y} v_y = \sum_{j \in \bar{Y}} v_j \leq 1, \\
&\quad v_y \leq 0, v_j \geq 0, \forall y \in Y, \forall j \in \bar{Y}\}.
\end{aligned}$$

To complete the proof, note that $L^*(v) = -\lambda$ if $v \in S_Y$. \square

A.5 Proof of Proposition 6

Proof. The convex conjugate of the SVM^{ML} loss is

$$L^*(v) = \begin{cases} \sum_{y \in Y} v_y, & \text{if } v \in S_Y, \\ +\infty, & \text{otherwise.} \end{cases}$$

Before we add $\frac{\gamma}{2} \|v\|^2$, recall that $\sum_{y \in Y} v_y = -\sum_{j \in \bar{Y}} v_j$, and so $\sum_{y \in Y} v_y = \frac{1}{2}(\sum_{y \in Y} v_y - \sum_{j \in \bar{Y}} v_j)$. We use the average instead of an individual sum for symmetry and improved numerical stability. The smoothed conjugate loss is then

$$L_\gamma^*(v) = \begin{cases} \frac{1}{2}(\sum_{y \in Y} v_y - \sum_{j \in \bar{Y}} v_j) + \frac{\gamma}{2} \|v\|^2, & \text{if } v \in S_Y, \\ +\infty, & \text{otherwise.} \end{cases}$$

To derive the primal loss, we take the conjugate again:

$$\begin{aligned}
L_\gamma(u) &= \sup_v \{ \langle u, v \rangle - L_\gamma^*(v) \} \\
&= \max_{v \in S_Y} \{ \langle u, v \rangle - \frac{1}{2}(\sum_{y \in Y} v_y - \sum_{j \in \bar{Y}} v_j) - \frac{\gamma}{2} \|v\|^2 \} \\
&= -\frac{1}{\gamma} \min_{v \in S_Y} \{ \frac{1}{2} \|v\|^2 + \frac{1}{2}(\sum_{y \in Y} v_y - \sum_{j \in \bar{Y}} v_j) - \langle u, v \rangle \} \\
&= -\frac{1}{\gamma} \min_{v \in S_Y} \{ \frac{1}{2} \|v\|^2 - \sum_{y \in Y} (\frac{1}{2} - u_y)(-v_y) \\
&\quad - \sum_{j \in \bar{Y}} (\frac{1}{2} + u_j)v_j \}.
\end{aligned}$$

Next, we define the following auxiliary variables:

$$\begin{aligned}
x_j &= -v_j, & b_j &= \frac{1}{2} - u_j, & \forall j \in Y, \\
y_j &= v_j, & \bar{b}_j &= \frac{1}{2} + u_j, & \forall j \in \bar{Y},
\end{aligned}$$

and rewrite the smooth loss $L_\gamma(u)$ equivalently as

$$L_\gamma(u) = -\frac{1}{\gamma} \min_{x, y} \frac{1}{2} \|x\|^2 - \langle x, b \rangle + \frac{1}{2} \|y\|^2 - \langle y, \bar{b} \rangle$$

A.6 Proof of Proposition 7

Proof. The conjugate loss is given by $L^*(v) = \sup\{\langle u, v \rangle - L(u) \mid u \in \mathbb{R}^m\}$. Since $L(u)$ is smooth and convex in u , we compute the optimal u^* by setting the partial derivatives to zero, which leads to $v_j = \frac{\partial}{\partial u_j} L(u)$. We have

$$\frac{\partial}{\partial u_l} L(u) = \frac{1}{|Y|} \sum_{y \in Y} \frac{\partial_{u_l} (\sum_j \exp(u_j - u_y))}{\sum_j \exp(u_j - u_y)},$$

$$\partial_{u_l} (\sum_j \exp(u_j - u_y)) = \begin{cases} \exp(u_l - u_y), & l \neq y, \\ -\sum_{j \neq y} \exp(u_j - u_y), & l = y. \end{cases}$$

Therefore,

$$\frac{\partial}{\partial u_l} L(u) = \frac{1}{|Y|} \sum_{y \in Y} \frac{1}{\sum_j \exp u_j} \begin{cases} \exp u_l, & \text{if } l \neq y, \\ -\sum_{j \neq y} \exp u_j, & \text{if } l = y. \end{cases}$$

Let $Z \triangleq \sum_{j \in Y} \exp u_j$, then

$$\frac{\partial}{\partial u_l} L(u) = \frac{1}{|Y|} \sum_{y \in Y} \frac{1}{Z} \begin{cases} \exp u_l, & \text{if } l \neq y, \\ \exp u_l - Z, & \text{if } l = y. \end{cases}$$

Let $k \triangleq |Y|$, we have

$$\begin{aligned}
l \notin Y &\implies \frac{\partial}{\partial u_l} L(u) = \frac{1}{k} \sum_{y \in Y} \frac{1}{Z} \exp u_l = \frac{1}{Z} \exp u_l, \\
l \in Y &\implies \frac{\partial}{\partial u_l} L(u) = \frac{1}{kZ} (\exp u_l - Z + (k-1) \exp u_l) \\
&= \frac{1}{Z} \exp u_l - \frac{1}{k}.
\end{aligned}$$

Thus, for the supremum to be attained, we must have

$$v_j = \begin{cases} \frac{1}{Z} \exp u_j - \frac{1}{k}, & \text{if } j \in Y, \\ \frac{1}{Z} \exp u_j, & \text{if } j \in \bar{Y}, \end{cases} \quad (21)$$

which means $v_j \geq -\frac{1}{k}$ if $j \in Y$, and $v_j \geq 0$ otherwise. Moreover, we have

$$\begin{aligned}
\langle \mathbf{1}, v \rangle &= \sum_{j \in Y} (\frac{1}{Z} \exp u_j - \frac{1}{k}) + \sum_{j \in \bar{Y}} \frac{1}{Z} \exp u_j \\
&= \frac{1}{Z} \sum_{j \in Y} \exp u_j - 1 = 0
\end{aligned}$$

and

$$\begin{aligned}
\sum_{j \in Y} v_j &= \sum_{j \in Y} (\frac{1}{Z} \exp u_j - \frac{1}{k}) \leq \frac{1}{Z} \sum_j \exp u_j - 1 = 0, \\
\sum_{j \in \bar{Y}} v_j &= \sum_{j \in \bar{Y}} \frac{1}{Z} \exp u_j \leq \frac{1}{Z} \sum_j \exp u_j = 1.
\end{aligned}$$

Solving (21) for u , we get

$$u_j^* = \begin{cases} \log(v_j + \frac{1}{k}) + \log Z, & \text{if } j \in Y, \\ \log v_j + \log Z, & \text{otherwise.} \end{cases}$$

Plugging the optimal u^* , we compute the conjugate as

$$\begin{aligned}
L^*(Y, v) &= \langle u^*, v \rangle - \frac{1}{|Y|} \sum_{y \in Y} \log \left(\sum_j \exp(u_j^* - u_y^*) \right) \\
&= \sum_{y \in Y} v_y \log(v_y + \frac{1}{k}) + \sum_{j \in \bar{Y}} v_j \log v_j \\
&\quad + \sum_j v_j \log Z - \frac{1}{k} \sum_{y \in Y} (\log Z - u_y^*) \\
&= \sum_{y \in Y} v_y \log(v_y + \frac{1}{k}) + \sum_{j \in \bar{Y}} v_j \log v_j \\
&\quad + \frac{1}{k} \sum_{y \in Y} \log(v_y + \frac{1}{k})
\end{aligned}$$

$$= \sum_{y \in Y} (v_y + \frac{1}{k}) \log(v_y + \frac{1}{k}) + \sum_{j \in \bar{Y}} v_j \log v_j,$$

where $\langle \mathbf{1}, v \rangle = 0$ and

$$\begin{aligned} \sum_{y \in Y} v_y &\leq 0, & v_y + \frac{1}{k} &\geq 0, \quad y \in Y, \\ \sum_{j \in \bar{Y}} v_j &\leq 1, & v_j &\geq 0, \quad j \in \bar{Y}. \end{aligned}$$

This leads to the definition of the effective domain D_Y , since

$$\begin{aligned} 0 = \langle \mathbf{1}, v \rangle &= \sum_{y \in Y} v_y + \sum_{j \in \bar{Y}} v_j \\ &= \sum_{y \in Y} (v_y + \frac{1}{k}) + \sum_{j \in \bar{Y}} v_j - 1. \end{aligned}$$

□

APPENDIX B PROOFS FROM § 4

B.1 Proof of Lemma 1

Proof. For any $g = f(x) \in \mathbb{R}^m$, let π be a permutation such that $g_{\pi_1} \geq g_{\pi_2} \geq \dots \geq g_{\pi_m}$. The expected top- k error at x is

$$\begin{aligned} \mathbb{E}_{Y|X}[\text{err}_k(Y, g) | X = x] &= \sum_{y \in Y} \mathbb{1}[g_{\pi_k} > g_y] p_y(x) \\ &= \sum_{y \in Y} \mathbb{1}[g_{\pi_k} > g_{\pi_y}] p_{\pi_y}(x) = \sum_{j=k+1}^m p_{\pi_j}(x) \\ &= 1 - \sum_{j=1}^k p_{\pi_j}(x). \end{aligned}$$

The error is minimal when $\sum_{j=1}^k p_{\pi_j}(x)$ is maximal, which corresponds to taking the k largest conditional probabilities $\sum_{j=1}^k p_{\tau_j}(x)$ and yields the Bayes optimal top- k error at x .

Since the relative order within $\{p_{\tau_j}(x)\}_{j=1}^k$ is irrelevant for the top- k error, any classifier $f(x)$, for which the sets $\{\pi_1, \dots, \pi_k\}$ and $\{\tau_1, \dots, \tau_k\}$ coincide, is Bayes optimal.

Note that we assumed w.l.o.g. that there is a clear cut $p_{\tau_k}(x) > p_{\tau_{k+1}}(x)$ between the k most likely classes and the rest. In general, ties can be resolved arbitrarily as long as we can guarantee that the k largest components of $f(x)$ correspond to the classes (indexes) that yield the maximal sum $\sum_{j=1}^k p_{\pi_j}(x)$ and lead to top- k Bayes optimality. □

B.2 Proof of Proposition 8

Proof. First, we show that the Bayes optimal function for the binary hinge loss is

$$f^*(x) = 2 \mathbb{1}[\Pr(Y = 1 | X = x) > \frac{1}{2}] - 1.$$

We decompose the expected loss as

$$\mathbb{E}_{X,Y}[L(Y, f(X))] = \mathbb{E}_X[\mathbb{E}_{Y|X}[L(Y, f(x)) | X = x]].$$

Thus, one can compute the Bayes optimal classifier f^* pointwise by solving

$$\arg \min_{\alpha \in \mathbb{R}} \mathbb{E}_{Y|X}[L(Y, \alpha) | X = x],$$

for every $x \in \mathbb{R}^d$, which leads to the following problem

$$\arg \min_{\alpha \in \mathbb{R}} \max\{0, 1 - \alpha\} p_1(x) + \max\{0, 1 + \alpha\} p_{-1}(x),$$

where $p_y(x) \triangleq \Pr(Y = y | X = x)$. It is obvious that the optimal α^* is contained in $[-1, 1]$. We get

$$\arg \min_{-1 \leq \alpha \leq 1} (1 - \alpha) p_1(x) + (1 + \alpha) p_{-1}(x).$$

The minimum is attained at the boundary and we get

$$f^*(x) = \begin{cases} +1 & \text{if } p_1(x) > \frac{1}{2}, \\ -1 & \text{if } p_1(x) \leq \frac{1}{2}. \end{cases}$$

Therefore, the Bayes optimal classifier for the hinge loss is not a strictly monotonically increasing function of $p_1(x)$.

To show that OVA hinge is not top- k calibrated, we construct an example problem with 3 classes and $p_1(x) = 0.4$, $p_2(x) = p_3(x) = 0.3$. Note that for every class $y = 1, 2, 3$, the Bayes optimal binary classifier is -1 , hence the predicted ranking of labels is arbitrary and may not produce the Bayes optimal top- k error. □

B.3 Proof of Proposition 9

Proof. First, we show that the Bayes optimal function for the binary logistic loss is

$$f^*(x) = \log \left(\frac{p_1(x)}{1 - p_1(x)} \right).$$

As above, the pointwise optimization problem is

$$\arg \min_{\alpha \in \mathbb{R}} \log(1 + \exp(-\alpha)) p_1(x) + \log(1 + \exp(\alpha)) p_{-1}(x).$$

The logistic loss is known to be convex and differentiable and thus the optimum can be computed via

$$\frac{-\exp(-\alpha)}{1 + \exp(-\alpha)} p_1(x) + \frac{\exp(\alpha)}{1 + \exp(\alpha)} p_{-1}(x) = 0.$$

Re-writing the first fraction we get

$$\frac{-1}{1 + \exp(\alpha)} p_1(x) + \frac{\exp(\alpha)}{1 + \exp(\alpha)} p_{-1}(x) = 0,$$

which can be solved as $\alpha^* = \log \left(\frac{p_1(x)}{p_{-1}(x)} \right)$ and leads to the formula for the Bayes optimal classifier stated above.

We check now that the function $\phi : (0, 1) \rightarrow \mathbb{R}$ defined as $\phi(x) = \log \left(\frac{x}{1-x} \right)$ is strictly monotonically increasing.

$$\begin{aligned} \phi'(x) &= \frac{1-x}{x} \left(\frac{1}{1-x} + \frac{x}{(1-x)^2} \right) \\ &= \frac{1-x}{x} \frac{1}{(1-x)^2} = \frac{1}{x(1-x)} > 0, \quad \forall x \in (0, 1). \end{aligned}$$

The derivative is strictly positive on $(0, 1)$, which implies that ϕ is strictly monotonically increasing. The logistic loss, therefore, fulfills the conditions of Lemma 2 and is top- k calibrated for any $1 \leq k \leq m$. □

B.4 Proof of Proposition 10

Proof. In order to derive the smooth hinge loss, we first compute the conjugate of the standard binary hinge loss,

$$\begin{aligned} L(\alpha) &= \max\{0, 1 - \alpha\}, \\ L^*(\beta) &= \sup_{\alpha \in \mathbb{R}} \{\alpha\beta - \max\{0, 1 - \alpha\}\} \\ &= \begin{cases} \beta & \text{if } -1 \leq \beta \leq 0, \\ \infty & \text{otherwise.} \end{cases} \end{aligned} \quad (22)$$

The smoothed conjugate is

$$L_\gamma^*(\beta) = L^*(\beta) + \frac{\gamma}{2} \beta^2.$$

The corresponding primal smooth hinge loss is given by

$$L_\gamma(\alpha) = \sup_{-1 \leq \beta \leq 0} \{ \alpha\beta - \beta - \frac{\gamma}{2}\beta^2 \} \\ = \begin{cases} 1 - \alpha - \frac{\gamma}{2} & \text{if } \alpha < 1 - \gamma, \\ \frac{(\alpha-1)^2}{2\gamma} & \text{if } 1 - \gamma \leq \alpha \leq 1, \\ 0, & \text{if } \alpha > 1. \end{cases} \quad (23)$$

$L_\gamma(\alpha)$ is convex and differentiable with the derivative

$$L'_\gamma(\alpha) = \begin{cases} -1 & \text{if } \alpha < 1 - \gamma, \\ \frac{\alpha-1}{\gamma} & \text{if } 1 - \gamma \leq \alpha \leq 1, \\ 0, & \text{if } \alpha > 1. \end{cases}$$

We compute the Bayes optimal classifier pointwise.

$$f^*(x) = \arg \min_{\alpha \in \mathbb{R}} L(\alpha)p_1(x) + L(-\alpha)p_{-1}(x).$$

Let $p \triangleq p_1(x)$, the optimal α^* is found by solving

$$L'(\alpha)p - L'(-\alpha)(1-p) = 0.$$

Case 0 $0 < \gamma \leq 1$. Consider the case $1 - \gamma \leq \alpha \leq 1$,

$$\frac{\alpha-1}{\gamma}p + (1-p) = 0 \implies \alpha^* = 1 - \gamma \frac{1-p}{p}.$$

This case corresponds to $p \geq \frac{1}{2}$, which follows from the constraint $\alpha^* \geq 1 - \gamma$. Next, consider $\gamma - 1 \leq \alpha \leq 1 - \gamma$,

$$-p + (1-p) = 1 - 2p \neq 0,$$

unless $p = \frac{1}{2}$, which is already captured by the first case. Finally, consider $-1 \leq \alpha \leq \gamma - 1 \leq 1 - \gamma$. Then

$$-p - \frac{-\alpha-1}{\gamma}(1-p) = 0 \implies \alpha^* = -1 + \gamma \frac{p}{1-p},$$

where we have $-1 \leq \alpha^* \leq \gamma - 1$ if $p \leq \frac{1}{2}$. We obtain the Bayes optimal classifier for $0 < \gamma \leq 1$ as follows:

$$f^*(x) = \begin{cases} 1 - \gamma \frac{1-p}{p} & \text{if } p \geq \frac{1}{2}, \\ -1 + \gamma \frac{p}{1-p} & \text{if } p < \frac{1}{2}. \end{cases}$$

Note that while $f^*(x)$ is not a continuous function of $p = p_1(x)$ for $\gamma < 1$, it is still a strictly monotonically increasing function of p for any $0 < \gamma \leq 1$.

Case $\gamma > 1$. First, consider $\gamma - 1 \leq \alpha \leq 1$,

$$\frac{\alpha-1}{\gamma}p + (1-p) = 0 \implies \alpha^* = 1 - \gamma \frac{1-p}{p}.$$

From $\alpha^* \geq \gamma - 1$, we get the condition $p \geq \frac{\gamma}{2}$. Next, consider $1 - \gamma \leq \alpha \leq \gamma - 1$,

$$\frac{\alpha-1}{\gamma}p - \frac{-\alpha-1}{\gamma}(1-p) = 0 \implies \alpha^* = 2p - 1,$$

which is in the range $[1 - \gamma, \gamma - 1]$ if $1 - \frac{\gamma}{2} \leq p \leq \frac{\gamma}{2}$. Finally, consider $-1 \leq \alpha \leq 1 - \gamma$,

$$-p - \frac{-\alpha-1}{\gamma}(1-p) = 0 \implies \alpha^* = -1 + \gamma \frac{p}{1-p},$$

where we have $-1 \leq \alpha^* \leq 1 - \gamma$ if $p \leq 1 - \frac{\gamma}{2}$. Overall, the Bayes optimal classifier for $\gamma > 1$ is

$$f^*(x) = \begin{cases} 1 - \gamma \frac{1-p}{p} & \text{if } p \geq \frac{\gamma}{2}, \\ 2p - 1 & \text{if } 1 - \frac{\gamma}{2} \leq p \leq \frac{\gamma}{2}, \\ -1 + \gamma \frac{p}{1-p} & \text{if } p < 1 - \frac{\gamma}{2}. \end{cases}$$

Note that f^* is again a strictly monotonically increasing function of $p = p_1(x)$. Therefore, for any $\gamma > 0$, the one-vs-all scheme with the smooth hinge loss (23) is top- k calibrated for all $1 \leq k \leq m$ by Lemma 2. \square

B.5 Proof of Proposition 11

Proof. Let $y \in \arg \max_{j \in \mathcal{Y}} p_j(x)$. Given any $c \in \mathbb{R}$, we will show that a Bayes optimal classifier $f^* : \mathbb{R}^d \rightarrow \mathbb{R}^m$ for the SVM^{Multi} loss is

$$f_y^*(x) = \begin{cases} c + 1 & \text{if } \max_{j \in \mathcal{Y}} p_j(x) \geq \frac{1}{2}, \\ c & \text{otherwise,} \end{cases} \\ f_j^*(x) = c, \quad j \in \mathcal{Y} \setminus \{y\}.$$

Let $g = f(x) \in \mathbb{R}^m$, then

$$\mathbb{E}_{Y|X}[L(Y, g) | X] = \sum_{l \in \mathcal{Y}} \max_{j \in \mathcal{Y}} \{ \mathbb{I}[j \neq l] + g_j - g_l \} p_l(x).$$

Suppose that the maximum of $(g_j)_{j \in \mathcal{Y}}$ is not unique. In this case, we have

$$\max_{j \in \mathcal{Y}} \{ \mathbb{I}[j \neq l] + g_j - g_l \} \geq 1, \quad \forall l \in \mathcal{Y}$$

as the term $\mathbb{I}[j \neq l]$ is always active. The best possible loss is obtained by setting $g_j = c$ for all $j \in \mathcal{Y}$, which yields an expected loss of 1. On the other hand, if the maximum is unique and is achieved by g_y , then

$$\max_{j \in \mathcal{Y}} \{ \mathbb{I}[j \neq l] + g_j - g_l \} \\ = \begin{cases} 1 + g_y - g_l & \text{if } l \neq y, \\ \max \{ 0, \max_{j \neq y} \{ 1 + g_j - g_y \} \} & \text{if } l = y. \end{cases}$$

As the loss only depends on the gap $g_y - g_l$, we can optimize this with $\beta_l = g_y - g_l$.

$$\mathbb{E}_{Y|X}[L(Y, g) | X = x] \\ = \sum_{l \neq y} (1 + g_y - g_l) p_l(x) \\ + \max \{ 0, \max_{l \neq y} \{ 1 + g_l - g_y \} \} p_y(x) \\ = \sum_{l \neq y} (1 + \beta_l) p_l(x) + \max \{ 0, \max_{l \neq y} \{ 1 - \beta_l \} \} p_y(x) \\ = \sum_{l \neq y} (1 + \beta_l) p_l(x) + \max \{ 0, 1 - \min_{l \neq y} \beta_l \} p_y(x).$$

As only the minimal β_l enters the last term, the optimum is achieved if all β_l are equal for $l \neq y$ (otherwise it is possible to reduce the first term without affecting the last term). Let $\alpha \triangleq \beta_l$ for all $l \neq y$. The problem becomes

$$\min_{\alpha \geq 0} \sum_{l \neq y} (1 + \alpha) p_l(x) + \max \{ 0, 1 - \alpha \} p_y(x) \\ \equiv \min_{0 \leq \alpha \leq 1} \alpha(1 - 2p_y(x))$$

Let $p \triangleq p_y(x) = \Pr(Y = y | X = x)$. The solution is

$$\alpha^* = \begin{cases} 0 & \text{if } p < \frac{1}{2}, \\ 1 & \text{if } p \geq \frac{1}{2}, \end{cases}$$

and the associated risk is

$$\mathbb{E}_{Y|X}[L(Y, g) | X = x] = \begin{cases} 1 & \text{if } p < \frac{1}{2}, \\ 2(1-p) & \text{if } p \geq \frac{1}{2}. \end{cases}$$

If $p < \frac{1}{2}$, then the Bayes optimal classifier $f_j^*(x) = c$ for all $j \in \mathcal{Y}$ and any $c \in \mathbb{R}$. Otherwise, $p \geq \frac{1}{2}$ and

$$f_j^*(x) = \begin{cases} c+1 & \text{if } j = y, \\ c & \text{if } j \in \mathcal{Y} \setminus \{y\}. \end{cases}$$

Moreover, we have that the Bayes risk at x is

$$\mathbb{E}_{Y|X}[L(Y, f^*(x)) | X = x] = \min\{1, 2(1-p)\} \leq 1.$$

It follows, that the multiclass hinge loss is not (top-1) classification calibrated at any x where $\max_{y \in \mathcal{Y}} p_y(x) < \frac{1}{2}$ as its Bayes optimal classifier reduces to a constant. Moreover, even if $p_y(x) \geq \frac{1}{2}$ for some y , the loss is not top- k calibrated for $k \geq 2$ as the predicted order of the remaining classes need not be optimal. \square

B.6 Proof of Proposition 12

Proof. The multiclass softmax loss is (top-1) calibrated for the zero-one error in the following sense. If

$$f^*(x) \in \arg \min_{g \in \mathbb{R}^m} \mathbb{E}_{Y|X}[L(Y, g) | X = x],$$

then for some $\alpha > 0$ and all $y \in \mathcal{Y}$

$$f_y^*(x) = \begin{cases} \log(\alpha p_y(x)) & \text{if } p_y(x) > 0, \\ -\infty & \text{otherwise,} \end{cases}$$

which implies

$$\arg \max_{y \in \mathcal{Y}} f_y^*(x) = \arg \max_{y \in \mathcal{Y}} \Pr(Y = y | X = x).$$

We now prove this result and show that it also generalizes to top- k calibration for $k > 1$. Using the identity

$$L(y, g) = \log \left(\sum_{j \in \mathcal{Y}} e^{g_j - g_y} \right) = \log \left(\sum_{j \in \mathcal{Y}} e^{g_j} \right) - g_y$$

and the fact that $\sum_{y \in \mathcal{Y}} p_y(x) = 1$, we write for a $g \in \mathbb{R}^m$

$$\begin{aligned} \mathbb{E}_{Y|X}[L(Y, g) | X = x] &= \sum_{y \in \mathcal{Y}} L(y, g) p_y(x) = \log \left(\sum_{y \in \mathcal{Y}} e^{g_y} \right) - \sum_{y \in \mathcal{Y}} g_y p_x(y). \end{aligned}$$

As the loss is convex and differentiable, we get the global optimum by computing a critical point. We have

$$\frac{\partial}{\partial g_j} \mathbb{E}_{Y|X}[L(Y, g) | X = x] = \frac{e^{g_j}}{\sum_{y \in \mathcal{Y}} e^{g_y}} - p_j(x) = 0$$

for $j \in \mathcal{Y}$. We note that the critical point is not unique as multiplication $g \rightarrow \kappa g$ leaves the equation invariant for any $\kappa > 0$. One can verify that $e^{g_j} = \alpha p_j(x)$ satisfies the equations for any $\alpha > 0$. This yields a solution

$$f_y^*(x) = \begin{cases} \log(\alpha p_y(x)) & \text{if } p_y(x) > 0, \\ -\infty & \text{otherwise,} \end{cases}$$

for any fixed $\alpha > 0$. We note that f_y^* is a strictly monotonically increasing function of the conditional class probabilities. Therefore, it preserves the ranking of $p_y(x)$ and implies that f^* is top- k calibrated for any $1 \leq k \leq m$. \square

B.7 Proof of Proposition 13

Proof. Given any $g = f(x) \in \mathbb{R}^m$, let π be a permutation such that $g_{\pi_1} \geq g_{\pi_2} \geq \dots \geq g_{\pi_m}$. Then, we have

$$\mathcal{J}_y = \begin{cases} \{\pi_{k+1}, \dots, \pi_m\} & \text{if } y \in \{\pi_1, \dots, \pi_{k-1}\}, \\ \{\pi_k, \dots, \pi_m\} \setminus \{y\} & \text{if } y \in \{\pi_k, \dots, \pi_m\}. \end{cases}$$

Therefore, the expected loss at x can be written as

$$\begin{aligned} \mathbb{E}_{Y|X}[L(Y, g) | X = x] &= \sum_{y \in \mathcal{Y}} L(y, g) p_y(x) \\ &= \sum_{r=1}^{k-1} \log \left(1 + \sum_{j=k+1}^m e^{g_{\pi_j} - g_{\pi_r}} \right) p_{\pi_r}(x) \\ &\quad + \sum_{r=k}^m \log \left(\sum_{j=k}^m e^{g_{\pi_j} - g_{\pi_r}} \right) p_{\pi_r}(x). \end{aligned}$$

Note that the sum inside the logarithm does not depend on g_{π_r} for $r < k$. Therefore, a Bayes optimal classifier will have $g_{\pi_r} = +\infty$ for all $r < k$ as then the first sum vanishes.

Let $p \triangleq (p_y(x))_{y \in \mathcal{Y}}$ and $q \triangleq (L(y, g))_{y \in \mathcal{Y}}$, then

$$q_{\pi_1} = \dots = q_{\pi_{k-1}} = 0 \leq q_{\pi_k} \leq \dots \leq q_{\pi_m}$$

and we can re-write the expected loss as

$$\mathbb{E}_{Y|X}[L(Y, g) | X = x] = \langle p, q \rangle = \langle p_\pi, q_\pi \rangle \geq \langle p_\tau, q_\pi \rangle,$$

where $p_{\tau_1} \geq p_{\tau_2} \geq \dots \geq p_{\tau_m}$ and we used the rearrangement inequality. Therefore, the expected loss is minimized when π and τ coincide (up to a permutation of the first $k-1$ elements), which already establishes top- s calibration for all $s \geq k$.

We can also derive a Bayes optimal classifier following the proof of Proposition 12. We have

$$\begin{aligned} \mathbb{E}_{Y|X}[L(Y, g) | X = x] &= \sum_{r=k}^m \log \left(\sum_{j=k}^m e^{g_{\tau_j} - g_{\tau_r}} \right) p_{\tau_r}(x) \\ &= \sum_{r=k}^m \left(\log \left(\sum_{j=k}^m e^{g_{\tau_j}} \right) - g_{\tau_r} \right) p_{\tau_r}(x). \end{aligned}$$

A critical point is found by setting partial derivatives to zero for all $y \in \{\tau_k, \dots, \tau_m\}$, which leads to

$$\frac{e^{g_y}}{\sum_{j=k}^m e^{g_{\tau_j}}} \sum_{r=k}^m p_{\tau_r}(x) = p_y(x).$$

We let $g_y = -\infty$ if $p_y(x) = 0$, and obtain finally

$$g_{\tau_j}^* = \begin{cases} +\infty & \text{if } j < k, \\ \log(\alpha p_{\tau_j}(x)) & \text{if } j \geq k \text{ and } p_{\tau_j}(x) > 0, \\ -\infty & \text{if } j \geq k \text{ and } p_{\tau_j}(x) = 0, \end{cases}$$

as a Bayes optimal classifier for any $\alpha > 0$.

Note that g^* preserves the ranking of $p_y(x)$ for all y in $\{\tau_k, \dots, \tau_m\}$, hence, it is top- s calibrated for all $s \geq k$. \square

APPENDIX C

PROOFS FROM § 5

C.1 Proof of Proposition 14

Proof. We follow the proof of [9, Proposition 4]. Choose an $i \in \{1, \dots, n\}$ and update a_i to maximize

$$-\frac{1}{n} L^*(y_i, -\lambda n a_i) - \frac{\lambda}{2} \text{tr} \left(A K A^\top \right).$$

For the nonsmooth top- k hinge loss, it was shown [9] that

$$L^*(y_i, -\lambda n a_i) = \langle c, \lambda n (a_i - a_{y_i, i} e_{y_i}) \rangle$$

if $-\lambda n(a_i - a_{y_i,i}e_{y_i}) \in \Delta_k^\alpha$ and $+\infty$ otherwise. Now, for the smoothed loss, we add regularization and obtain

$$-\frac{1}{n} \left(\frac{\gamma}{2} \|\lambda n(a_i - a_{y_i,i}e_{y_i})\|^2 + \langle c, \lambda n(a_i - a_{y_i,i}e_{y_i}) \rangle \right)$$

with $-\lambda n(a_i - a_{y_i,i}e_{y_i}) \in \Delta_k^\alpha$. Using $c = \mathbf{1} - e_{y_i}$ and $\langle \mathbf{1}, a_i \rangle = 0$, one can simplify it to

$$-\frac{\gamma n \lambda^2}{2} \|a_i^{\setminus y_i}\|^2 + \lambda a_{y_i,i},$$

and the feasibility constraint can be re-written as

$$-a_i^{\setminus y_i} \in \Delta_k^\alpha \left(\frac{1}{\lambda n} \right), \quad a_{y_i,i} = \langle \mathbf{1}, -a_i^{\setminus y_i} \rangle.$$

For the regularization term $\text{tr}(AKA^\top)$, we have

$$\text{tr}(AKA^\top) = K_{ii} \langle a_i, a_i \rangle + 2 \sum_{j \neq i} K_{ij} \langle a_i, a_j \rangle + \text{const.}$$

We let $q = \sum_{j \neq i} K_{ij} a_j = AK_i - K_{ii} a_i$ and $x = -a_i^{\setminus y_i}$:

$$\begin{aligned} \langle a_i, a_i \rangle &= \langle \mathbf{1}, x \rangle^2 + \langle x, x \rangle, \\ \langle q, a_i \rangle &= q_{y_i} \langle \mathbf{1}, x \rangle - \langle q^{\setminus y_i}, x \rangle. \end{aligned}$$

Now, we plug everything together and multiply with $-2/\lambda$.

$$\begin{aligned} \min_{x \in \Delta_k^\alpha \left(\frac{1}{\lambda n} \right)} \gamma \lambda n \|x\|^2 - 2 \langle \mathbf{1}, x \rangle + 2(q_{y_i} \langle \mathbf{1}, x \rangle - \langle q^{\setminus y_i}, x \rangle) \\ + K_{ii} (\langle \mathbf{1}, x \rangle^2 + \langle x, x \rangle). \end{aligned}$$

Collecting the corresponding terms finishes the proof. \square

C.2 Proof of Proposition 15

Proof. Let $v \triangleq -\lambda n a_i$ and $y = y_i$. Using Proposition 3,

$$L^*(v) = \sum_{j \neq y} v_j \log v_j + (1 + v_y) \log(1 + v_y),$$

where $\langle \mathbf{1}, v \rangle = 0$ and $v^{\setminus y} \in \Delta_k^\alpha$. Let $x \triangleq v^{\setminus y}$ and $s \triangleq -v_y$. We have $s = \langle \mathbf{1}, x \rangle$ and from $\text{tr}(AKA^\top)$ we get

$$K_{ii} (\langle x, x \rangle + s^2) / (\lambda n)^2 - 2 \langle q^{\setminus y} - q_y \mathbf{1}, x \rangle / (\lambda n),$$

where $q = \sum_{j \neq i} K_{ij} a_j = AK_i - K_{ii} a_i$. Finally, we plug everything together as in Proposition 14. \square

C.3 Proof of Proposition 16

Proof. The Lagrangian of (11) is given by

$$\begin{aligned} \mathcal{L}(x, s, t, \lambda, \mu, \nu) &= \frac{\alpha}{2} (\langle x, x \rangle + s^2) - \langle b, x \rangle + \langle x, \log x \rangle \\ &+ (1-s) \log(1-s) + t (\langle \mathbf{1}, x \rangle - s) \\ &+ \lambda (s-1) - \langle \mu, x \rangle + \langle \nu, x - \frac{s}{k} \mathbf{1} \rangle, \end{aligned}$$

where $t \in \mathbb{R}$, $\lambda, \mu, \nu \geq 0$ are the dual variables. Computing partial derivatives of \mathcal{L} w.r.t. x_j and s , and setting them to zero, we obtain

$$\begin{aligned} \alpha x_j + \log x_j &= b_j - 1 - t + \mu_j - \nu_j, \quad \forall j, \\ \alpha(1-s) + \log(1-s) &= \alpha - 1 - t - \lambda - \frac{1}{k} \langle \mathbf{1}, \nu \rangle, \quad \forall j. \end{aligned}$$

Note that only $x_j > 0$ and $s < 1$ satisfy the above constraints, which implies $\mu_j = 0$ and $\lambda = 0$. We re-write the above as

$$\begin{aligned} \alpha x_j + \log(\alpha x_j) &= b_j - 1 - t + \log \alpha - \nu_j, \\ \alpha(1-s) + \log(\alpha(1-s)) &= \alpha - 1 - t + \log \alpha - \frac{\langle \mathbf{1}, \nu \rangle}{k}. \end{aligned}$$

These equations correspond to the Lambert W function of the exponent, $V(t) = W(e^t)$, discussed in § 5.1. Let $p \triangleq \langle \mathbf{1}, \nu \rangle$ and re-define $t \leftarrow 1 + t - \log \alpha$.

$$\begin{aligned} \alpha x_j &= W(\exp(b_j - t - \nu_j)), \\ \alpha(1-s) &= W(\exp(\alpha - t - \frac{p}{k})). \end{aligned}$$

Finally, we obtain the following system:

$$\begin{aligned} \alpha x_j &= V(b_j - t - \nu_j), \quad \forall j \\ \alpha(1-s) &= V(\alpha - t - \frac{p}{k}), \\ s &= \langle \mathbf{1}, x \rangle, \quad p = \langle \mathbf{1}, \nu \rangle. \end{aligned}$$

Note that $V(t)$ is a strictly monotonically increasing function, therefore, it is invertible and we can write

$$\begin{aligned} b_j - t - \nu_j &= V^{-1}(\alpha x_j), \\ \alpha - t - \frac{p}{k} &= V^{-1}(\alpha(1-s)). \end{aligned}$$

Next, we use the definition of the sets U and M ,

$$\begin{aligned} s &= \langle \mathbf{1}, x \rangle = \sum_U \frac{s}{k} + \sum_M \frac{1}{\alpha} V(b_j - t), \\ p &= \langle \mathbf{1}, \nu \rangle = \sum_U b_j - |U| (t + V^{-1}(\frac{\alpha s}{k})). \end{aligned}$$

Let $\rho \triangleq \frac{|U|}{k}$ and $A \triangleq \frac{1}{k} \sum_U b_j$, we get

$$\begin{aligned} (1-\rho)s &= \frac{1}{\alpha} \sum_M V(b_j - t), \\ \frac{p}{k} &= A - \rho(t + V^{-1}(\frac{\alpha s}{k})). \end{aligned}$$

Finally, we eliminate p and obtain the system:

$$\begin{aligned} \alpha(1-\rho)s - \sum_M V(b_j - t) &= 0, \\ (1-\rho)t + V^{-1}(\alpha(1-s)) - \rho V^{-1}(\frac{\alpha s}{k}) + A - \alpha &= 0. \end{aligned}$$

Moreover, when U is empty, it simplifies into a single equation

$$V(\alpha - t) + \sum_M V(b_j - t) = \alpha. \quad \square$$

C.4 Proof of Proposition 17

Proof. We continue the derivation started in the proof of Proposition 4. First, we write the system that follows directly from the KKT [109] optimality conditions.

$$\begin{aligned} x_j &= \min\{\exp(a_j - t), \frac{s}{k}\}, \quad \forall j, \\ \nu_j &= \max\{0, a_j - t - \log(\frac{s}{k})\}, \quad \forall j, \\ 1-s &= \exp(-t - \frac{p}{k}), \\ s &= \langle \mathbf{1}, x \rangle, \quad p = \langle \mathbf{1}, \nu \rangle. \end{aligned} \quad (24)$$

Next, we define the two index sets U and M as follows

$$U \triangleq \{j \mid x_j = \frac{s}{k}\}, \quad M \triangleq \{j \mid x_j < \frac{s}{k}\}.$$

Note that the set U contains at most k indexes corresponding to the largest components of a_j . Now, we proceed with finding a t that solves (24). Let $\rho \triangleq \frac{|U|}{k}$. We eliminate p as

$$\begin{aligned} p &= \sum_j \nu_j = \sum_U a_j - |U| (t + \log(\frac{s}{k})) \implies \\ \frac{p}{k} &= \frac{1}{k} \sum_U a_j - \rho(t + \log(\frac{s}{k})). \end{aligned}$$

Let $Z \triangleq \sum_M \exp a_j$, we write for s

$$\begin{aligned} s &= \sum_j x_j = \sum_U \frac{s}{k} + \sum_M \exp(a_j - t) \\ &= \rho s + \exp(-t) \sum_M \exp a_j = \rho s + \exp(-t) Z. \end{aligned}$$

We conclude that

$$\begin{aligned} (1 - \rho)s &= \exp(-t)Z \implies \\ t &= \log Z - \log((1 - \rho)s). \end{aligned}$$

Let $A \triangleq \frac{1}{k} \sum_U a_j$. We further write

$$\begin{aligned} \log(1 - s) &= -t - \frac{\rho}{k} = -t - A + \rho(t + \log(\frac{s}{k})) \\ &= \rho \log(\frac{s}{k}) - A - (1 - \rho)[\log Z - \log((1 - \rho)s)], \end{aligned}$$

which yields the following equation for s

$$\begin{aligned} \log(1 - s) - \rho(\log s - \log k) + A \\ + (1 - \rho)[\log Z - \log(1 - \rho) - \log s] &= 0. \end{aligned}$$

Therefore,

$$\begin{aligned} \log(1 - s) - \log s + \rho \log k + A \\ + (1 - \rho) \log Z - (1 - \rho) \log(1 - \rho) &= 0, \\ \log\left(\frac{1 - s}{s}\right) &= \log\left(\frac{(1 - \rho)^{(1 - \rho)} \exp(-A)}{k^\rho Z^{(1 - \rho)}}\right). \end{aligned}$$

We finally get

$$\begin{aligned} s &= 1/(1 + Q), \\ Q &\triangleq (1 - \rho)^{(1 - \rho)} / (k^\rho Z^{(1 - \rho)} e^A). \end{aligned}$$

We note that: a) Q is readily computable once the sets U and M are fixed; and b) $Q = 1/Z$ if $k = 1$ since $\rho = A = 0$ in that case. This yields the formula for t as

$$t = \log Z + \log(1 + Q) - \log(1 - \rho).$$

As a sanity check, we note that we again recover the softmax loss for $k = 1$, since $t = \log Z + \log(1 + 1/Z) = \log(1 + Z) = \log(1 + \sum_j \exp a_j)$.

To verify that the computed s and t are compatible with the choice of the sets U and M , we check if this holds:

$$\begin{aligned} \exp(a_j - t) &\geq \frac{s}{k}, \quad \forall j \in U, \\ \exp(a_j - t) &\leq \frac{s}{k}, \quad \forall j \in M, \end{aligned}$$

which is equivalent to

$$\max_M a_j \leq \log(\frac{s}{k}) + t \leq \min_U a_j.$$

To compute the actual loss (15), we have

$$\begin{aligned} \langle a, x \rangle - \langle x, \log x \rangle - (1 - s) \log(1 - s) \\ &= \sum_U a_j \frac{s}{k} + \sum_M a_j \exp(a_j - t) - \sum_U \frac{s}{k} \log(\frac{s}{k}) \\ &\quad - \sum_M (a_j - t) \exp(a_j - t) - (1 - s) \log(1 - s) \\ &= As - \rho s \log(\frac{s}{k}) + t \exp(-t) Z - (1 - s) \log(1 - s) \\ &= As - \rho s \log(\frac{s}{k}) + (1 - \rho)st - (1 - s) \log(1 - s). \end{aligned}$$

□

C.5 Proof of Proposition 18

Proof. We update the dual variables $a \triangleq a_i \in \mathbb{R}^m$ corresponding to the training example (x_i, Y_i) by solving the following optimization problem.

$$\max_{a \in \mathbb{R}^m} -\frac{1}{n} L_\gamma^*(Y_i, -\lambda n a) - \frac{\lambda}{2} \text{tr}(AKA^\top),$$

where $\lambda > 0$ is a regularization parameter. Equivalently, we can divide both the primal and the dual objectives by λ and use $C \triangleq \frac{1}{\lambda n} > 0$ as the regularization parameter instead. The optimization problem becomes

$$\max_{a \in \mathbb{R}^m} -CL^*(Y_i, -\frac{1}{C}a) - \frac{1}{2} \text{tr}(AKA^\top). \quad (25)$$

Note that

$$\text{tr}(AKA^\top) = K_{ii} \langle a, a \rangle + 2 \sum_{j \neq i} K_{ij} \langle a_j, a \rangle + \text{const},$$

where the const does not depend on a . We ignore that constant in the following derivation and also define an auxiliary vector $q \triangleq \sum_{j \neq i} K_{ij} a_j = AK_i - K_{ii} a_i$. Plugging the conjugate from Proposition 6 into (25), we obtain

$$\begin{aligned} \max_{a \in \mathbb{R}^m} -C \left(\frac{1}{2C} (-\sum_{y \in Y_i} a_y + \sum_{j \in \bar{Y}_i} a_j) + \frac{\gamma}{2C^2} \|a\|^2 \right) \\ - (1/2)(K_{ii} \|a\|^2 + 2 \langle q, a \rangle) \\ \text{s.t. } -\frac{1}{C} a \in S_{Y_i} \end{aligned}$$

We re-write the constraint $-\frac{1}{C} a \in S_{Y_i}$ as

$$\begin{aligned} \sum_{y \in Y_i} a_y &= -\sum_{j \in \bar{Y}_i} a_j \leq C \\ a_y &\geq 0, \quad \forall y \in Y_i; \quad a_j \leq 0, \quad \forall j \in \bar{Y}_i; \end{aligned}$$

and switch to the equivalent minimization problem below.

$$\begin{aligned} \min_{a \in \mathbb{R}^m} \frac{1}{2} (K_{ii} + \frac{\gamma}{C}) \|a\|^2 - \frac{1}{2} \sum_{y \in Y_i} a_y - \frac{1}{2} \sum_{j \in \bar{Y}_i} (-a_j) \\ + \langle q, a \rangle \\ \sum_{y \in Y_i} a_y &= \sum_{j \in \bar{Y}_i} -a_j \leq C \\ a_y &\geq 0, \quad \forall y \in Y_i; \quad -a_j \geq 0, \quad \forall j \in \bar{Y}_i. \end{aligned}$$

Note that

$$\begin{aligned} -\frac{1}{2} \sum_{y \in Y_i} a_y - \frac{1}{2} \sum_{j \in \bar{Y}_i} (-a_j) + \langle q, a \rangle \\ = -\sum_{y \in Y_i} (\frac{1}{2} - q_y) a_y - \sum_{j \in \bar{Y}_i} (\frac{1}{2} + q_j) (-a_j), \end{aligned}$$

and let us define

$$\begin{aligned} x \triangleq (a_y)_{y \in Y_i} \in \mathbb{R}^{|Y_i|}, \quad b \triangleq \frac{1}{K_{ii} + \gamma/C} (\frac{1}{2} - q_y)_{y \in Y_i} \in \mathbb{R}^{|Y_i|}, \\ y \triangleq (-a_j)_{j \in \bar{Y}_i} \in \mathbb{R}^{|\bar{Y}_i|}, \quad \bar{b} \triangleq \frac{1}{K_{ii} + \gamma/C} (\frac{1}{2} + q_j)_{j \in \bar{Y}_i} \in \mathbb{R}^{|\bar{Y}_i|}. \end{aligned}$$

The final projection problem for the update step is

$$\begin{aligned} \min_{x, y} \frac{1}{2} \|x - b\|^2 + \frac{1}{2} \|y - \bar{b}\|^2 \\ \langle \mathbf{1}, x \rangle = \langle \mathbf{1}, y \rangle \leq C \\ x \geq 0, \quad y \geq 0. \end{aligned} \quad (26)$$

□

C.6 Proof of Proposition 19

Proof. We sketch the main parts of the proof that show correctness of the algorithm. A complete and formal derivation would follow the proof given in [65].

The Lagrangian for the optimization problem (17) is

$$\mathcal{L}(x, y, t, s, \lambda, \mu, \nu) = \frac{1}{2} \|x - b\|^2 + \frac{1}{2} \|y - \bar{b}\|^2 + t(\langle \mathbf{1}, x \rangle - r) + s(\langle \mathbf{1}, y \rangle - r) + \lambda(r - \rho) - \langle \mu, x \rangle - \langle \nu, y \rangle,$$

and it leads to the following KKT conditions

$$\begin{aligned} x_j &= b_j - t + \mu_j, & \mu_j x_j &= 0, & \mu_j &\geq 0, \\ y_k &= \bar{b}_k - s + \nu_k, & \nu_k y_k &= 0, & \nu_k &\geq 0, \\ \lambda &= t + s, & \lambda(r - \rho) &= 0, & \lambda &\geq 0. \end{aligned} \quad (27)$$

If $\rho = 0$, the solution is trivial. Assume $\rho > 0$ and let

$$x(t) = \max\{0, b - t\}, \quad y(s) = \max\{0, \bar{b} - s\},$$

where t, s are the dual variables from (27) and we have

$$(t + s)(r - \rho) = 0, \quad t + s \geq 0, \quad 0 \leq r \leq \rho.$$

We define index sets for x as

$$I_x = \{j \mid b_j - t > 0\}, \quad L_x = \{j \mid b_j - t \leq 0\}, \quad m_x = |I_x|,$$

and similar sets I_y, L_y for y . Solving a reduced subproblem

$$\min\{\frac{1}{2} \|x - b\|^2 \mid \langle \mathbf{1}, x \rangle = r\},$$

for t and a similar problem for s , yields

$$t = \frac{1}{m_x} (\sum_{j \in I_x} b_j - r), \quad s = \frac{1}{m_y} (\sum_{j \in I_y} \bar{b}_j - r). \quad (28)$$

We consider two cases: $r = \rho$ and $r < \rho$. If $r = \rho$, then we have two variables t and s to optimize over, but the optimization problem (17) decouples into two simplex projection problems which can be solved independently.

$$\begin{aligned} \min\{\frac{1}{2} \|x - b\|^2 \mid \langle \mathbf{1}, x \rangle = \rho, x_j \geq 0\}, \\ \min\{\frac{1}{2} \|y - \bar{b}\|^2 \mid \langle \mathbf{1}, y \rangle = \rho, y_j \geq 0\}. \end{aligned} \quad (29)$$

Let t' and s' be solutions to the independent problems (29). If $t' + s' \geq 0$, we have that the KKT conditions (27) are fulfilled and we have, therefore, the solution to the original problem (17). Otherwise, we have that the optimal $t^* + s^* > t' + s'$ and so at least one of the two variables must increase. Let $t^* > t'$, then $\langle \mathbf{1}, x(t^*) \rangle < \langle \mathbf{1}, x(t') \rangle = \rho$, therefore $r^* < \rho$.

If $r < \rho$, then $t + s = 0$. We eliminate s , which leads to

$$\frac{1}{m_x} (\sum_{j \in I_x} b_j - r) = -\frac{1}{m_y} (\sum_{j \in I_y} \bar{b}_j - r).$$

This can now be solved for r as

$$r = (m_y \sum_{I_x} b_j + m_x \sum_{I_y} \bar{b}_j) / (m_x + m_y). \quad (30)$$

One can verify that $r < \rho$ if r is computed by (30) and $t' + s' < 0$. Plugging (30) into (28), we get

$$t = (\sum_{I_x} b_j - \sum_{I_y} \bar{b}_j) / (m_x + m_y). \quad (31)$$

One can further verify that $t > t'$ and $-t > s'$, where t is computed by (31), t', s' are computed by (28) with $r = \rho$, and $t' + s' < 0$. Therefore, if $x_j(t') = 0$ for some $j \in L_x(t')$, then $x_j(t) = 0$, and so $L_x(t') \subset L_x(t)$. The variables that were fixed to the lower bound while solving (29) with $r = \rho$ remain fixed when considering $r < \rho$. \square

C.7 Proof of Proposition 20

Proof. Let $q \triangleq \sum_{j \neq i} K_{ij} a_j = AK_i - K_{ii} a_i$ and $C \triangleq \frac{1}{\lambda n}$, as before. We need to solve

$$\max_{a \in \mathbb{R}^m} -CL^*(Y_i, -\frac{1}{C}a) - \frac{1}{2} (K_{ii} \|a\|^2 + 2 \langle q, a \rangle).$$

Let x and y be defined as

$$\begin{cases} x = (-\frac{1}{C}a_j + \frac{1}{k})_{j \in Y_i} \\ y = (-\frac{1}{C}a_j)_{j \in \bar{Y}_i}, \end{cases} \implies \begin{cases} a_j = -C(x_j - \frac{1}{k}), \\ a_j = -Cy_j. \end{cases}$$

We have that

$$\begin{aligned} K_{ii} \|a\|^2 + 2 \langle q, a \rangle &= K_{ii} C^2 (\|x - \frac{1}{k} \mathbf{1}\|^2 + \|y\|^2) \\ &\quad - 2C (\langle q_{Y_i}, x - \frac{1}{k} \mathbf{1} \rangle + \langle q_{\bar{Y}_i}, y \rangle). \end{aligned}$$

Ignoring the constant terms and switching the sign, we obtain

$$\begin{aligned} \min_{x \geq 0, y \geq 0} &\langle x, \log x \rangle + \frac{1}{2} K_{ii} C \|x\|^2 - K_{ii} C \frac{1}{k} \langle \mathbf{1}, x \rangle - \langle q_{Y_i}, x \rangle \\ &\langle y, \log y \rangle + \frac{1}{2} K_{ii} C \|y\|^2 - \langle q_{\bar{Y}_i}, y \rangle \\ \text{s.t.} &\langle \mathbf{1}, x \rangle + \langle \mathbf{1}, y \rangle = 1 \end{aligned}$$

Let $\alpha \triangleq K_{ii} C$ and define

$$b_j = \frac{1}{\alpha} q_j + \frac{1}{k}, \quad j \in Y_i, \quad \bar{b}_j = \frac{1}{\alpha} q_j, \quad j \in \bar{Y}_i.$$

The final proximal problem for the update step is given as

$$\begin{aligned} \min_{x \geq 0, y \geq 0} &\langle x, \log x \rangle + \frac{\alpha}{2} \|x - b\|^2 + \langle y, \log y \rangle + \frac{\alpha}{2} \|y - \bar{b}\|^2 \\ &\langle \mathbf{1}, x \rangle + \langle \mathbf{1}, y \rangle = 1. \end{aligned}$$

Next, we discuss how to solve (18). The Lagrangian for this problem is given by

$$\begin{aligned} \mathcal{L}(x, y, \lambda, \mu, \nu) &= \langle x, \log x \rangle + \frac{\alpha}{2} \|x - b\|^2 + \langle y, \log y \rangle \\ &\quad + \frac{\alpha}{2} \|y - \bar{b}\|^2 + \lambda (\langle \mathbf{1}, x \rangle + \langle \mathbf{1}, y \rangle - 1) - \langle \mu, x \rangle - \langle \nu, y \rangle. \end{aligned}$$

Setting the partial derivatives to zero, we obtain

$$\begin{aligned} \log x_j + \alpha x_j &= \alpha b_j - \lambda - 1 + \mu_j, \\ \log y_j + \alpha y_j &= \alpha \bar{b}_j - \lambda - 1 + \nu_j. \end{aligned}$$

We $x_j > 0$ and $y_j > 0$, which implies $\mu_j = 0$ and $\nu_j = 0$.

$$\begin{aligned} \log(\alpha x_j) + \alpha x_j &= \alpha b_j - \lambda - 1 + \log \alpha, \\ \log(\alpha y_j) + \alpha y_j &= \alpha \bar{b}_j - \lambda - 1 + \log \alpha. \end{aligned}$$

Let $t \triangleq \lambda + 1 - \log \alpha$, we have

$$\begin{aligned} \alpha x_j &= W(\exp(\alpha b_j - t)) = V(\alpha b_j - t), \\ \alpha y_j &= W(\exp(\alpha \bar{b}_j - t)) = V(\alpha \bar{b}_j - t), \end{aligned}$$

where W is the Lambert W function. Let

$$g(t) = \sum_{j \in Y_i} V(b_j + \frac{\alpha}{k} - t) + \sum_{j \in \bar{Y}_i} V(b_j - t) - \alpha,$$

then the optimal t^* is the root of $g(t) = 0$, which corresponds to the constraint $\langle \mathbf{1}, x \rangle + \langle \mathbf{1}, y \rangle = 1$. \square